Alaska Department of Transportation & Public Facilities

Research & Technology Transfer

ALASKA DEPARTMENT OF TRANSPORTATION

Evaluation of Wearing Surfaces for the Yukon River Bridge

Prepared by: J. Leroy Hulsey, Professor of Civil & Environmental Engineering
Zachary Jerla,, M.S.Civil Engineering
Wilhelm Muench, Graduate Student

July 2009

Prepared for:
Alaska Department of Transportation
Statewide Research Office
3132 Channel Drive
Juneau, AK 99801-7898

FHWA-AK-RD-09-07

REPORT DOCUMENTATION PAGE			Form approved OMB No.
Public reporting for this collection of information is estimated to average 1 hour per response, including the time for reviewing instructions, searching existing data sources, gathering and maintaining the data needed, and completing and reviewing the collection of information. Send comments regarding this burden estimate or any other aspect of this collection of information, including suggestion for reducing this burden to Washington Headquarters Services, Directorate for Information Operations and Reports, 1215 Jefferson Davis Highway, Suite 1204, Arlington, VA 22202-4302, and to the Office of Management and Budget, Paperwork Reduction Project (0704-1833), Washington, DC 20503			
1. AGENCY USE ONLY (LEAVE BLANK) FHWA-AK-RD-09-07	2. REPORT DATE July 2009	3. REPORT TYPE AND DATES COVERED Final	
4. TITLE AND SUBTITLE Evaluation of Wearing Surfaces for the Yukon River Bridge			5. FUNDING NUMBERS DOT & PF AKSAS # 62848 STP-065-2(14)/T2-06-10
6. AUTHOR(S) J. Leroy Hulsey, Zachary Jerla, Wilhelm Muench			
7. PERFORMING ORGANIZATION NAME(S) AND ADDRESS(ES) Alaska University Transportation Center / University of Alaska Institute of Northern Engineering P.O. Box 755910 University of Alaska Fairbanks Fairbanks, Alaska 99775-5900			8. PERFORMING ORGANIZATION REPORT NUMBER INE/AUTC09.02
9. SPONSORING/MONITORING AGENCY NAME(S) AND ADDRESS(ES) State of Alaska, Alaska Dept. of Transportation and Public Facilities Research, Development and Technology Transfer 2301 Peger Rd Fairbanks, AK 99709-5399			10. SPONSORING/MONITORING AGENCY REPORT NUMBER FHWA-AK-RD-09-07
11. SUPPLENMENTARY NOTES Performed in cooperation with the U.S. Department of Transportation, Federal Highway Administration.			
12a. DISTRIBUTION / AVAILABILITY STATEMENT No restrictions. This document is available to the public through the National Technical Information Service, Springfield, VA 22161 (http://www.ntis.gov)			12b. DISTRIBUTION CODE
13. ABSTRACT (Maximum 200 words) The Dalton Highway's E. L. Patton Bridge is the only span crossing the Yukon River in Alaska. Since 1976, this bridge has carried the Trans-Alaskan Pipeline, and is expected to be used in the future for a natural gas pipeline. The bridge is 2,295 feet long with a deck width of 30 feet, two traffic lanes on a 6% grade over an orthotropic closed-cell steel deck. The bridge experiences extreme temperature conditions (-60˚F to 100˚F) and wear from heavily loaded trucks using tire chains. The original 5 inch thick, two-layer timber wearing surface has been replaced four times to date, with escalating costs and decreasing timber quality. This study involved researching and testing several different material systems in an attempt to find a lightweight, durable, and traction-resistant material that could be used to minimize life-cycle costs of the bridge's wearing surface. The resulting performance ranking showed the Cobra X system (a lightweight high-density polyethylene) to be the best alternative to timber. Because the Cobra X system is no longer manufactured, the researchers provided specific recommendations that the AK DOT&PF could use to request proposals for development of a similarly performing surfacing system.			
14. KEYWORDS : Highway bridges, long span bridge, bridge decks, maintenance, traction, durability			15. NUMBER OF PAGES 242
			16. PRICE CODE N/A
17. SECURITY CLASSIFICATION OF REPORT Unclassified	18. SECURITY CLASSIFICATION OF THIS PAGE Unclassified	19. SECURITY CLASSIFICATION OF ABSTRACT Unclassified	20. LIMITATION OF ABSTRACT N/A

NSN 7540-01-280-5500

STANDARD FORM 298 (Rev. 2-98)
Prescribed by ANSI Std. 239-18 298-102

SI* (MODERN METRIC) CONVERSION FACTORS

APPROXIMATE CONVERSIONS TO SI UNITS

Symbol	When You Know	Multiply By	To Find	Symbol
		LENGTH		
in	inches	25.4	millimeters	mm
ft	feet	0.305	meters	m
yd	yards	0.914	meters	m
mi	miles	1.61	kilometers	km
		AREA		
in^2	square inches	645.2	square millimeters	mm^2
ft^2	square feet	0.093	square meters	m^2
yd^2	square yard	0.836	square meters	m^2
ac	acres	0.405	hectares	ha
mi^2	square miles	2.59	square kilometers	km^2
		VOLUME		
fl oz	fluid ounces	29.57	milliliters	mL
gal	gallons	3.785	liters	L
ft^3	cubic feet	0.028	cubic meters	m^3
yd^3	cubic yards	0.765	cubic meters	m^3
		NOTE: volumes greater than 1000 L shall be shown in m^3		
		MASS		
oz	ounces	28.35	grams	g
lb	pounds	0.454	kilograms	kg
T	short tons (2000 lb)	0.907	megagrams (or "metric ton")	Mg (or "t")
		TEMPERATURE (exact degrees)		
^oF	Fahrenheit	5 (F-32)/9 or (F-32)/1.8	Celsius	^oC
		ILLUMINATION		
fc	foot-candles	10.76	lux	lx
fl	foot-Lamberts	3.426	candela/m^2	cd/m^2
		FORCE and PRESSURE or STRESS		
lbf	poundforce	4.45	newtons	N
lbf/in^2	poundforce per square inch	6.89	kilopascals	kPa

APPROXIMATE CONVERSIONS FROM SI UNITS

Symbol	When You Know	Multiply By	To Find	Symbol
		LENGTH		
mm	millimeters	0.039	inches	in
m	meters	3.28	feet	ft
m	meters	1.09	yards	yd
km	kilometers	0.621	miles	mi
		AREA		
mm^2	square millimeters	0.0016	square inches	in^2
m^2	square meters	10.764	square feet	ft^2
m^2	square meters	1.195	square yards	yd^2
ha	hectares	2.47	acres	ac
km^2	square kilometers	0.386	square miles	mi^2
		VOLUME		
mL	milliliters	0.034	fluid ounces	fl oz
L	liters	0.264	gallons	gal
m^3	cubic meters	35.314	cubic feet	ft^3
m^3	cubic meters	1.307	cubic yards	yd^3
		MASS		
g	grams	0.035	ounces	oz
kg	kilograms	2.202	pounds	lb
Mg (or "t")	megagrams (or "metric ton")	1.103	short tons (2000 lb)	T
		TEMPERATURE (exact degrees)		
^oC	Celsius	1.8C+32	Fahrenheit	^oF
		ILLUMINATION		
lx	lux	0.0929	foot-candles	fc
cd/m^2	candela/m^2	0.2919	foot-Lamberts	fl
		FORCE and PRESSURE or STRESS		
N	newtons	0.225	poundforce	lbf
kPa	kilopascals	0.145	poundforce per square inch	lbf/in^2

*SI is the symbol for the International System of Units. Appropriate rounding should be made to comply with Section 4 of ASTM E380. (Revised March 2003)

EVALUATION OF WEARING SURFACES FOR THE YUKON RIVER BRIDGE

Final Report

Prepared for
Alaska Department of Transportation & Public Facilities

Authors:

J. Leroy Hulsey
Professor of Civil & Environmental Engineering

Zachary Jerla, M.S. Civil Engineering
Wilhelm Muench (Graduate Student)

Institute of Northern Engineering
College of Engineering and Mines
University of Alaska Fairbanks
Fairbanks, AK 99775

INE/AUTC09.02

July 2009

Table of Contents

List of Figures

List of Tables

Acknowledgments

The authors thank the Alaska Department of Transportation & Public Facilities, Martin Marietta, Inc., Ultra Poly, Inc., Creative Pultrusions, Inc., and Compositech, Inc. for supplying timber and test samples for use in this research.

We appreciate the funding support that was provided by the Alaska University Transportation Center (AUTC), the Institute of Northern Engineering at the University of Alaska Fairbanks, and the Alaska Department of Transportation & Public Facilities.

For their assistance with administrative matters regarding this contract, we thank Billy Connor, Director of AUTC; Kathy Peterson, Grant Manager for AUTC; and Saundra Jefko and Jill M. Dewey-Davidson, Program Assistants for AUTC.

Abstract

Consider that a lightweight, durable, and traction-resistant material is needed as a wearing surface replacement for a two-lane bridge deck that is on a 6% grade. The wearing surface to be replaced is 30 ft (9.2 m) wide and is attached to an orthotropic closed-cell steel deck that is supported by two steel box girders that are 61 in. (155.9 cm) wide by 163 in. (414 cm) deep. The six-span bridge, which is 2295 ft (699.5 m) long, is located on the Dalton Highway, a gravel road about 50 mi (80 km) north of Fairbanks, Alaska. This structure is expected to support the oil pipeline, a future gas line, and heavily loaded trucks; it is also expected to respond to mild summers and harsh winters, with air temperature extremes of -58°F (-50°C) to 100°F (40°C).

A 5 in. (127 mm) two-layer timber wearing surface was installed in 1976. This timber system was replaced in 1981, 1992, 1999, and 2007. Should timber be the next wearing surface? Thermal cracking, abrasion, durability, flexural strain, traction, weight, and fastening methods to the steel deck are important parameters for selecting a replacement material for this wearing surface. Live load fatigue in the wearing surface should not be an issue. The driving surface may be dry, wet, or ice- and snow-covered. During the winter, because of the steep grade, trucks typically use tire chains, which damage the timber.

Alternate wearing surfaces were laboratory tested for structural durability, traction, and resistance to tire chains. In addition to laboratory testing, field performance of bridge wearing surfaces was evaluated. Laboratory test results are presented, with each wearing surface ranked for structural integrity, traction and chain damage, and field performance. Cobra X (the company no longer exists) will likely provide more than a 15-year satisfactory service life. All other wearing surfaces including timber were rejected.

Executive Summary

This study was commissioned to find a cost effective wearing surface to replace the wooden deck on the Yukon River Bridge, located on the Dalton Highway. Unfortunately, wood has proven to be unsatisfactory because of its short life of five to seven years and because it provides low traction during wet and freezing conditions. Of the materials tested, only Cobra X, which has been in service on the bridge for twelve years, proved promising. Since Cobra X is no longer available, a substitute will be needed if the Alaska Department of Transportation & Public Facilities (AKDOT&PF) wishes to pursue this option.

The Yukon River Bridge is on a 6% grade and is subjected to

- air temperature extremes from -60°F to 100°F;
- heavy truck loads;
- snow removal equipment; and
- tire chains commonly used by truck drivers during the winter.

The wearing surface, which lies on an orthotropic steel deck spliced with plates and bolts, must meet the following design restrictions:

- It must not exceed 30 psf.
- The thickness must be between 3 and 5 in.
    - It must cover splices and bolts (minimum of 3 in.).
    - Its 5-in. upper limit is controlled by the bridge railing.
- The wearing surface must be sufficiently flexible to lay on an uneven deck and bridge, across steel deck splices and bolts.
- Thermal strains and thermal deformations must be accommodated.

A 5-in. (127 mm) two-layer timber wearing surface was installed at the time of construction. Since then, the wearing surface has been replaced four times: in 1981, 1992, 1999, and 2007. Each time, repair and replacement costs have increased, and the timber quality has decreased; thus, AKDOT&PF is seeking a safe and more cost-effective solution. An experimental study was conducted to evaluate alternate wearing surfaces being considered for possible use on this bridge.

We tested wearing surfaces in the laboratory for (a) structural durability; (b) static and dynamic coefficients of friction at wet, dry, and icy conditions; and c) tire chain damage resulting from tires rolling, lashing, or dragging across the surface. Traction and tire-chain damage tests were carried out in the laboratory on timber, uncoated UHMW, coated UHMW, Super Panel, Cobra X, and asphalt concrete. Cobra X and asphalt were used as a base of comparison. Both were previously in service for about 14 years. A partial summary of findings for a moving vehicle is provided in the following table. The American Association of State Highway and Transportation Officials (AASHTO) recommends a minimum traction value of 0.40 for moderate temperature conditions. The AKDOT&PF may want to establish its own criteria for this facility.

Table of Traction and Tire Chain Damage for Various Wearing Surfaces

		Coefficient of Friction							Damage (0.001 in.)		
		70°F		20°F		-20°F		Field	-20°F		
	Status	Dry	Wet	Dry	Icy	Wet	Icy	Dry	Rolling	Lashing	Dragging
Moving tests:											
UHMW	L	0.50	0.47	0.37	0.13	0.37	0.18	NT	29	21	13
Coated UHMW	L	0.54	0.55	0.60	0.25	0.48	0.12	NT	NT	NT	NT
Timber running board[a]	L,F	0.58	0.64	0.71	0.21	0.53	0.41	0.70	131	16	13
Transonite	L,F	0.62	0.63	0.75	0.51	0.63	0.29	0.90	33	47	26
Super Panel	L	0.76	0.75	0.89	0.60	0.75	0.47	NT	38	60	28
Asphalt[c]	L,F	0.62	0.63	NT	NT	NT	NT	0.84	NT	NT	NT
Cobra X[b]	L,F	0.58	0.45	0.65	0.53	0.55	0.33	0.52	37	22	0
Prodeck 4	F	NT	NT	NT	NT	NT	NT	0.94	NT	NT	NT

a) Timber running board studies included timber on timber, timber on UHMW, and timber on M-shaped UHMW.

b) Cobra X was in use for 14 years prior to testing in the laboratory. Its field test age was 15 years.

c) The asphalt was used for 14 years prior to testing. Field tests were conducted on 10-year-old asphalt.

During this study on the Yukon River Bridge, we inspected bridge wearing surfaces in the summer of 2006 and 2007. In 2007, we also performed traction tests on the in-place bridge deck wearing surfaces. Each wearing surface was ranked as a possible future wearing surface on this bridge structure, based on a compilation of laboratory tests and field inspections.

Summary of Laboratory Tests, Field Tests, and Field Inspections

Wearing Surface	Where	Laboratory Studies			Field Evaluation	Is it acceptable for this bridge?
		Durability	Traction	Chain Damage		
Cobra X	F,L	1	3	1	Good	Yes, Recommended
Timber/timber	F,L	3	4	5	Poor	No, Not recommended
Transonite	F,L	2	2	3	Failed	No, Reject
Timber on solid UHMW	L	4	4	5	NA	No, Reject
Timber on M-shaped UHMW	L	5	4	5	NA	No, Reject
Super Panel	L	6	1	4	NA	No, Reject
UHMW	L	NA	5	NA	NA	No, Reject
Uncoated UHMW	L	NA	6	2	NA	No, Reject
Prodeck 4	F	NA	NA	NA	Failed	No, Reject
Concrete-filled metal grid	F	NA	NA	NA	Poor	Weight is a problem, and traction could be an issue, as the concrete abrades below the metal grid.

Note: F stands for field; L stands for laboratory

Recommendations:

1. Specifications for selecting a future wearing surface should be provided. Selection requirements should include:
   a. a minimum dynamic friction coefficient for wet conditions.
   b. the thickness limitation for the wearing surface.
   c. the maximum weight of the wearing surface (30 psf).
   d. either thin coatings (such as an aggregate epoxy that can be applied by Maintenance and Operations) or a traction surface that is more flexible than the substrata.
   e. a wearing surface that provides sufficient flexibility. This may be measured by performing a bending test on a flat plate. One of the following conditions should be met:

- ✓ Test a two-way slab of the design thickness that is 48 square in. Each edge is pinned supported. Apply pressure of 500 psi over 36 square in. at the center of the plate. Center deflection should exceed 0.25 in.
- ✓ Alternatively, test a beam of the design thickness that is 6 in. wide, 48 in. long. The beam should be loaded by applying a pressure of 500 psi, acting over a 36-square-in. area at the center of the beam. The center deflection should exceed 3.25 in.

2. Future wearing surfaces should be one layer, with provisions to accommodate thermal differences between the surface and the steel deck.
3. We suggest requesting manufacturer-produced systems that are modular and will allow for easy replacement and repair.
4. We suggest that trial wearing surfaces be installed for field observation.
5. Wearing surfaces worthy of consideration include:
   a. modular rubber grade crossings;
   b. products like Cobra X;
   c. coatings used by the U.S. Navy for aircraft carriers that improve both traction and gouge resistance; and
   d. other coatings such as aggregate epoxy that may be field applied by maintenance forces.

CHAPTER 1 – SUMMARY OF FINDINGS

Alternate wearing surfaces were evaluated for possible use on the Yukon River Bridge, located 50 mi (80 km) north of Fairbanks, Alaska, on the Dalton Highway.

The bridge is 2295 ft (699.5 m) long on a 6% downgrade from south to north. It was opened to traffic in 1976 with a temporary two-layer timber deck wearing surface. During winter months, trucks typically use tire chains to climb the 6% grade.

The problem is that timber wearing surfaces are damaged by both traffic and weather, and these surfaces do not last beyond five to six years before extensive maintenance or replacement is needed (see Figures 1.1 and 1.2).

Figure 1.1 Timber deck repair, a maintenance activity.

Figure 1.2 Timber deck at the end of its service life.

The bridge superstructure is an orthotropic steel deck, supported by two steel box girders with six spans. Steel beams, spaced at 15-ft spans between the two box girders, support the orthotropic steel deck. A suitable wearing surface must meet the following criteria:

- Thickness should be limited to 6 in.
- Wearing-surface system must clear splice plates and bolts that were used for the steel deck.
- Wearing surface must be fastened to the orthotropic steel deck.
- Weight should be less than 30 psf.
- Traction should be better than wood.

- Surface must resist wear and damage from tire chains.
- Thermal strains should be accounted for.
- Flexibility should be compatible with the steel deck.

This study addressed three issues for six different types of alternative wearing-surface solutions:

1. Structural durability
2. Traction and resistance to wear and damage caused by truck tire chains
3. Field performance

Structural Durability

We evaluated and ranked six experimental bridge decks based on structural durability. Durability was determined through testing and analytical modeling by the finite element method (Jerla, 2008). Factors considered in the ranking were stiffness, cold-temperature response, behavior during testing, and material properties. During tests for structural durability, we did not instrument Cobra X, though we did monitor the product for deflection versus load. Table 1.1 shows the structural durability ranking for each wearing surface.

Table 1.1 Structural Durability Ranking for Wearing Surfaces

Test Panel	Ranking	Advantages	Disadvantages
Cobra X	1	Lightweight and flexible.	A connection to the deck is needed.
Transonite	2	Lightweight and flexible; little change in stiffness with temperature; stronger than the others.	Instability at low compressive stresses may cause the wearing surface to delaminate.
Timber/ Timber	3	Lightweight and flexible; stiffness is similar to Transonite.	Differences in stiffness between layers in the lower layer caused it to carry more load. This caused premature cracking.
Timber on Solid UHMW	4	Top timber layer was jointed and fastened to the UHMW; the low flexural modulus plastic is ideal for fastening to the deck.	The material property mismatch caused timber planks to crack. Thermal strains are a problem. It stiffens in cold temperatures, and attachments using screws into the plastic are permanent.
Timber on M-shaped UHMW	5	Advantages are the same as timber on solid UHMW and its weight is reduced.	M-shape was significantly more flexible than the solid; this caused timber running planks to crack at lower loads. Other disadvantages are the same as the solid except it stiffened more in cold temperatures.
Super Panel	6	By comparison, stiffer and stronger than the other systems. Material properties were somewhat insensitive to cold temperatures.	Too stiff and too brittle for use on the Yukon River Bridge.

Cobra X was tested as a one-way plate (beam action). Deflection was excessive at 1000 lb, so loading was stopped. During testing, we observed that Cobra X is very flexible, an ideal condition for this bridge. The stiffness of the Super Panel was 46 times the stiffness of Cobra X (Jerla, 2008).

Traction and Chain Damage

Traction

In the laboratory, we tested traction for six wearing surfaces and a sample of asphalt pavement. These tests were conducted at temperatures of 70°F (room temperature), 20°F, and

-20°F. Both static friction and dynamic friction coefficients were measured for four new products and two used older products. Wood, UHMW, Transonite, and the Super Panel were the new products. Cobra X had been in service on the Yukon River Bridge for 14 years prior to testing. The asphalt concrete sample was from an Anchorage intersection and was 14 years old.

We conducted between three and four tests for each test condition, and we compiled and averaged the resulting traction values for each type of test. Using laboratory data, we ranked the traction performance of each wearing surface for temperature conditions of 20°F and -20°F.

Traction rankings for dry and icy conditions were determined for a moving vehicle (dynamic friction coefficient). Wearing surfaces were ranked for traction under icy conditions with a stalled vehicle (static friction). Tables 1.2 and 1.3 show the rankings, with figures in the gray columns sorted from high to low. These tables show that:

- Cobra X ranked in the top three products for all icy cases.
- UHMW, uncoated and coated, ranked near the bottom of the products for 20°F and -20°F.
- Timber, under icy conditions, ranked near zero at 20°F (both the static and dynamic friction coefficients).
    - For a stalled vehicle on a 6% grade, this lack of traction is problematic; yet at -20°F and icy, timber is one of the better traction surfaces.

Table 1.2 Wearing Surfaces Ranked by Traction Performance at -20°F (Dry and Icy)

Ranking	Sample	70°F		20°F		-20°F	
		Dry	Wet	Dry	Icy	Dry	Icy
Ranked for dynamic friction at -20°F and icy:							
1	Wood	0.54	0.61	0.69	0.05	0.47	0.38
2	Super Panel	0.66	0.70	0.78	0.65	0.70	0.34
3	Cobra X	0.58	0.45	0.65	0.53	0.55	0.33
4	Transonite	0.62	0.63	0.75	0.51	0.63	0.29
5	Uncoated UHMW	0.50	0.47	0.37	0.13	0.37	0.18
6	UHMW	0.54	0.55	0.60	0.25	0.48	0.12
--	Asphalt Concrete	0.59	0.61	NT	NT	NT	NT
Ranked for static friction at -20°F and icy:							
1	Super Panel	0.76	0.75	0.89	0.60	0.75	0.47
2	Cobra X	0.65	0.52	0.77	0.61	0.64	0.43
3	Wood	0.58	0.64	0.71	0.21	0.53	0.41
4	Transonite	0.67	0.69	0.82	0.57	0.69	0.37
5	Uncoated UHMW	0.55	0.50	0.47	0.25	0.44	0.30
6	UHMW	0.56	0.57	0.62	0.28	0.51	0.19
--	Asphalt Concrete	0.62	0.63	NT	NT	NT	NT
Ranked for dynamic friction at -20°F and dry:							
1	Super Panel	0.66	0.70	0.78	0.65	0.70	0.34
2	Transonite	0.62	0.63	0.75	0.51	0.63	0.29
3	Cobra X	0.58	0.45	0.65	0.53	0.55	0.33
4	UHMW	0.54	0.55	0.60	0.25	0.48	0.12
5	Wood	0.54	0.61	0.69	0.05	0.47	0.38
6	Uncoated UHMW	0.50	0.47	0.37	0.13	0.37	0.18
--	Asphalt Concrete	0.59	0.61	NT	NT	NT	NT

NT = Not tested

Table 1.3 Wearing Surfaces Ranked by Traction Performance

Ranking	Sample	70°F Dry	70°F Wet	20°F Dry	20°F Icy	-20°F Dry	-20°F Icy
Ranked for dynamic friction at 20°F and icy:							
1	Super Panel	0.66	0.70	0.78	0.65	0.70	0.34
2	Cobra X	0.58	0.45	0.65	0.53	0.55	0.33
3	Transonite	0.62	0.63	0.75	0.51	0.63	0.29
4	UHMW	0.54	0.55	0.60	0.25	0.48	0.12
5	Uncoated UHMW	0.50	0.47	0.37	0.13	0.37	0.18
6	Wood	0.54	0.61	0.69	0.05	0.47	0.38
--	Asphalt Concrete	0.59	0.61	NT	NT	NT	NT
Ranked for static friction at 20°F and icy:							
1	Cobra X	0.65	0.52	0.77	0.61	0.64	0.43
2	Super Panel	0.76	0.75	0.89	0.60	0.75	0.47
3	Transonite	0.67	0.69	0.82	0.57	0.69	0.37
4	UHMW	0.56	0.57	0.62	0.28	0.51	0.19
5	Uncoated UHMW	0.55	0.50	0.47	0.25	0.44	0.30
6	Wood	0.58	0.64	0.71	0.21	0.53	0.41
--	Asphalt Concrete	0.62	0.63	NT	NT	NT	NT
Ranked for dynamic friction at 20°F and dry:							
1	Super Panel	0.66	0.70	0.78	0.65	0.70	0.34
2	Transonite	0.62	0.63	0.75	0.51	0.63	0.29
3	Wood	0.54	0.61	0.69	0.05	0.47	0.38
4	Cobra X	0.58	0.45	0.65	0.53	0.55	0.33
5	UHMW	0.54	0.55	0.60	0.25	0.48	0.12
6	Uncoated UHMW	0.50	0.47	0.37	0.13	0.37	0.18
--	Asphalt Concrete	0.59	0.61	NT	NT	NT	NT

NT = Not tested

In 2007, the Yukon River Bridge deck wearing surfaces were replaced with a new two-layer timber wearing surface. Before replacement, we field tested for traction of the bridge timber deck wearing surface and the experimental features (see Figure 1.3). Test results represent end-of-life values.

Except for a sample of asphalt pavement and a 14-year-old sample of Cobra X, the samples measured for traction in the laboratory were new. These traction values are beginning-of-life values.

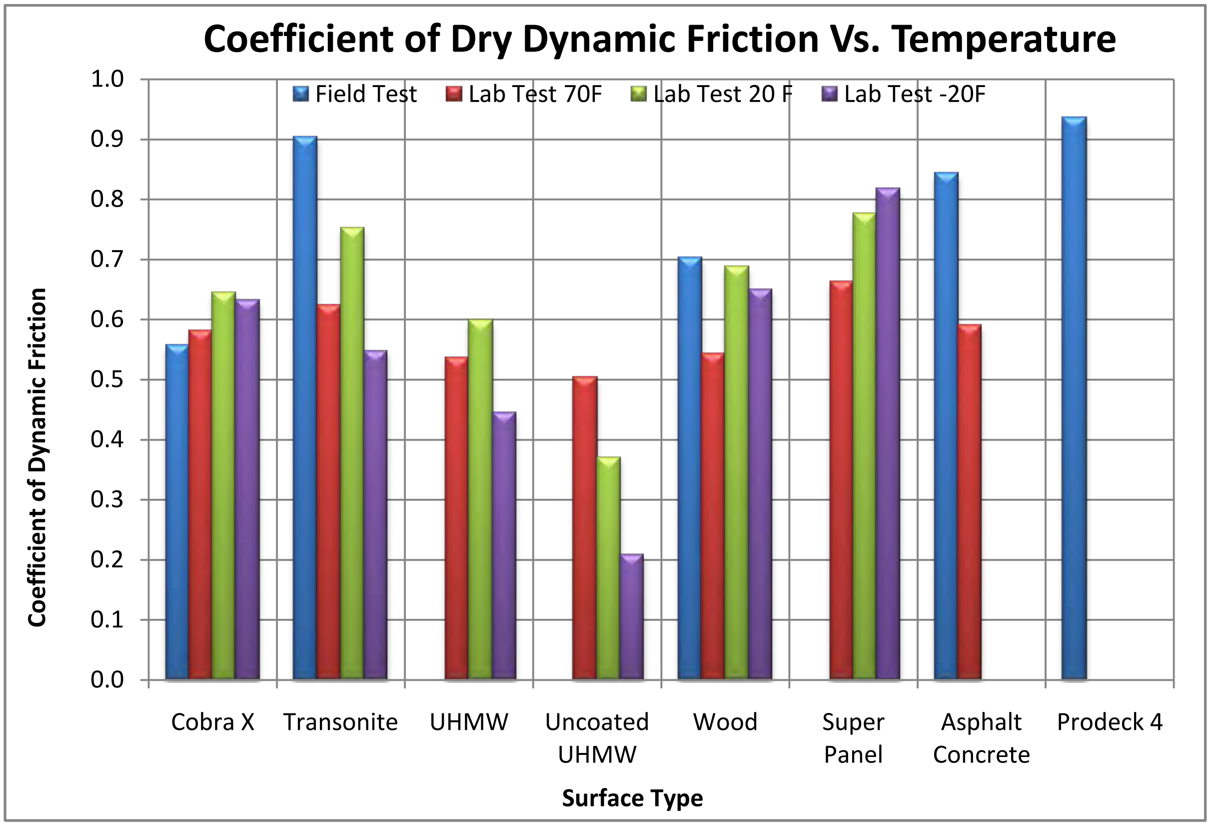

Figure 1.3 Dynamic traction values from field and laboratory tests

We compared the laboratory-measured dynamic friction coefficients for the six different samples of wearing surfaces by examining minimum, maximum, and most frequent for all test exposures. The test conditions were 70°F dry and wet, 20°F dry and icy, and -20°F dry and icy. Figure 1.4 shows ranges for each wearing surface.

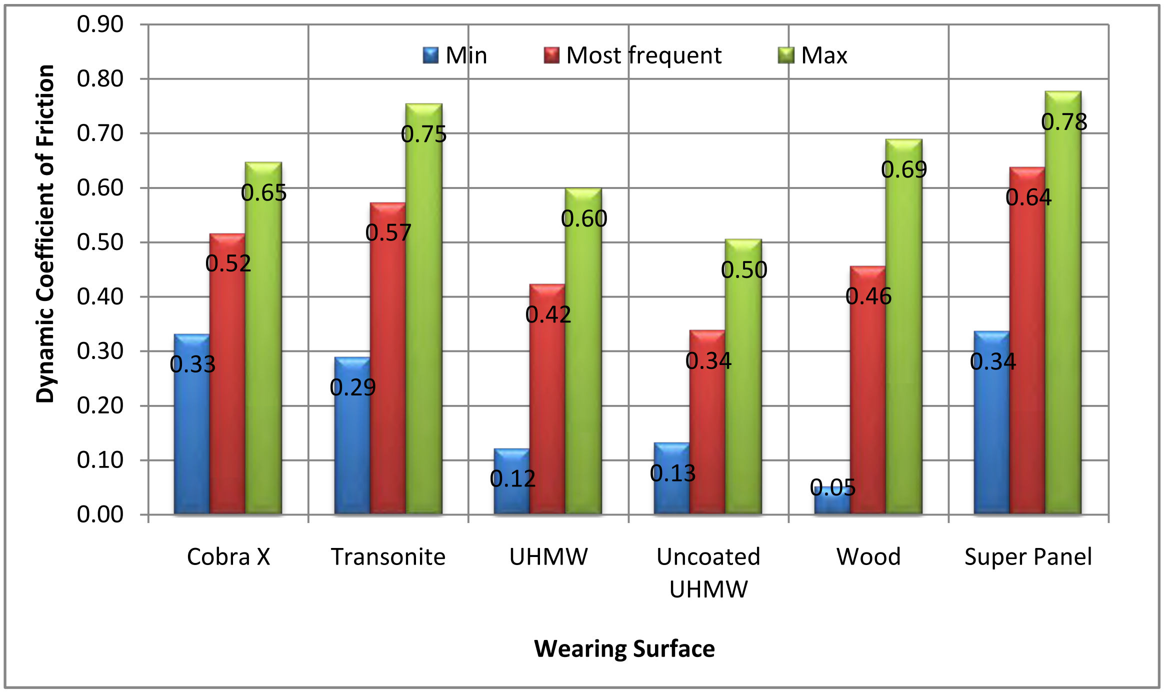

Figure 1.4 Range of dynamic coefficients (summer to winter) for the wearing surfaces.

A similar evaluation was done for the static coefficients of friction. These values represent what may occur for a stalled vehicle (see Figure 1.5).

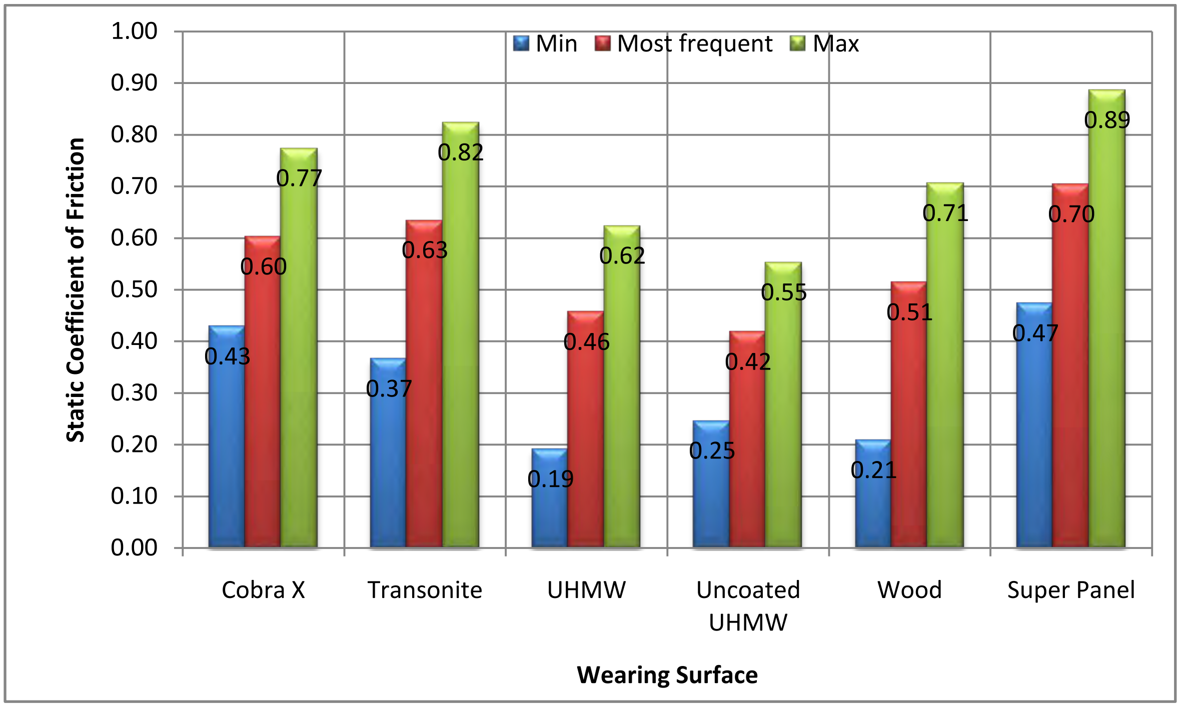

Figure 1.5 Range of static coefficients (summer to winter) for the wearing surfaces.

On June 21, 2007, we conducted preliminary traction test measurements on asphalt pavement at the Duckering Building parking lot of the University of Alaska Fairbanks (UAF) campus. This pavement has been in service over ten years. The purpose of these tests was to become familiar with our testing equipment and to provide a field-test measurement that would serve as a baseline for used pavement measurements. The average traction for the parking lot was 0.84. Traction for end-of-life wearing surfaces at the Yukon River Bridge was measured the following day, on June 22, 2007 (see Figure 1.6 and Table 1.4).

Figure 1.6 Field traction measurements using Grip Tester Type 292/16.

Table 1.4 Range of Field Traction Coefficients, Dry (June, 2007)

	Wood (8 yr)			Cobra X (15 yr)			Prodeck 4 (2 yr)			Transonite (2 yr)		
Test	Min	Avg	Max	Min	Avg	Max	Min	Avg	Max	Min	Avg	Max
1:39 PM	0.20	0.62	0.8	0.50	0.50	0.57	0.59	0.91	1.01	0.78	0.86	0.98
1:47 PM	0.07	0.70	0.9	0.60	0.64	0.7	0.66	0.91	0.99	0.64	0.92	1.01
1:54 PM	0.21	0.73	0.9	0.50	0.5	0.55	0.88	0.96	1.02	0.88	0.91	0.96
2:00 PM	0.09	0.76	0.9	0.60	0.59	0.63	0.8	0.94	1.01	0.7	0.91	1.03
2:07 PM	0.22	0.68	0.8	0.50	0.51	0.56	0.86	0.94	0.99	0.77	0.89	1.02
2:13 PM	0.35	0.72	0.9	0.60	0.6	0.63	0.82	0.95	1.03	0.82	0.93	1.01
Extremes	0.07		0.9	0.50		0.63	0.59		1.01	0.64		1.03

The measured end-of-life field dynamic traction coefficients were for a dry summer day. The measured values showed that

- Transonite (2 years old) and Prodeck 4 (2 years old) provided better traction than others did.

- Wood (8 years old) had coefficients from 0.07 to 0.9; that is, the traction varied significantly along the bridge deck. In some instances, traction was near zero; in other instances, traction was very good. This can be a problem for the driver.
- Cobra X (15 years old) provided coefficients from 0.5 to 0.63; that is, the coefficients for Cobra X are small. The average field traction coefficient for the Cobra X was 0.56. The laboratory traction-test value for this same product at age 14 years was 0.58.

Summary Ranking for Traction

Laboratory-measured dynamic coefficients of friction at 70°F, 20°F, -20°F for dry, wet, and icy exposures were reviewed for each test sample. These values and those for static coefficients of friction are presented in Table 1.5.

Table 1.5 Laboratory-Measured Traction Coefficients vs. Exposure

	70°F		**20°F**		**-20°F**				
Sample	**Dry**	**Wet**	**Dry**	**Icy**	**Dry**	**Icy**	**Min**	**Most frequent**	**Max**
Dynamic Friction:									
Cobra X	0.58	0.45	0.65	0.53	0.55	0.33	0.33	0.52	0.65
Transonite	0.62	0.63	0.75	0.51	0.63	0.29	0.29	0.57	0.75
UHMW	0.54	0.55	0.60	0.25	0.48	0.12	0.12	0.42	0.60
Uncoated UHMW	0.50	0.47	0.37	0.13	0.37	0.18	0.13	0.34	0.50
Wood	0.54	0.61	0.69	0.05	0.47	0.38	0.05	0.46	0.69
Super Panel	0.66	0.70	0.78	0.65	0.70	0.34	0.34	0.64	0.78
Asphalt Concrete	0.59	0.61	NT	NT	NT	NT	NT	NT	NT
Static Friction:									
Cobra X	0.65	0.52	0.77	0.61	0.64	0.43	0.43	*0.60*	0.77
Transonite	0.67	0.69	0.82	0.57	0.69	0.37	0.37	*0.63*	0.82
UHMW	0.56	0.57	0.62	0.28	0.51	0.19	0.19	*0.46*	0.62
Uncoated UHMW	0.55	0.50	0.47	0.25	0.44	0.30	0.25	*0.42*	0.55
Wood	0.58	0.64	0.71	0.21	0.53	0.41	0.21	*0.51*	0.71
Super Panel	0.76	0.75	0.89	0.60	0.75	0.47	0.47	*0.70*	0.89
Asphalt Concrete	0.62	0.63	NT	NT	NT	NT	NT	*NT*	NT

NT - Not tested

In this study, we graded each wearing surface for traction, based on a normalized rating for a moving vehicle in accordance with the following formula:

$$\bar{g} = 80\%\left(\frac{t_{\min}}{0.5}\right) + 20\%\left(\frac{t_{\max}}{0.9}\right)$$

in which $t_{\min}$ is the minimum dynamic coefficient of friction for a given wearing surface, $t_{\max}$ is the maximum dynamic coefficient of friction for this wearing surface, and $\bar{g}$ is a grade that is used to rank traction effectiveness.

The ideal wearing surface will have a $\bar{g}$ of 1.0, and its minimum will be greater than 0.5. Using the above equation, we ranked wearing surfaces using the dynamic coefficients of friction that are within the grayed area of Table 1.5; these are shown in Table 1.6. The Super Panel was graded the best, and wood was given the lowest grade. UHMW products did not have sufficient traction resistance for use on this structure.

Table 1.6 Samples Graded and Ranked for Dynamic Traction

		Traction Coefficients			
Sample	Grade	Min	Most frequent	Max	Largest change
Super Panel	0.71	0.34	0.64	0.78	0.44
Cobra X	0.67	0.33	0.52	0.65	0.32
Transonite	0.63	0.29	0.57	0.75	0.47
UHMW	0.32	0.12	0.42	0.60	0.48
Uncoated UHMW	0.32	0.13	0.34	0.50	0.37
Wood	0.23	0.05	0.46	0.69	0.64

Tire Chain Damage

Rolling Damage

Rolling damage is a measure of the damage caused by one chained truck tire moving across the bridge deck. Our test for rolling damage involved moving a normally loaded (4500 lb) test panel while the chained tire rotated at about 40 mph. The damage caused by the high pressure of chain links against the bridge-deck surface is cumulative with time; therefore, the test was designed to represent a year of rolling damage. We conducted three tests on each test panel; that is, we tested the left side, the center, and the right side of each panel. Table 1.7 lists the damage for each wearing surface for 70°F and -20°F. The temperature of -20°F was used to rank the wearing surfaces. Wood was the most vulnerable to rolling damage, and unlike other wearing surfaces, the most damage was caused at cold temperatures when trucks are likely to use chains.

Table 1.7 Wearing Surfaces, Ranked by the Least Rolling Damage

		Damage Depth (0.001 in.)		
Ranking	Surface	-20°F	20°F	70°F
1	UHMW	29	NT	46
2	Transonite	33	NT	62
3	Cobra X	37	NT	55
4	Super Panel	38	NT	65
5	Wood	131	NT	121

NT = Not tested

Lashing Damage

We conducted lashing tests by spinning a tire with chains at approximately 40 mph. The tire with a chain 1 in. above the surface was rotated for a period of 2 sec. In this test, our objective was to evaluate damage caused by loose links of chain that strike the wearing surface. Two seconds of lashing time represented nearly a year of use on the Yukon River Bridge. We ranked samples based on the least lashing damage (see Table 1.8).

Table 1.8 Wearing Surfaces Ranked for Damage by Lashing

Ranking	Surface	Damage Depth (0.001 in.)
1	Wood	16
2	UHMW	21
3	Cobra X	22
4	Transonite	47
5	Super Panel	60

Dragging Damage

We tested for dragging damage by cyclically moving the test panel 11 cycles under the tire with chains. The tire was subjected to a normal force of 4500 lb while locked and prevented from rotating (a drag condition). The normal force of 4500 lb was used to approximate the force on a single tire in an 18,000 lb equivalent single axle load (ESAL). Two seconds of lashing time and 11 cycles of dragging were used as an approximate for one year of damage at the Yukon River Bridge. The findings were ranked for performance in resistance to dragging damage (see Table 1.9).

Table 1.9 Ranking of Wearing Surfaces in Resistance to Dragging Damage

Ranking	Surface	Damage Depth (0.001 in.)
1	Cobra X	-5
2	UHMW	13
3	Wood	13
4	Transonite	26
5	Super Panel	28

Summary Rankings for Tire Chain Damage

Wearing surfaces may be damaged by a combination of rolling, lashing, and dragging. The weighted contribution of each is dependent on traffic and weather, and on what percentage of the surface is damaged by each. In this research, we did not identify the weighted values that should be assigned to accumulated damage. Each type of damage is presented in a combined table for review and consideration (see Table 1.10). The values for rolling damage listed in this table are based on one pass instead of 30 to 36 passes. Accumulated damage, which is beyond the scope of this study, is left for future research.

Table 1.10 Summary of Damage by Tire Chains

Surface Depth (0.001 in.)									
	Lashing			Dragging			Rolling		
Sample	70°F	20°F	-20°F	70°F	20°F	-20°F	70°F	20°F	-20°F
Cobra X	26	14	14	-1	7	-5	1	NT	13
Transonite	39	31	31	24	25	26	40	NT	14
UHMW	21	13	13	22	11	13	18	NT	12
Wood	38	27	27	20	28	13	93	NT	95
Super Panel	32	50	50	15	39	28	44	NT	19
NT = Not tested									

Performance was ranked based on accumulated damage, assuming each type of damage is weighted equally. Rankings for these wearing surfaces at -20°F are shown in Table 1.11.

Table 1.11 Wearing-Surface Damage by Tire Chains

Accumulated Damage for -20°F (0.001 in.)					
Ranking	Sample	Rolling	Lashing	Dragging	Totals
1	Cobra X	13	14	-5	22
2	UHMW	12	13	13	38
3	Transonite	14	31	26	71
4	Super Panel	19	50	28	97
5	Wood	95	27	13	135

Field Performance

We inspected the Yukon River Bridge wearing surfaces in 2006 and again in 2007. Based on these inspections, we ranked each wearing surface for performance (see Table 1.12).

Table 1.12 Ranking Performance for In-Service Yukon River Bridge Wearing Surfaces

Ranking	Future use	Wearing surface	Age (yr)	Condition	Performance
1	yes	Cobra X on timber under layer	15	Fastened to timber underlayment	This experimental feature was installed in 1992. *Observed*: It has performed well.
2	yes	Two-layer timber system	8	Timbers layers are lagged together	Installed in 1999. *Observed*: It is slick when wet or icy. Its life is reduced by decay, chains, and equipment damage. *Predicted*: It likely will prematurely crack because one layer carries more load.
3	no	Concrete-filled grid	8	Metal grid with concrete between	This is an experimental feature. *Observed*: Its condition was better than expected; however, concrete was below the metal grid, which will cause a traction problem.
4	no	Transonite	2	Composite is fastened to the steel deck	This experimental feature was installed in 2005. *Observed*: The wearing surface was damaged the first year. In addition, it appears that the panel was not sealed at the fastener penetrations, and subsequently, it was unable to drain.
5	no	Prodeck 4	2	FRP supported by a rail	This experimental feature was installed in 2005. *Observed*: The wearing surface was delaminating, and there were stress cracks at the web flange interface. It appears that this system is too stiff and too brittle for this application. There appeared to be water damage.

Findings and Conclusions

Except for Cobra X, none of the wearing-surface options tested in this study will provide a satisfactory long-term solution for use on the Yukon River Bridge. Each material was problematic (see Table 1.13).

Table 1.13 Summary of Laboratory Tests, Field Tests, and Field Inspections

Wearing Surface	Where	Laboratory Studies			Field Evaluation	Is it acceptable for this bridge?
		Durability	Traction	Chain Damage		
Cobra X	F,L	1	3	1	Good	Yes, Recommended
Timber/timber	F,L	3	4	5	Poor	No, Not recommended
Transonite	F,L	2	2	3	Failed	No, Reject
Timber on solid UHMW	L	4	4	5	NA	No, Reject
Timber on M-shaped UHMW	L	5	4	5	NA	No, Reject
Super Panel	L	6	1	4	NA	No, Reject
UHMW	L	NA	5	NA	NA	No, Reject
Uncoated UHMW	L	NA	6	2	NA	No, Reject
Prodeck 4	F	NA	NA	NA	Failed	No, Reject
Concrete-filled metal grid	F	NA	NA	NA	Failed	Weight is a problem, and traction will be an issue as the concrete abrades below the metal grid.
Note: F stands for field; L stands for laboratory						

We tested five materials for mechanical properties, dynamic and static coefficients of friction, and resistance to tire chain damage. The materials tested were untreated Douglas Fir #2, Cobra X (polyethylene that was in service for 14 years), Super Panel, a fiberglass reinforced plastics (FRP) composite supplied by Creative Pultrusions, Inc., UHMW (ultra-high molecular weight) polyethylene supplied by Ultra Poly, Inc., and Transonite supplied by Martin Marietta. The material-property test results show:

Mechanical properties

- The most flexible material was Cobra X.
- The stiffest and most brittle material was the Super Panel FRP composite.

Traction

- Super Panel was the best material.
- Wood was the worst material and the UHMW products were nearly as bad.

Chain damage

- Cobra X suffered the least damage.
- Wood suffered the most damage.

We conducted laboratory structural durability tests to evaluate possible wearing-surface systems for the Yukon River Bridge. The systems studied included timber on timber, timber on UHMW, timber on M-shaped UHMW, Transonite, Super Panel, and Cobra X.

Test results revealed the following:

- Timber/timber – Loads acting on a two-layer timber system (one longitudinal layer and one transverse layer, lagged together) carry the loads by one layer carrying more than its share. This reduces the life of the two-layer timber composite.
- Timber/UHMW – A timber running board lagged to UHMW is not a good solution in that the boards are stiffer than the UHMW. Subsequently, more load is carried by timbers than by the UHMW. Further, using lag bolts is not an option. Once fastened, lag bolts cannot be removed without producing damage.
- Timber/M-shaped UHMW – The timber running board carried load quicker than timber and the solid UHMW. The bottom layer was significantly more flexible, causing the timbers to carry more of the load earlier, which resulted in the running boards cracking sooner than the timber/UHMW sample. The other issues are the same as stated above.
- Transonite – In the laboratory, this product outperformed most of the others. In the field, the traction surface was badly damaged after the first year. Based on material tests, two issues were revealed: (1) The traction surface for this panel is

significantly stiffer than the substrate, and will likely experience a brittle failure in the field. (2) Compression of the inner fiberglass columns may be a cause for concern.

- Super Panel – The FRP composite is too stiff and brittle for this application.
- Cobra X – This product has the lowest stiffness and in this case is the best choice for this application.

An acceptable wearing surface should be nearly as flexible as the Cobra X. It should be tough and resistant to chain damage, and the dynamic coefficients of friction should be at least 0.7 when dry and no less than 0.5 when icy.

Any future wearing surface involving a composite should have the more flexible layer on top. The traction coat should not be stiffer than the support layers; otherwise, it will likely fail prematurely.

Recommendations

Given that timber is not a cost-effective wearing surface, the following suggestions are presented for consideration:

We recommend that a wearing surface similar to Cobra X be developed for the Yukon River Bridge. The patent for Cobra X ran out in November 2007. Therefore, other manufactures should be able to provide this or similar products. We do not recommend that it be fastened to a timber underlayment, but rather fastened directly to the deck. The wearing surface should be designed to (a) rest on an orthotropic steel deck, (b) accommodate steel deck splice plates, and (c) resist wear and damage from tire chains. The dry dynamic coefficient of friction should exceed 0.7 and 0.5 when wet.

We recommend that a fastening system between wearing surface and steel deck be evaluated in the laboratory prior to installation. The connection system should be tested for static forces, dynamic forces, and thermal strains. Some composites appear to stiffen with a drop in temperature. Any wearing surface should be looked at for compatibility with an orthotropic steel deck and should be evaluated analytically and experimentally in the laboratory. Evaluation should be followed by installation and monitoring of test samples installed on a 6% grade on the Dalton Highway, though it will not be necessary to put test samples on the bridge if a condition similar to a 6% grade can be found that is used by trucks with tire chains.

Our studies for structural durability should be sufficient to address structural compatibility. The remaining questions to be answered are (a) is the traction of a given surface coating sufficient for use on a 6% grade, and (b) will the wearing surface resist damage from tire chains.

1. The outcome of this research shows that any wearing surface that is proposed for the Yukon River Bridge should meet the following criteria:
    a. It should be less than 30 psf.
    b. If any two-layer wearing surface is proposed, the top layer should be more flexible than the bottom layer.
    c. Surface traction coatings should be more flexible than the support system, and should be resistant to gouges and abrasion.
    d. The system should be thermally compatible with the orthotropic steel deck, or if not, connections to the steel deck should allow it to breath.
    e. If possible, the wearing surface should be modular, easy to remove and replace.

2. We know that Cobra X was successful; thus, we suggest requesting that a similar system be manufactured for testing.
3. There are companies that provide rubber grade crossings for railroads. These companies may be willing to manufacture a custom product for this structure. Based on the literature, it appears that this may be a viable option.
4. The U.S. Navy has awarded numerous research contracts for the development of gouge-resistant tractable surfaces, needed for takeoffs and landings on aircraft carriers.
5. Before installing a wearing surface on the bridge, we suggest it be tested in the laboratory for traction and resistance to damage by tire chains.
6. We recommend that AKDOT&PF prepares a competitive proposal, requesting design and manufacture of alternate wearing surfaces that may be installed on a section of road where trucks typically use tire chains. The grade should be 6% or greater.
    a. Test panels should be first tested in the laboratory for traction and resistance to chain damage. If the laboratory test results are encouraging, then a field test would be appropriate.
    b. Installation of test sections somewhere near Fairbanks on the Dalton Highway should be sufficient.
        i. Installation on the Yukon River Bridge should not be necessary, because we understand the structural-durability issues for this bridge.
        ii. We need to know if the traction coat on a given wearing surface holds up to traffic and weather.

CHAPTER 2 – INTRODUCTION

This study evaluates alternative wearing-surface materials that may be applied to the orthotropic steel deck (6% grade) on the Yukon River Bridge. The material must be lightweight (no more than 30 psf), durable, and ductile, and have a surface that will provide winter traction. In addition, it must perform well for a number of years, exposed to winter temperatures that may be below -60°F and to trucks that cross with tire chains (see Figures 2.1 and 2.2).

Figure 2.1 Yukon River Bridge in summer.

Figure 2.2 Yukon River Bridge in winter looking up the 6% grade.

A series of laboratory tests were developed specifically for the project to measure traction, surface damage, and structural flexibility and strength for each wearing surface. Two types of tests were conducted, each by a different researcher:

1. Structural durability at 70°F and at -11°F
   - Mechanical properties of the panel materials
   - Panel stiffness
   - Panel strength
2. Traction and chain damage at 70°F, 20°F, and -20°F
   - Dry static and dynamic friction tests
   - Wet static and dynamic friction tests
   - Damage measurements due to chains under rolling and lash

Pavement traction was measured in the laboratory for an aged section of pavement. These results were compared with field traction measurements for asphalt pavement that had been in service more than ten years at the Duckering Building parking lot on the UAF campus.

Problem Definition

A sustainable wearing surface is needed for the Yukon River Bridge, located about 50 mi (80 km) north of Fairbanks. The bridge has two lanes that are on a 6% downgrade from south to north. The bridge loads are primarily trucks and the oil pipeline. The superstructure is an orthotropic steel deck, supported by transverse beams spaced at 15 ft on center that transfer loads to two closed steel box girders that cross the river with six spans.

The bridge deck is 30 ft wide by 2295 ft long. The structure was opened to traffic in 1976, and at the time, a 5-in. (127 mm) two-layer temporary timber wearing surface was placed over the steel deck. Because of the steep grade, trucks typically use chains, and this has caused several problems. Chains tend to plane the timber deck, reducing thickness and traction. The timber deteriorates rapidly under severe climate and loads.

Over a 30-year period, the temporary timber solution has been replaced four times. Between replacements, significant maintenance expenditures have been required to keep the deck in satisfactory operating condition. The wearing surface was replaced in 1981, 1992, 1999, and again in 2007.

In 1992, AKDOT&PF installed Cobra X as an experimental feature on a small portion of the bridge. Cobra X is a high-density polyethylene that was manufactured for use at railroad crossings. The company that manufactured the product is no longer in business, and the product is no longer available.

In the summer of 2005, two different reinforced fiberglass panels were installed as test panels. Martin Marietta supplied one product and Bedford Plastics provided the other. AKDOT&PF hoped to have sufficient information from the experimental feature program to make a choice between wearing-surface alternatives. Both panels have grit manufactured in the top surface. These products are manufactured with an inner stiff plate over an inner cellular system. Both products are patented, and details were unavailable.

Initially, both the Martin Marietta product and the Bedford Plastics product were to be studied in this research. Prior to the start of our research, however, Bedford Plastics withdrew their product from the market. The product is no longer available, and was not made a part of this study.

We were looking for a wearing surface that meets these parameters:

An ideal wearing surface for the Yukon River Bridge must be flexible, durable, ductile, and lightweight. It must also have sufficient traction to accommodate winter truck chains on a 6% grade. Connections between the wearing surface and the orthotropic steel deck should be designed to accommodate differential thermal strains between the wearing surface and the orthotropic steel deck (Hulsey et.al, 1999, 2002 and Appendix D).

Research Objectives

The objective of this research was to determine by comparative evaluation the best choice of available wearing surfaces for use on the Yukon River Bridge.

Five different wearing surfaces were supplied for this study:

- Transonite, fiber-reinforced plastic panels, supplied by Martin Marietta Composites:
    - One 4 ft × 4 ft panel
    - Five 18 in. × 24 in. panels with top surface grit for traction
- UHMW, ultra high-density polyethylene, supplied by Ultra Poly, Inc.:
    - One 4 ft × 4 ft solid panel
    - One 4 ft × 4 ft M-shaped panel
    - Five 18 in. × 24 in. solid panels with top surface grit for traction
- Super Panel, fiber-reinforced polymer (FRP), was supplied by Creative Pultrusions, Inc. and Compositech, Inc. (a local contractor).
- Timber, supplied by AKDOT&PF:

- Five 2½ in. × 12 in. × 8 ft timbers that are of the same type as previously used on the bridge. These timbers were assembled into a 4 ft × 4 ft flexural test panel and 2½ in. × 12 in. × 12 ft boards for traction and chain damage tests.

- Cobra X, a high-density polyethylene panel, removed from the Yukon River Bridge by AKDOT&PF in the summer of 2006. This panel was subjected to service conditions from 1992 to 2006 (14 years).

Except for Cobra X and the Super Panel, we conducted structural durability tests on 4 ft by 4 ft panels. Since Cobra X and the Super Panel were not 4 ft wide, the durability tests conducted on these samples involved one-way plate action tests.

In the laboratory, we conducted a series of tests for traction and surface damage caused by tire chains on 18 in. by 24 in. test samples. We conducted traction and chain damage studies on Cobra X after structural durability tests were complete; then an 18 in. by 24 in. sample was cut from the panel. Composite structural durability was tested on the following systems:

- Timber on timber system, see Figure 2.3 (new).
- Transonite, see Figure 2.4 (new).
- Timber on solid UHMW, see Figure 2.5 (new).
- Timber on M-shaped UHMW, see Figure 2.6 (new).
- Super Panel, see Figure 2.7 (new).
- Cobra X, see Figures 2.8 and 2.9 (14 years of service on the bridge).

Figure 2.3 Timber on timber composite (rough sawn, two layers of 2½ in. by 12 in.

Figure 2.4 Transonite by Martin Marietta (side view).

Figure 2.5 Timber driving surface lagged to UHMW solid.

Figure 2.6 Timber driving surface lagged to UHMW M-shape.

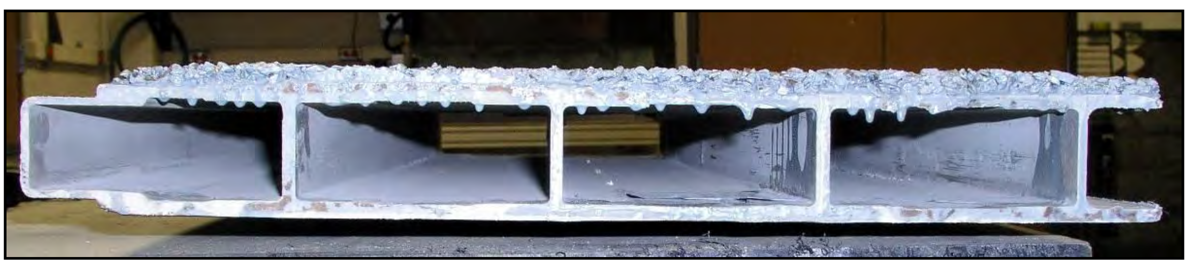

Figure 2.7 Super Panel (side view).

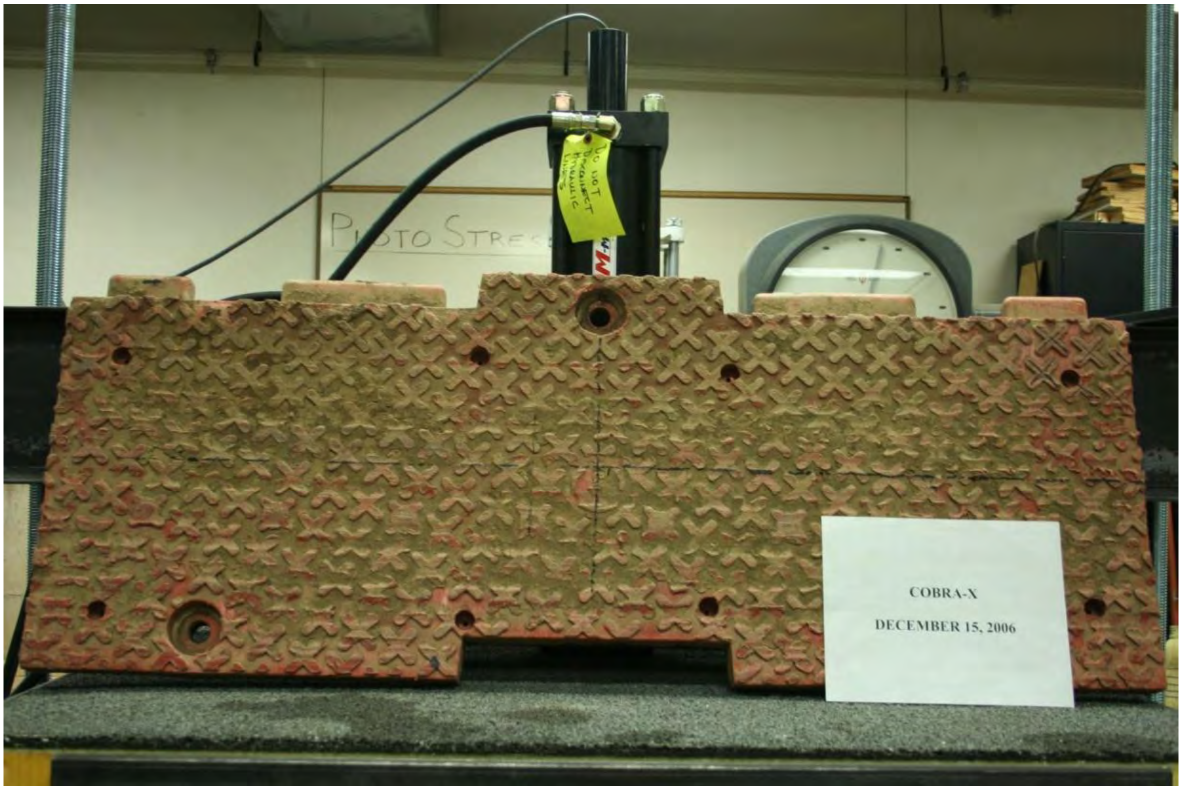

Figure 2.8 Cobra X top surface, typical bridge-deck panel.

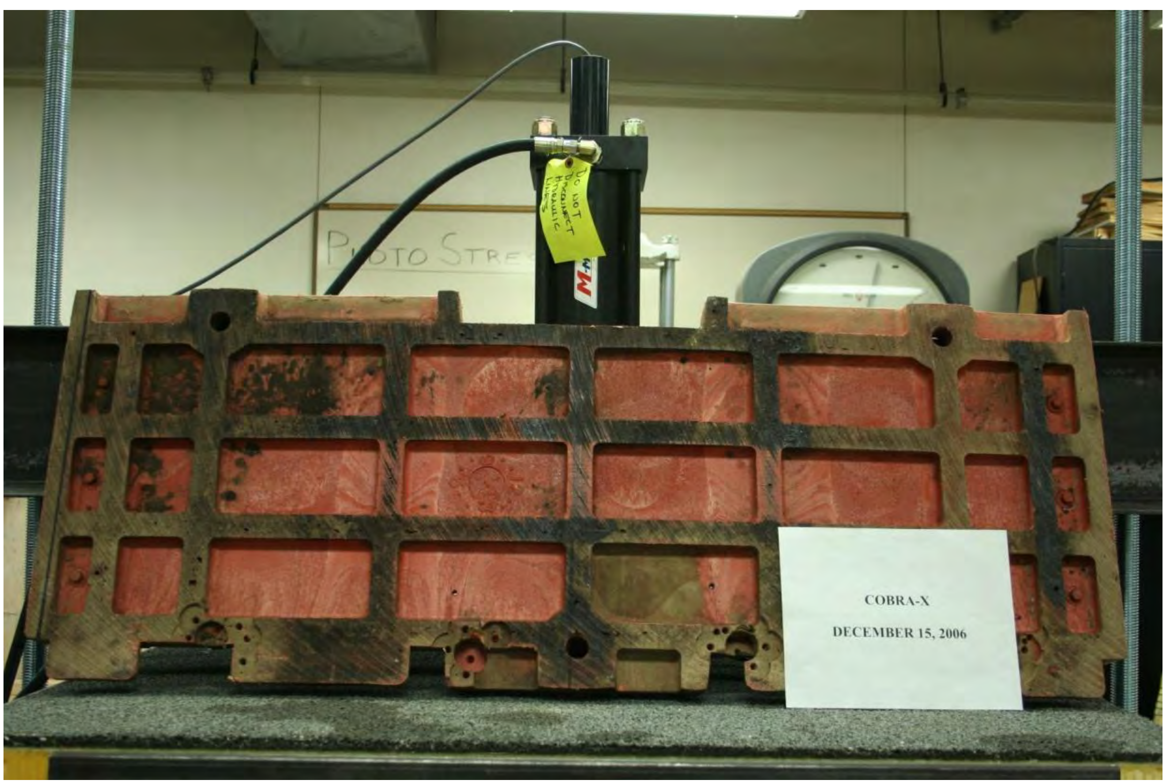

Figure 2.9 Cobra X bottom side, typical bridge-deck panel.

Before testing, we expanded the study to include a field component. This involved inspecting the condition of the bridge's wearing surfaces. One year later, after the laboratory tests were completed, we measured traction of the surfaces at the bridge and performed a follow-up inspection of the wearing surfaces on this structure. Field measurements for traction were obtained using a Grip Tester (manufactured by Findlay Irvine).

This study addressed three issues for five different types of alternative wearing-surface solutions:

1. Structural durability
2. Traction (laboratory and field), and wear and damage caused by truck tire chains
3. Field performance (inspection of wearing surfaces at the bridge site)

Structural Durability

One part of this study focused on the structural durability for alternate wearing-surface systems. This was done by Zachery Jerla as part of the requirements for a master's degree in Civil Engineering. He tested five experimental bridge-deck panels at room temperature and cold temperature, and evaluated structural behavior and stiffness. His studies provided a basis for ranking structural durability and applicability of these panels to the Yukon River Bridge. A design procedure for analyzing future wearing surfaces is available for study (Jerla, 2008).

Wearing-Surface Traction and Damage by Tire Chains

Part of this study focused on evaluating surface traction. We also conducted laboratory tests to determine the possible extent of damage caused by tire chains rolling, lashing, or dragging (applying breaks and stopping) over the surface. This part of the study was conducted by Wilhelm Muench as part of the requirements for a master's degree in Civil

Engineering. Initially, Muench's work focused on developing test equipment and test procedures that would provide a reliable scientific method for finding the coefficient of friction for a wearing surface. In addition, he developed test procedures and measurement methods for assessing the amount of damage caused by tire chains. Once the equipment was developed and tested, tests for traction and wear and chain damage were measured. Test results for traction and wear and chain damage were used as a basis for ranking the various wearing surfaces for possible use on the Yukon River Bridge.

CHAPTER 3 – TEST RESULTS

Structural Durability

Five bridge-deck wearing surfaces were investigated experimentally, theoretically, and by finite element analysis (Jerla, 2008). Two experimental panels were FRP (fiber-reinforced plastics) composites. The other three were timber composites manufactured in the laboratory by Jerla. The FRP composites were Transonite and Super Panel (see Figure 3.1).

Transonite by Martin Marietta Composites: This product is a pultruded 3-D reinforced composite “sandwich” that consists of FRP laminates and a foam core. The top and bottom face skins are supported by and tied together with through-thickness fibers.

Super Panel by Creative Pultrusions, Inc.: This was a custom floor panel made for use on the North Slope. The FRP product was made to form a cellular composite floor panel. The remaining three panels were constructed and instrumentated by Jerla to give a two-part jointed system.

The remaining three systems were manufactured to give a two-part jointed system. Once assembled, it was instrumentated using strain gauges and displacement transducers. Each of the manufactured test panels were 4 ft square and 5 in. thick. The panels were timber on timber, timber on solid UHMW, and timber on M-shaped UHMW (see Figure 3.2).

Timber on timber: A 5-in.-thick two-layer timber system that was fastened together with 5/16 in. lag bolts. The assembly was produced to simulate the temporary wood deck that has been used since 1976.

Timber on solid UHMW: A 5-in.-thick two-layer system that was fastened together with 5/16 in. lag bolts. The top had four 2½-in.-thick 12 in. boards fastened to a solid 4-ft-square by 2½-in.-thick plate of UHMW.

Timber on M-shaped UHMW: A 5-in.-thick two-layer system that was fastened together with 5/16 in. lag bolts. The top had four 2½-in.-thick 12 in. boards fastened to a 4-ft-square corrugated plate of UHMW.

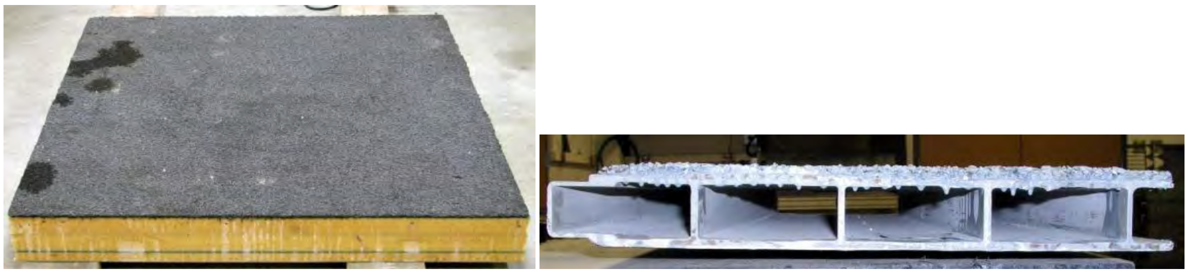

Figure 3.1 Transonite (left) and Super Panel (right).

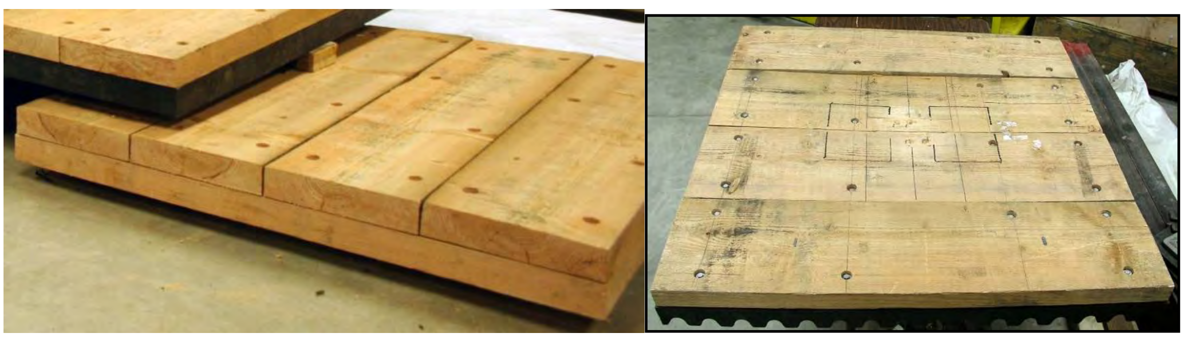

Figure 3.2 Timber on timber and timber on solid UHMW (left); timber on M-shaped UHMW (right).

These panels were tested in a load frame to 16,000 lb. During the test, displacements and strains were monitored for each 4-ft-square test panel. A typical test is illustrated in Figure 3.3.

Figure 3.3 Static test for the timber on UHMW test panel.

We performed panel tests and material tests. Material tests were conducted in accordance with ASTM standards using the UAF MTS 55K machine. We used the material properties and the finite element method to evaluate panel behavior. These analytical results were compared with the experimental results. Some of the material properties obtained by testing in the UAF laboratories are provided in Tables 3.1 to 3.3.

Table 3.1 Tensile Properties

Material	Tensile Properties		
	Maximum Tensile Stress (psi)	Tensile Strain at Max. Stress (με)	Tensile Modulus of Elasticity (psi)
UHMW Polyethylene	4,250	150,758	118,000

Table 3.2 Flexural Properties

Material	Flexural Properties		
	Maximum Flexural Stress (psi)	Flexural Strain at Max. Stress (με)	Flexural Modulus of Elasticity (ksi)
Transonite	645	3,390	253
Douglas Fir	11,066	9,697	2,021
UHMW Polyethylene	4,758	50,758	151
Super Panel	12,801	27,524	365

Table 3.3 Compressive Properties

Material	Compressive Properties		
	Maximum Compressive Stress (psi)	Compressive Strain at Max. Stress (με)	Compressive Modulus of Elasticity (psi)
Transonite	355	10,584	26,842
Douglas Fir Perpendicular To Grain	607	25,576	52,660
Douglas Fir Parallel To Grain	7,672	8,814	856,380
UHMW Polyethylene (Loading Rate 0.05 in./min)	1,457	30,750	54,147
UHMW Polyethylene (Loading Rate 0.25 in./min)	3,469	135,506	63,345
Super Panel	15,760	52,010	140,900

The timber composite panels were 4 ft square, and when tested, these panels were simply supported around the perimeter. Tests were performed two ways: One test was performed with the duals parallel to the running boards; the other test was performed with the duals transverse to the running boards. Load was applied with a computerized ram. Load, strains, and displacements were monitored with a data acquisition system. Timber joints and distribution of load to the various parts is complex; therefore, we developed an equivalent stiffness for these panels (see Table 3.4). Test results revealed that the timber on solid UHMW stiffened considerably when it was exposed to cold temperatures.

Table 3.4 Stiffness Comparisons for All Five Panels

Experimental Panel	Room-Temperature Test, Longitudinal Orientation, k_{room} (lb/in.)	Room-Temperature Test, Transverse Orientation, k (lb/in.)	Cold-Temperature Test, Longitudinal Orientation, k_{cold} (lb/in.)	k_{cold}/k_{room}
Timber/Timber	44,422	46,420	48,439	1.09
Transonite	29,657	28,519	30,691	1.03
Super Panel	26,634	27,922	28,989	1.09
Timber on Solid UHMW	28,256	26,455	34,816	1.23
Timber on M-shaped UHMW	20,520	18,490	22,861	1.11

After panels were tested at room temperature and cold temperature, they were tested to failure. Once failed, materials needed for material testing were obtained and tested. The load deflections for these panel tests are shown in Figure 3.4.

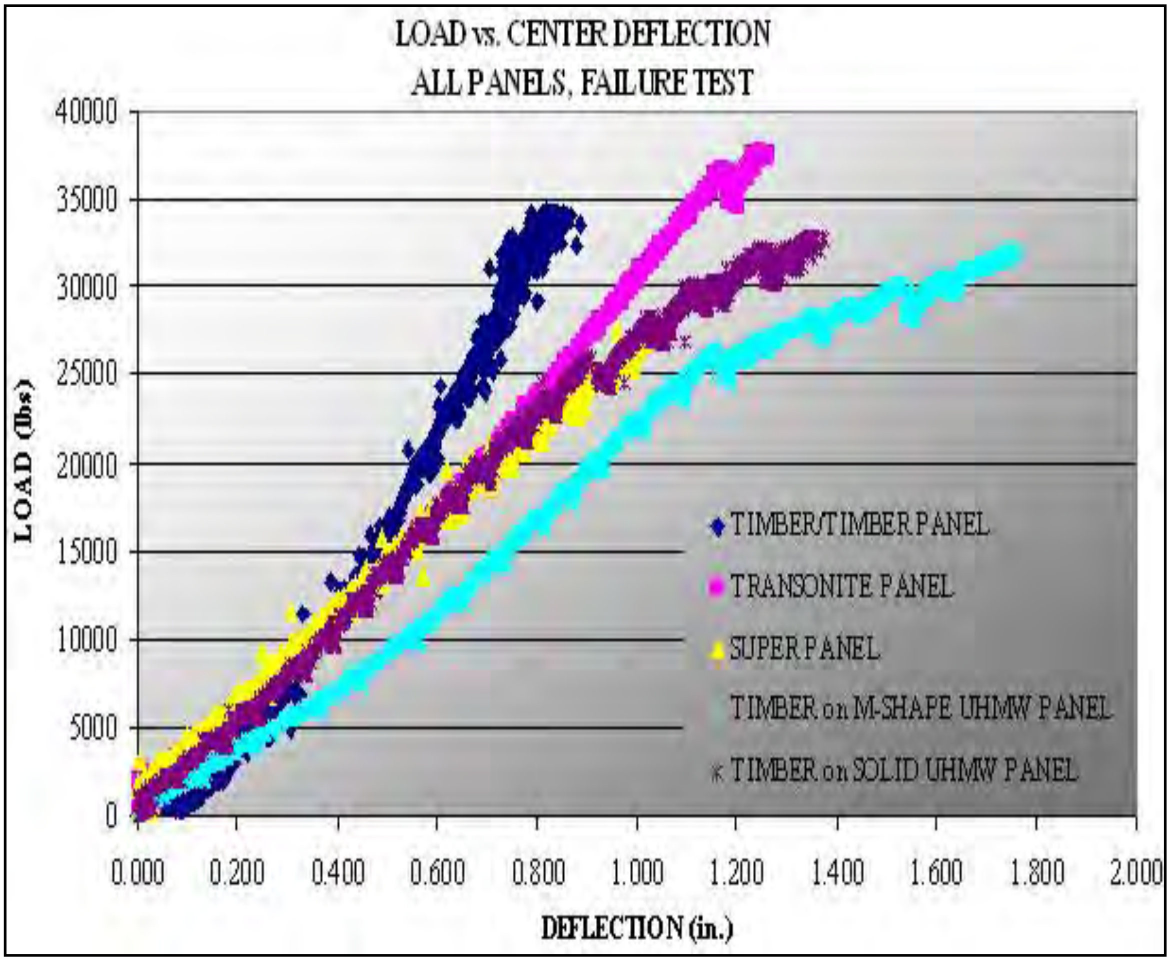

Figure 3.4 Laboratory-tested stiffness comparison for wearing-surface systems

General Design Information

Tables 3.5 and 3.6 provide a summary of experimental material properties along with the published material properties for the test panels.

Table 3.5 Experimental Material Properties

Material	Material Properties			
	Flexural Modulus of Elasticity (ksi)	Maximum Tensile Stress (psi)	Maximum Compressive Stress (psi)	Maximum Flexural Stress (psi)
Transonite	253	Not Available	355	645
Douglas Fir	2,021	Not Available	7,672[a]	11,066
UHMW Polyethylene	151	4,250	3,469	4,758
Super Panel	254	Not Available	15,760	12,801

a. Maximum compressive stress for Douglas Fir was tested parallel to grain.

Table 3.6 Published Material Properties

Material	Material Properties			
	Flexural Modulus of Elasticity (ksi)	Maximum Tensile Stress (psi)	Maximum Compressive Stress (psi)	Maximum Flexural Stress (psi)
Transonite	Not Available	25,000[b] to 60,000[b]	400 to 1,470	Not Available
Douglas Fir	1,613	7,540[a]	3,610[a]	Not Available
UHMW Polyethylene	120	6,000	Not Available	Not Available
Super Panel	3,500	Not Available	26,213	33,000

a. Maximum compressive stress for Douglas Fir tested parallel to grain.
b. Tensile stress for the FRP sheets of the Transonite panel.

All the test panels except Cobra X consisted of a complex composite. Two were complex FRP composites and the others were either a two-layer timber on timber or timber on UHMW. Experimental, theoretical, and finite element analysis led to the development of a flexural rigidity value and stiffness reduction ratios. A flexural rigidity value should provide the bridge engineer with the tool to access panel performance. If using rigidity, material properties and internal geometry of the panel structure for the wearing surface may be neglected. A stiffness-reduction ratio reflects loss of stiffness due to jointing. Table 3.7 shows the flexural rigidity and the corresponding stiffness-reduction ratio for these panels.

Table 3.7 Flexural Rigidity and Stiffness-Reduction Ratio for Experimental Panels

Experimental Panel	Theoretical Flexural Rigidity ($in.^2 \cdot kips$)	Stiffness Reduction Ratio, k_{ratio}
Timber/Timber	436	1.78
Timber on Solid UHMW	350	1.67
Transonite	345	1.22
Timber on M-shaped UHMW	288	Not Available
Super Panel	29,401	Not Available
Cobra X Panel	640	Not Available

Tables 3.5 through 3.7 provide material properties for wearing surfaces that can be designed as solid homogenous systems, FRP composite bridge decks, and two-part jointed bridge decks. Effects due to cold temperatures are shown in Table 3.8. The stiffness at -11°F was stiffer than at room temperature.

Table 3.8 Room and Cold Panel Stiffness Values

Experimental Panel	Room-Temperature Test, Longitudinal Orientation, k_{room} (lb/in.)	Cold-Temperature Test, Longitudinal Orientation, k_{cold} (lb/in.)
Timber/Timber	44,422	48,439
Transonite	29,657	30,691
Super Panel	26,634	28,989
Timber on Solid UHMW	28,256	34,816
Timber on M-shaped UHMW	20,520	22,861

Material properties and stiffness values shown in Tables 3.5 through 3.8 are available to account for critical states of stress and strain in the wearing surface. A detailed design procedure is provided by Jerla (2008). A wearing surface fastened to the orthotropic steel deck may act compositely. In this case, stresses tend to occur at locations of large local positive and negative curvatures in the steel deck. Three zones on a typical orthotropic steel deck have indicated areas of high stress (Wolchuk, 2001). The first is near the transverse beams (see Figure 3.5).

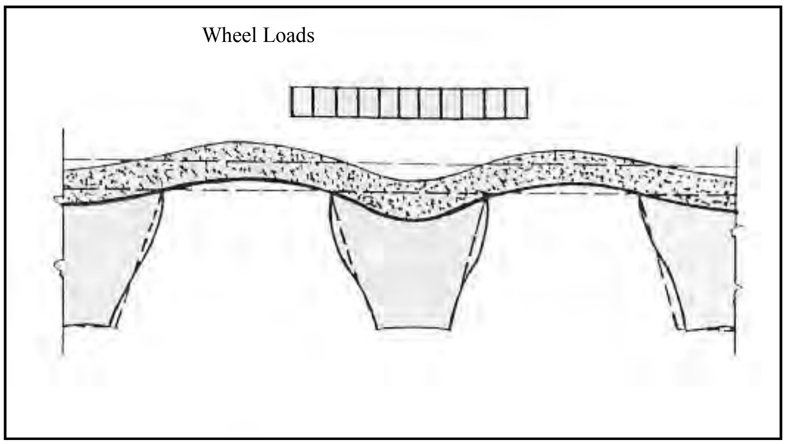

Figure 3.5 Local deformations near the transverse floor beams (Wolchuk, 2001).

At mid span between floor beams, the effect of closed rib deflections tends to increase the magnitude of stress; this area is shown in Figure 3.7.

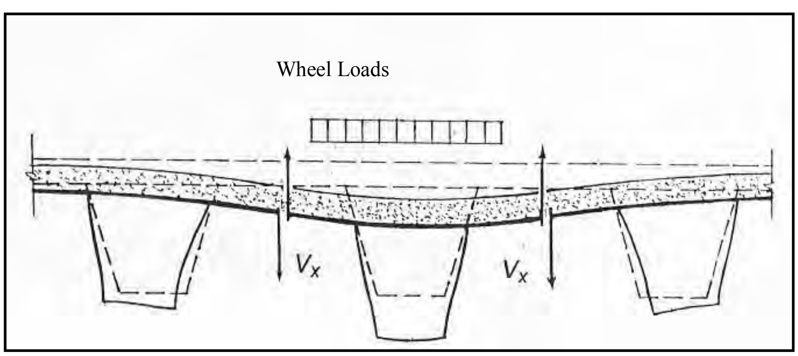

Figure 3.6 Local deformations between floor beams (Wolchuk, 2001).

The state of stress over the longitudinal girder web may be excessive, as this location is where large local plate curvatures and states of stress occur (see Figure 3.7).

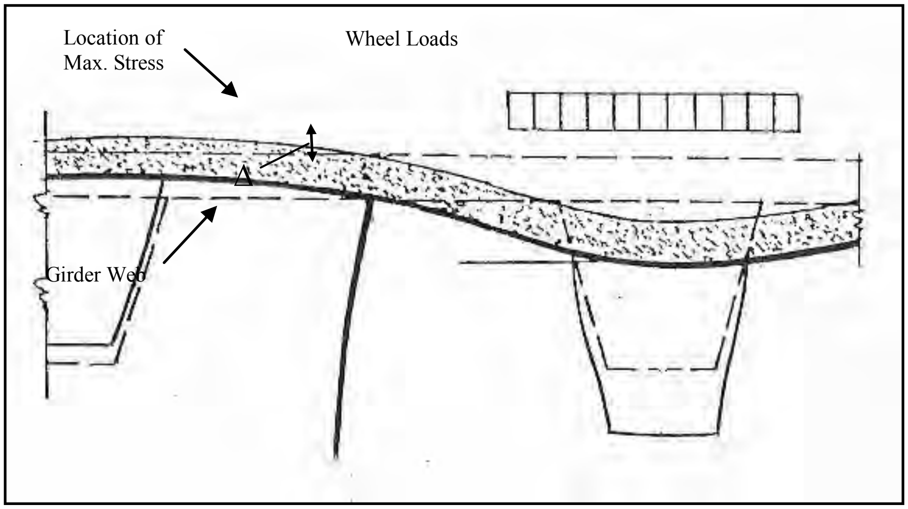

Figure 3.7 Local deformations near longitudinal girders (Wolchuk, 2001).

Fatigue cracking will occur in any one of these zones if tensile stress in the wearing surface exceeds the fatigue strength of the surfacing (Wolchuk, 2001). Previous research for this structure showed that maximum static strains recorded for the orthotropic steel deck of the Yukon River Bridge were 139.1 $\mu\varepsilon$ (Hulsey et al., 1995). If the analysis of the composite superstructure shows strains within the range of 139.1 $\mu\varepsilon$, the wearing surface should be adequate for the Yukon River Bridge.

We ranked the five experimental bridge decks that were evaluated for this study, based on structural durability. Factors considered in the ranking procedure were stiffness, susceptibility to cold temperatures, behavior during testing, and material properties. Table 3.9 shows the ranking, advantages, and disadvantages for each panel.

Table 3.9 Structural Rankings for the Test Panels

Test Panel	Ranking	Advantages	Disadvantages
Transonite	1	The panel was ranked higher than others because: a) it is lighter than the other panels; b) it is more flexible; c) it was the only panel with a small increase in stiffness at cold temperatures; and d) the strength of this panel was higher than others (it did not fail).	Issues: a) During material property compression testing, specimens failed due to crushing, and lateral instability existed at very low compressive tests; b) during flexural tests, the traction coating delaminated in the presence of excessive deflections; and c) as a wearing surface, local material failure may be a problem.
Timber/ Timber	2	a) It is light weight; b) only small changes occurred due to cold temperatures; and c) it performed well when tested to failure; i.e., load-deflection and load-strain curves were similar to that of the Transonite panel.	This is a two-layer jointed timber wearing surface. The top layer is perpendicular to the second, and these layers are 3x12s with ¼″ joint between. Issues: a) Directional stiffness of one layer is significantly different from the other; b) because of jointing, a high stiffness reduction ratio was calculated; and c) ―Failure” tests showed that planks in the bottom layer prematurely cracked, causing load to be carried by the upper planks.
Timber on Solid UHMW	3	a) Only the top timber layer was jointed and this minimized loss of stiffness; b) UHMW has a low modulus that results in a low flexural rigidity, making it an ideal material for fastening to orthotropic steel decks.	Issues: a) Voids and cracks present in the timber running planks and the connection from running planks to the UHMW polyethylene cause a loss in stiffness; b) mismatch of material properties caused timber planks to crack; this would be a concern in the field; c) thermal strain is a concern; d) the panel was sensitive to cold temperatures; and e) once fastened with lag bolts, it is permanently attached; this could be a maintenance issue.
Timber on M-shaped UHMW	4	This has the same advantages as the timber on solid UHMW and in addition, its weight is reduced due to the removed UHMW geometry.	Issues: a) The UHMW is significantly more flexible than the solid, and this caused the timber running planks to crack under lower loads; b) through e) are the same as above; and f) the panel stiffened under cold temperatures.
Super Panel	5	a) The Super Panel has both high strength and high stiffness values; and b) material properties were only slightly affected by cold temperatures.	Issues: a) It is very stiff and this may be a problem, as it will not flex as needed to accommodate the flexibility of the orthotropic steel deck; b) very little ductile behavior; ―Material” test results show that the Super Panel fails suddenly; and c) during ―Failure” tests, the web-flange intersection fractured. Fractures seen on the Bedford Prodeck 4 test panels were similar to those seen on the Bridge.

Traction

Friction coefficients were consistent on most samples (see Table 3.10). The Transonite sample (supplied by Martin Marietta) and the UHMW sample (supplied by Ultra Poly) lost a small amount of loosely bonded surface aggregate during these tests. Frictional coefficients for wood appeared high, but the wood was rough-sawn and in good condition—not aged bridge planks. The tire moved smoothly over the surface on all but the wet wood samples, where the tire went from a slip-to-stick condition; therefore, only one reading could be obtained for dynamic friction on wet wood. A typical traction test is shown in Figure 3.8.

Table 3.10 Traction Test Results at 70°F (20°C)

Condition/sample	# of Samples	Average	Standard Deviation	95% Confidence Interval
Dry Dynamic				
Cobra X	4	0.58	0.01	0.54 to 0.62
Transonite	3	0.62	0.02	0.55 to 0.70
UHMW	3	0.54	0.02	0.49 to 0.59
Uncoated UHMW	3	0.50	0.05	0.33 to 0.67
Wood	3	0.54	0.00	0.53 to 0.55
Super Panel	4	0.66	0.03	0.58 to 0.75
Wet Dynamic				
Cobra X	4	0.45	0.02	0.39 to 0.51
Transonite	3	0.63	0.01	0.60 to 0.66
UHMW	3	0.55	0.02	0.50 to 0.60
Uncoated UHMW	4	0.47	0.01	0.43 to 0.51
Wood	1	0.61	NA	NA
Super Panel	4	0.70	0.01	0.66 to 0.74
Dry Static				
Cobra X	4	0.65	0.02	0.59 to 0.70
Transonite	3	0.67	0.03	0.57 to 0.77
UHMW	3	0.56	0.01	0.52 to 0.60
Uncoated UHMW	3	0.55	0.07	0.31 to 0.79
Wood	3	0.58	0.01	0.56 to 0.60
Super Panel	4	0.76	0.03	0.68 to 0.83
Wet Static				
Cobra X	4	0.52	0.02	0.46 to 0.58
Transonite	3	0.69	0.01	0.67 to 0.70
UHMW	3	0.57	0.02	0.50 to 0.63
Uncoated UHMW	4	0.50	0.01	0.48 to 0.53
Wood	3	0.64	0.02	0.59 to 0.69
Super Panel	4	0.75	0.01	0.73 to 0.78

Figure 3.8 Typical traction test.

Additionally, laboratory friction coefficients (traction) were measured for various exposures. For example, we measured friction coefficients at 70°F (20°C) for dry and wet conditions. We also measured the friction coefficients at 20°F (-6.7°C), and -20°F (-28.9°C) for dry, wet, and icy conditions. Values for a stalled vehicle that is stopped on the bridge (static friction) or for a moving vehicle (dynamic friction) are provided in Table 3.11.

The Compositech panel has the highest coefficient of friction of all samples tested. The dynamic friction coefficient for wood varied from 0.38 to 0.61 for temperatures of 70°F and -20°F. However, when the temperature is 20°F and icy, the friction coefficient is approximately zero (0.05). Other than wood, friction coefficients for icy conditions are about 50% of those for a dry surface at -20°F. In all cases, traction for the UHMW did not seem to vary with surface moisture.

Table 3.11 Laboratory Traction Values for Different Wearing Surfaces

	70°F (20°C)		20°F (-6.7°C)		-20°F(-28.9°C)	
Sample	Dry	Wet	Dry	Icy	Dry	Icy
Dynamic Friction:						
Cobra X	0.58	0.45	0.65	0.53	0.55	0.33
Transonite	0.62	0.63	0.75	0.51	0.63	0.29
UHMW	0.54	0.55	0.60	0.25	0.48	0.12
Uncoated UHMW	0.50	0.47	0.37	0.13	0.37	0.18
Wood	0.54	0.61	0.69	0.05	0.47	0.38
Super Panel	0.66	0.70	0.78	0.65	0.70	0.34
Asphalt Concrete	0.59	0.61	NT	NT	NT	NT
Static Friction:						
Cobra X	0.65	0.52	0.77	0.61	0.64	0.43
Transonite	0.67	0.69	0.82	0.57	0.69	0.37
UHMW	0.56	0.57	0.62	0.28	0.51	0.19
Uncoated UHMW	0.55	0.50	0.47	0.25	0.44	0.30
Wood	0.58	0.64	0.71	0.21	0.53	0.41
Super Panel	0.76	0.75	0.89	0.60	0.75	0.47
Asphalt Concrete	0.62	0.63	NT	NT	NT	NT
NT - Not tested						

Chain Damage Tests

Prior to testing, we measured the surface of each sample by using a rolling linear variable displacement transducer (LVDT). This procedure was used to define the surface topography prior to testing. The sample was placed under the wheel and, for either dragging, rolling or lashing, was implemented for a given number of cycles. After a number of cycles, we removed the sample from the test frame and measured the surface and the surface topography once again to evaluate the level of damage. We used these beginning and ending conditions to evaluate surface damage.

Wear measurements are taken by profiling the surface before and after testing. The surface of the panel is in contact with a disk 3/4 in. (19.05 mm) in diameter and 3/8 in. (9.53 mm) wide. The position of the disk is recorded in the horizontal and vertical directions as it is moved over the panel in the long direction of the panel. Values listed are for the largest change in surface as recorded by the profiler. Rolling tests failed to show significant damage. This was due to the tendency of the tire chains to cause highly localized damage to the panel in the form of depressions about 5/16 in. (8 mm) in diameter. The chains then returned to these damaged locations on subsequent cycles of the test, resulting in panel depressions in the shape of the chain, and little increase in damage on subsequent cycles. The profile disk will not enter these small depressions.

Because of the problem just mentioned, we determined rolling damage on the panels with a depth gage at random locations to find an average surface-depression depth. The tire was rolled over the test panel, and the depth of local damage was measured. The increase in depth of the damage minus the average depression depth was counted as depth of damage.

Rolling Damage

We conducted rolling tests for 60 cycles at 70°F and again at -20°F. The length of test approximated a year of rolling wear for the Yukon River Bridge deck. The depth of damage was significantly higher for wood than for any other remaining wearing surfaces that were tested (see Table 3.12). Transonite and UHMW samples lost a small amount of surface aggregate.

Table 3.12 Wearing Surfaces Ranked by the Least Rolling Damage

		Damage Depth (0.001 in.)	
Ranking	Surface	-20°F	70°F
1	UHMW	29.49	45.85
2	Transonite	32.63	61.99
3	Cobra X	36.59	55.27
4	Super Panel	37.56	64.69
5	Wood	130.70	121.10

Lashing Damage

We conducted a lashing-chain wear test by rotating a wheel about 1 in. above the wearing surface with a loose chain that struck the surface. The damage caused by this type of test is provided in Table 3.13.

Table 3.13 Damage by Lashing as a Function of Temperature

	Damage Depth (0.001 in.)		
Test Sample	70°F	20°F	-20°F
Cobra X	26	14	22
Transonite	39	31	47
UHMW	21	13	16
Wood	38	27	21
Super Panel	32	50	60

We ranked the panels according to their ability to resist damage by lashing. The ranking is presented in Table 3.14.

Table 3.14 Wearing Surfaces Ranked for Lashing Damage at -20°F (0.001)

Ranking	Surface	Damage (in.)
1	Wood	16
2	UHMW	21
3	Cobra X	22
4	Transonite	47
5	Super Panel	60

Dragging

Between 11 and 36 cycles were applied to the test samples when testing for dragging. Both wood and Cobra X samples showed very uneven wear during these tests. We determined wear by measuring the amount of wear within a grid; then using this grid, we determined the average amount of damage over an area (see Table 3.15). Transonite and

UHMW samples wore more evenly but only lost a small amount of surface, making accurate measurement difficult.

Table 3.15 Damage by Dragging as a Function of Temperature

Test Samples	Damage Depth (0.001 in.)		
	70°F	20°F	-20°F
Cobra X	-1	7	-5
Transonite	24	25	26
UHMW	22	11	13
Wood	20	28	13
Super Panel	15	39	28

The test samples were ranked for their ability to resist damage by dragging (see Table 3.16).

Table 3.16 Ranked Wearing Surfaces by Least Dragging Damage (0.001 in.)

Ranking	Surface	Damage
1	Cobra X	-5
2	UHMW	13
3	Wood	13
4	Transonite	26
5	Super Panel	28

Summary of Test Results

Structural Durability

Transonite – This panel had better structural durability performance in the laboratory than any other system; yet on the bridge, it performed poorly. We rejected Transonite for use as an alternative.

Super Panel – This panel was strong but brittle, and when tested in the laboratory, it failed at the web flange intersection. This product is similar to Prodeck 4, an experimental feature supplied by Bedford Plastics, Inc. Prodeck 4 displayed similar behavior, seen at the bridge site. Therefore, we rejected this material as a future alternative.

Timber/material – When two layers of jointed timbers fastened together with lag bolts are loaded, directional differences in stiffness for these layers causes one layer to carry more load than another. In the field, if boards on one layer weaken, the other board will carry more than its proportionate share of load, which will likely accelerate failure of this surfacing system. It is not advisable to place stiff running boards on a more flexible product like UHMW. Two issues occur when doing so: (1) Installing wood with lag bolts into the UHMW will likely result in a maintenance issue. Once the lag bolts are installed, it is nearly impossible to remove them; thus, replacing boards will be a problem. We found that the lag bolts must be at least 5/16 in. in diameter; otherwise, they will twist off during installation. (2) Running planks were stiffer than the UHMW, and the boards attempted to carry more load until cracking and some slippage occurred. In addition, the thermal strains for UHMW are significantly different from steel or wood; thus, a design for a fastening system would be needed to accommodate thermal change.

We evaluated analytically each wearing-surface system tested in this study, and if a similar system was at the bridge, we inspected it to determine service performance.

Traction and Chain Damage

We tested both static and dynamic traction coefficients for icy conditions in the laboratory. The top performing wearing surfaces for icy conditions at -20°F were wood, the Super Panel, and Cobra X. At icy and 20°F, the top three wearing surfaces were Transonite, Cobra X, and the Super Panel. At 20°F and icy, wood became the worst performer. The traction of wood at 20°F and icy for static friction was 0.21, and for dynamic friction, it was

0.05. Thus, a wood wearing surface will likely be a problem for a stalled vehicle on this bridge.

We tested six wearing surfaces for resistance to chain damage. The damages considered in this study were rolling damage (chained tire rolling over the wearing surface), lashing (when loose chain strikes the wearing surface), and dragging (when brakes are applied to tires with chains). The best performers were Cobra X, UHMW, and Transonite. There was more damage to wood by the tire chains than the other alternatives (see Table 3.17).

Table 3.17 Wear Damage Caused by Tire Chains at Different Temperatures

	Damage Depth (0.001 in.)								
	Lashing			Dragging			Rolling		
	70°F	20°F	-20°F	70°F	20°F	-20°F	70°F	20°F	-20°F
Cobra X	26	14	14	-1	7	-5	1	NT	13
Transonite	39	31	31	24	25	26	40	NT	14
UHMW	21	13	13	22	11	13	18	NT	12
Wood	38	27	27	20	28	13	93	NT	95
Super Panel	32	50	50	15	39	28	44	NT	19

What Wearing Surface Should Be Used?

Findings from the structural durability tests, field inspections, traction studies, and chain-damage tests suggest that Cobra X would be a good choice for wearing surface, provided there are design changes to accommodate better fastening systems and provisions for replacement of damaged panels. If possible, this or a similar product should allow for the maintenance or repair of the tractable surface coating. The traction surface should have a dynamic minimum dry friction coefficient of 0.9 and a dynamic minimum icy friction coefficient at all temperatures of 0.5.

We do not recommend wood as a viable wearing-surface choice. This is because quality is decreasing as cost is rising. Wood is vulnerable to decay, easily damaged by tire chains, and slick when icy and 20°F. Table 3.18 shows the choices.

Table 3.18 Wearing Surfacing Systems for the Yukon River Bridge

Test Panel	Possible Usage	Comments
Systems tested in the laboratory and inspected in the field		
Transonite	Rejected	This performed well in the laboratory. Yet in the field, there were installation details that allowed water to infiltrate the panel that may, through freezing and thawing, cause deterioration. Further, there was significant damage to the wearing surface the first year. There needs to be a way to repair the wearing surface. It is not advisable to have a stiff wearing surface on a softer substrate; this is asking for trouble.
Timber/ Timber	Rejected	Differences in stiffness between layers in the lower layer caused the lower layer to carry more load. This caused premature cracking. The fastening system between timber layers should allow slippage between the layers. Load carrying issues with this system causes premature cracking in the various boards when new. The jointing system should be flexible and bend, or it should provide relief so that each layer can deform with little restraint from the other.
Cobra X	Accepted with change	This system is no longer manufactured. However, it is flexible, was compatible to the Yukon River Bridge, and it performed satisfactorily for 15 years. A material like this product should be considered with the following suggestions: Instead of using a timber underlayment, it may be better to fasten it to the steel deck using a thicker system to cover splice plates and connection bolts. A wear-resistant traction surface that could be reapplied in the field between replacements would be helpful in maintaining the integrity of this bridge.
Systems tested in the laboratory; there was not one like any of these on the bridge		
Timber on Solid UHMW	Rejected	The material property mismatch caused timber planks to crack. Thermal strains are a problem. It stiffens with colder temperatures. Attachments using screws or lag bolts into the plastic are nearly permanent. This is problematic. Using a material like UHMW is not recommended because the timbers are stiffer than the underlayment. The UHMW is more flexible than the timber, which at a given strain causes the timbers to carry a larger proportion of the load.
Timber on M-shaped UHMW	Rejected	The M-shape was significantly more flexible than the solid and this caused timber running planks to crack at lower loads. Other disadvantages are the same as the solid, except that it stiffened more in cold temperatures. This has the same issues as the solid UHMW, except the level of load-causing problems to the timbers is lower.
Super Panel	Rejected	It is too stiff and too brittle for use on the Yukon River Bridge.
Systems on the bridge, but not available for testing in the laboratory		
Concrete with steel grid	Rejected	Although, this seems like a good choice and its condition after 8 years of service appeared okay, we found that the truckers avoid this section of the bridge. The traction of this section was very poor.

CHAPTER 4 – CONCLUSIONS

Except for Cobra X, none of the wearing surfaces tested in this study are acceptable for use on the Yukon River Bridge. The two-layer timber system used in the past is easily damaged by tire chains, it is slick when it is 20°F, and the product quality decreases as cost increases.

Any wearing surface proposed for this structure should weigh less than 30 psf; its traction coating should be resistant to damage by tire chains, and it should have a traction coating that is more flexible than the member is. The system should be thermally compatible, and there must be provisions for carefully connecting the system to the orthotropic steel deck.

CHAPTER 5 – LITERATURE SEARCH

The Yukon River Bridge, recognized as an outstanding civil engineering design, has been a major research project for a number of institutions throughout Alaska. The first study of the bridge was initiated shortly after the bridge was completed and opened to traffic in October 1975. The U.S. Army Cold Regions Research and Engineering Laboratory (CRREL), University of Alaska, and Alaska Department of Transportation began studying the breakup pattern of the Yukon River at the bridge and methods of measuring ice forces exerted on the bridge during the winter of 1975–76. The Federal Highway Administration developed an interest in the measurement and prediction of ice forces on highway bridges using the Yukon River Bridge as a test site. Due to low water levels during the 1978 breakup and the formation of an ice jam between the instrumented pier and shore, no ice-load data could be obtained. Despite the disappointing breakup of 1978, the Yukon River Bridge remains an outstanding site of ice-force measurements (Johnson and McFadden, 1979).

Shortly after the investigation of ice forces on the Yukon River Bridge, risk analysis criteria were established by Peratrovich and Nottingham, Inc. in 1981. The engineering consultants recognized that risk criteria for the bridge should not be simplified to the point of merely studying the material under stress due to certain loads. Concerns were expressed which involved loss of revenue, creation of energy problems, possible defense needs, and Alaska North Slope access. Alyeska Pipeline Service Company realized that most parts of the pipeline could be temporarily repaired and put back into service in a few days or less. However, when one of the largest, most difficult rivers in the world is involved, repair time could be up to one year or even longer. To complicate matters, the Yukon River Bridge is the only highway link to the Alaska North Slope. For these and other reasons, it was recommended that risk assessment be approached in two basic simultaneous ways: risk and contingency suitability, and risk and economics. Within the assessment of risk and contingency suitability, Peratrovich and Nottingham (1981) posed two questions of primary concern relevant to the present research. The questions were (1) ―Will the solution add weight that may negate the existing structure's contingency design for loss of one girder?" and (2) ―Will this solution add weight on the existing bridge which may limit future overload highway transportation to the North Slope and impact shipping efficiency?"

The answers to these questions led to a restricted dead-load allowance on the steel orthotropic deck of the Yukon River Bridge, thus limiting the selection of an adequate wearing surface. Bridge designers, along with Peratrovich and Nottingham, saw that an increase in dead load on the Yukon River Bridge could be critical to the orthotropic steel deck. Therefore, it was suggested that a future deck wearing surface should be limited to a maximum dead load of 30 lb/ft^2, and an even lighter dead load would be more desirable.

During the summer of 1993, researchers from the University of Alaska Fairbanks (UAF) took static strain measurements of the orthotropic steel deck for several trucks at different positions. The focus of the research was to analyze both thermal and truck-induced strains on the Yukon River Bridge deck and provide a method for selecting a wearing surface that would resist live-load flexural strain and thermal cracking. The magnitude of the measured live-load flexural strains in the deck was found to be minimal, with the largest strain recorded at 139.1 $\mu\varepsilon$. Minimum strains were -127.7 $\mu\varepsilon$, and the largest range in strain was 186.9 $\mu\varepsilon$. Due to the low magnitude of flexural strain, researchers suggested that alternative wearing-surface materials might be suitable for the bridge. The experimental results were correlated with a computer model to predict interface strains for surfacing alternatives. A five-step method for selecting alternative wearing surfaces was presented in a report following the research. A simultaneous study was conducted in which literature was reviewed that addressed past experiences with alternative wearing surfaces and analytical methods for calculating strains for orthotropic steel deck bridges. In conjunction with the literature review, a two-part national survey of state Departments of Transportation (DOT) was performed. The survey presented questions to assimilate DOT experiences with wearing surfaces on orthotropic steel deck bridges and to identify computer programs used by DOT to analyze and design orthotropic steel deck bridges. No wearing surfaces were identified by the literature or the national survey of DOT to suggest that common wearing-surface materials would meet the criteria needed for the Yukon River Bridge (Hulsey et al., 1995).

AKDOT&PF began to realize that the selection of an alternative wearing surface for the Yukon River Bridge was not a textbook design problem. The bridge presents three unusual features: a 6% grade, extreme temperatures during winter months, and a low volume of heavy loads. Factors significantly influencing wearing-surface life are surface traction, cold weather fatigue, permeability, ductility, abrasion resistance, and shear resistance of the bonding material at the steel interface. A wearing surface that can withstand the unusual features of the bridge and overcome the factors influencing the life of the surface will be an expensive solution. Therefore, it was suggested that several promising wearing surfaces be selected for study (Hulsey et al., 1999).

In 2002, the UAF Civil and Environmental Engineering Department and AKDOT&PF made a joint research effort to create wearing-surface selection criteria for the Yukon River Bridge. Selection criteria were demonstrated through two examples that illustrated design procedure for selecting a wearing surface on the bridge. The examples took advantage of design charts created during the 1995 Yukon River Bridge study that account for truckloads and temperature change. The examples presented for consideration were an asphalt wearing surface with an AC-5 mix and a rubber asphalt concrete wearing surface. The analysis showed similar results with limiting tensile strains of 200 με and 400 με, respectively, for the examples described. The induced thermal stress on the steel deck resulting from a 3 in. asphalt wearing surface with an AC-5 mix was 4641 lb/in.^{2}, and a 2.25 in. rubber asphalt concrete wearing surface yielded thermal stresses around 6092 lb/in.^{2}. The research also included a chronological inspection report of the wearing surface on the Yukon River Bridge (Hulsey et al., 2002).

AKDOT&PF was determined to replace the timber deck surface on the Yukon River Bridge with a synthetic material to reduce maintenance. Prospective materials were expected to remain functional and in service for a minimum of thirty years. The wearing or friction course material of the prospective deck was expected to last a minimum of ten years and be economically and conveniently renewed or replaced. For a wearing surface to meet the standards established by AKDOT&PF, the surfacing on the steel orthotropic deck should be regarded as an integral part of the deck system and must be designed accordingly. Under these conditions, the surfacing acts compositely with the deck, causing a substantial increase in rigidity. The surfacing may be subjected to significant tensile or compressive stresses. To assure reliable surfacing performance on a steel orthotropic deck, the analysis of the stresses must be calculated for an integrated structural system created by the wearing surface bonded to the steel deck (Wolchuk, 2001). This is specifically mandated by *AASHTO-LRFD Bridge Design Specifications* (AASHTO, 1998), Article 9.8.3.3 Wearing Surface:

> The wearing surface should be regarded as an integral part of the total orthotropic deck system and shall be specified to be bonded to the top of the deck plate …
>
> Force effects in the wearing surface and at the interface with the deck plate shall be investigated with consideration of engineering properties of the wearing surface at anticipated extreme service temperatures …
>
> For the purpose of designing the wearing surface itself, and its adhesion to the deck plate, the wearing surface shall be assumed to be composite with the deck plate, regardless of whether or not the deck plate is designed on that basis.

The essential requirements to be satisfied by wearing surfaces on steel decks are durability to resist rutting, shoving, and wearing; ductility and strength to accommodate thermal expansion, contraction, and imposed deformations without cracking; and fatigue strength to withstand flexural stresses due to composite action of the wearing surface with the deck plate and a secure and long-lasting bond with the deck plate. The intensity of the elastic and inelastic strains and stresses due to composite action of the wearing surface with the deck plate, and the ability to resist them, determine the longevity and fatigue strength of the surfacing, subject to repetitive wheel loads. For the purpose of a wearing-surface design, surfacing must be assumed to act compositely with the steel plate, and the flexural and shear bond stresses in the surfacing must be calculated for the applicable temperature range using the mechanical properties of the surfacing material. These properties (elastic modulus, tensile and bond strength, as functions of temperature) generally are not readily available and should be determined by tests (Wolchuk, 1997).

Literature reviewed on the research and practical design of orthotropic decks and their surfaces agrees that, when the wearing surface and steel deck act compositely, deformations and stresses in the orthotropic decks may be reduced. The magnitude of the deck-stiffening effect of the wearing surface is dependent upon its thickness, the elastic modulus that is dependent on temperature, and the load application, that is, static or dynamic, and bond characteristics. *AASHTO LRFD Bridge Design Specifications* (AASHTO, 1998), Article 9.8.3.3 Wearing Surface, provides a definitive design guideline, which states:

> Safety against surfacing cracking may be best assured by using surfacing materials with semi plastic properties or with low elastic modulus not subject to much variation with temperature.

The primary wearing surfaces discussed in the review of literature on steel orthotropic decks suggest using thinner (2 in.) surfacing, provided that the material does not become unduly rigid and brittle at extreme low temperatures, nor very soft at high temperatures. Polyurethane surfaces demonstrate these characteristics and are relatively soft throughout a wide temperature range, with only moderate rigidity increase at cold temperatures (Wolchuk, 2001). A polyurethane or similar surface may have been considered for the Yukon River Bridge, but AKDOT&PF specified that a prospective wearing surface must allow for removal of any portion of the wearing surface via mechanical means (i.e., unbolting, unscrewing, saw cutting) without damage to the steel deck. Removal of the wearing surface is to accommodate inspection of the orthotropic steel deck of the Yukon River Bridge. A removable wearing surface, along with the unusual features of the bridge and composite action needed between the wearing surface and steel deck, added a level of complexity in the investigation for a replacement deck.

Between April 2001 and January 2004, the Department of Civil Engineering at Kansas State University (KSU) conducted research on the evaluation of stiffness and ultimate load-carrying capacity of glass fiber-reinforced polymer (GFRP) honeycomb sandwich panels, with a sinusoidal core, used in bridge applications. The research also investigated the fatigue performance of sixteen full-scale GFRP panels. The panels were developed by Kansas Structural Composites, Inc., which has successfully installed fully composite bridges in several states including Kansas, Missouri, and West Virginia. Using the findings from experimental and analytical work done at KSU, a simple procedure for stiffness determination, based on material properties from coupon tests and geometrical properties of an idealized transformed section, was found to predict deflection within 20% accuracy. Analytical expressions to estimate both flexural and shear stiffness were presented as part of the stiffness determination. The research also observed that the GFRP panels demonstrated outstanding fatigue performance, and change in stiffness was insignificant during cyclic loading. The factors influencing the ultimate load-carrying capacity were clearly identified in the study, but a reliable analytical prediction of the ultimate flexural capacity was not attained. Failure occurring in the bond lines between the outer faces and core can significantly vary from specimen to specimen, making the prediction of failure difficult. Kansas State University constructed a preliminary proposal for design procedure of external wraps and internal ties that shift the failure of the specimens from the bond lines to the glass fibers. Finally, several 3-D finite element models were developed and analyzed to better understand the behavior of these complex structural systems (Kalný and Peterman, 2005).

The research performed at KSU provided evidence that a fiber-reinforced polymer (FRP) deck can be used in bridge applications, and when subjected to cyclic loading, the change in stiffness was insignificant. Outstanding fatigue performance of the panels is a critical characteristic required for a wearing surface on the Yukon River Bridge. Kansas State

University also demonstrated that it was possible to predict deflection, and derived a simple formula for flexural and shear stiffness. Knowing the stiffness of these complex composite bridge decks is also crucial in the integrated design of the wearing surface and steel orthotropic deck. One area of research, valuable to the Yukon River Bridge but which KSU did not investigate, was the effect of extreme temperatures on FRP panels.

Limited research was found pertaining to the analysis of FRP bridge decks under cold temperatures (-40°F). However, an informative research effort was undertaken by the Department of Civil Engineering at West Virginia University to analyze, theoretically and experimentally, FRP bridge decks under cold temperatures. Experimental data showed that induced thermal strain could be as high as 15% to 25% of allowable strain in the weak direction of FRP bridge decks. Two FRP composite bridge decks were experimentally evaluated: (1) a 4 in. deep hollow box core section, and (2) an 8 in. deep hollow box core section with diagonal stiffeners. Boundary conditions were varied for the experimental tests, and strain and deflection were monitored as the top surface of the FRP bridge deck was cooled with dry ice and the bottom surface of the FRP bridge deck was left at room temperature, which resulted in a top-surface temperature of -30°F to -40°F. The FRP decks exhibited upward convexity when the temperature of the top surface was higher than that of the bottom surface, and downward concavity when the temperature of the top surface was lower than that of the bottom surface. The deflections also increased with an increasing magnitude of temperature difference between the top and bottom surfaces. The theoretical and finite element results of deflection and strain were in agreement with experimental results. Result correlations led to accurate prediction of the maximum deflection for a FRP deck under a linear temperature gradient. The prediction was shown to be accurate only while considering the thermal effects between induced thermal strain and stress. The strain and stress were dependent on the effectiveness of boundary restraints in the horizontal plane and vertical plane. The large temperature difference (120°F) between the top and bottom of a FRP bridge deck can be attributed to low thermal conductivity of FRP materials and low thermal mass because of the hollow-core FRP decks (Prachasaree et al., 2007).

The Yukon River Bridge has been an area of continuous research since the first pile was driven for the abutments. Issues regarding the Yukon River Bridge have led institutions to conduct research on ice forces, use risk-analysis criteria development, and timber bridge-deck replacement. A significant amount of research has investigated steel orthotropic decks and their wearing surfaces. Fiber-reinforced polymer bridge decks have been tested experimentally, and successful analytical predictions and finite element models have been establish to evaluate their performance. Despite all this, a reliable wearing surface for the Yukon River Bridge remains unknown. Continuous research is needed and creative solutions are required to solve the problem. The following chapter presents research performed on experimental bridge decks for the Yukon River Bridge. Some bridge-deck materials have previously been installed on this bridge and others have not yet been tried. Inspired by past research on the Yukon River Bridge and the work conducted at KSU, a research plan was developed. The conclusions of the Department of Civil Engineering at West Virginia University have shown that to properly design FRP decks for cold temperatures, thermal-response studies including thermally induced stress, strains, deformations, and thermal fatigue effects have to be evaluated in a systematic manner (Prachasaree et al., 2007). With their suggestions, the present research evaluates experimental bridge decks in cold-temperature environments.

When crossing the Yukon River Bridge during winter months, truck drivers often need tire chains. Lack of traction on this 6% grade, combined with traction surface damage, is another complexity that must be solved as part of obtaining a cost-effective wearing surface for this bridge. The literature reveals a number of studies on skid resistance and surface coatings, such as SafeLane developed at Michigan Tech (Persichetti, 2005; 2007). These studies attempted to improve the traction of known materials by applying coatings, such as an epoxy. Other studies have developed coatings for bridges such as SafeLane. Alternative products available for rail grade crossings look promising for this type of structure (Matoba, 2001; Wanek, 2004; 2005). For example, products such as polyethylene and rubber are being used in the rail industry for grade crossings.

The literature did not reveal methods for measuring damage caused by tire chains, and only limited articles were available on traction measurements for bridge structures. There were numerous articles on damage caused by studded tires; however, these articles were not that helpful. Thus, in this research, we developed laboratory test equipment to measure the extent of damage in the wear surface caused by tire chains. In addition, equipment was developed to measure static and dynamic coefficients of friction for various temperatures and exposures such as dry, wet, or icy.

CHAPTER 6 – STRUCTURAL PANEL TESTS

We compared test results for load, strain, and deflection, and calculated flexural stiffness of panel tests at room temperature and in cold temperature. In addition, we compared material-property test results to average and published property values. Material property values are in Chapter 7.

Room- and Cold-Temperature Tests

This section provides tests results for room-temperature and cold-temperature tests. Comparisons are made between experimental results for test panels, and conclusions are provided for panel stiffness, performance, and compatibility with the steel orthotropic deck of the Yukon River Bridge.

Panel Tests

We tested panels for stiffness and strength by subjecting a 4-ft-by-4-ft simply supported plate to a center load that simulated truck dual tires. All five panels were tested at room temperature with the loading foot longitudinal to the running planks. This same test was repeated, with the loading foot transverse to the running planks. We compared results for displacement and strain at a 16,000 lb load.

We performed tests at room temperature and at cold temperature, with the loading foot oriented longitudinally to the direction of traffic. The same tests were repeated with the loading foot rotated ninety degrees. We then compared results for all five of the test panels.

We compared structural behavior for these experimental bridge decks, and summarized strains and deflections at critical locations for room temperature and cold temperature. Additionally, we compared panel stiffness at room temperature with panel stiffness at cold temperature. Panel strengths were compared by testing each panel to failure.

Strain Gage Locations

We installed strain gages at or near the points of maximum stress. Assuming that maximum stress would occur in the center of the panel and along the boundaries of the loading foot, we placed gages on a projected outline of the loading foot on the bottom of the panel. An x–y coordinate system was used to identify strain gage location with direction of traffic on the Yukon River Bridge running longitudinal to the x-axis. Figure 6.1 shows an outline of the loading foot in both the longitudinal and transverse directions, with strain gages positioned in the assumed areas of maximum stress.

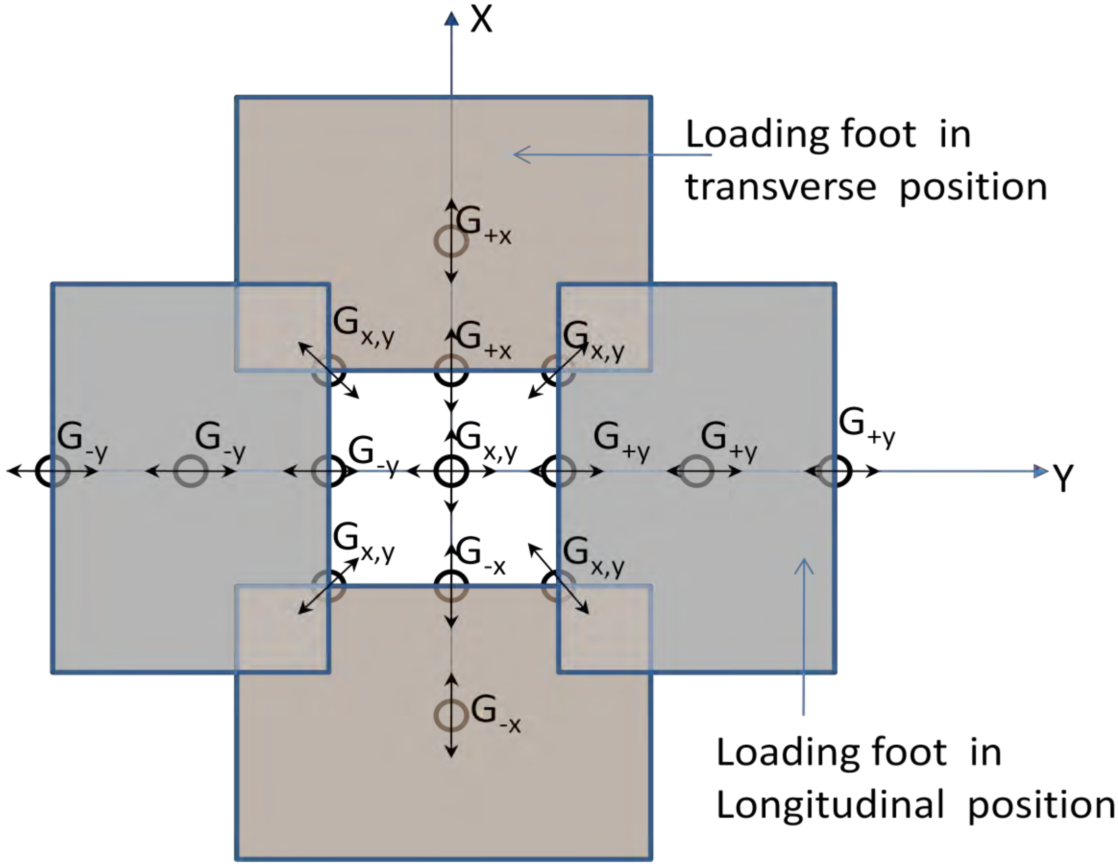

Figure 6.1 Desired locations of strain gages.

Though the desired locations of the strain gages are shown in Figure 6.1, the gage locations for some panels deviated from this drawing due to individual characteristics and geometry. The letter *G,* followed by gage number and axis denoting where the gage was measuring strain, developed as a naming convention to identify panel strains at various locations (Jerla, 2008).

Timber/Timber Panel

Five room-temperature tests conducted on the timber/timber panel revealed that, as the panel was unloaded and loaded, stiffness increased (see Figure 6.2). In these tests, the loading foot was longitudinal to the running planks.

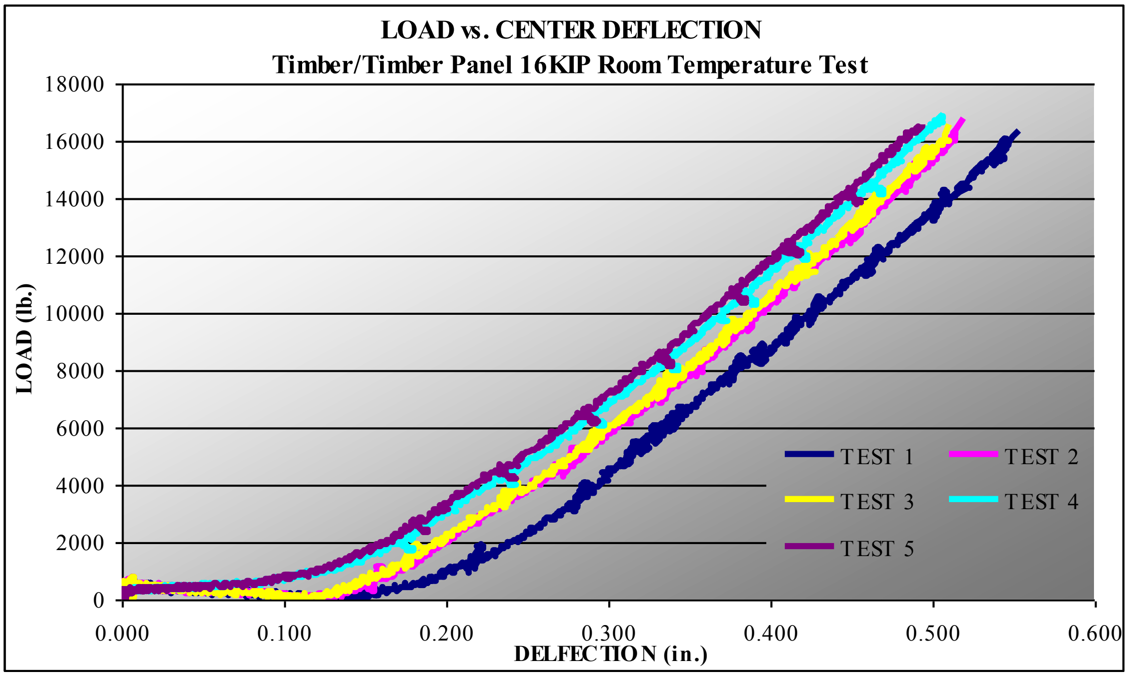

Figure 6.2 Timber/timber panel: Load vs. center deflection.

A change in panel stiffness was exhibited after the first test. In the remaining tests, change in stiffness was minimal. The panel deflected more during the first test because initial gaps and irregularities between the two layers of timbers acted as a more flexible system. The initial region in Figure 6.2 shows that the panel attempted to reposition itself on the load frame. This occurred because the timbers shrank and the timber/timber panel rested unevenly on the loading frame. The panel did not begin taking load until all edges were in contact with the loading frame.

Comparative room-temperature test results, when the load foot is oriented longitudinal versus transverse to the running planks, are shown in Figure 6.3.

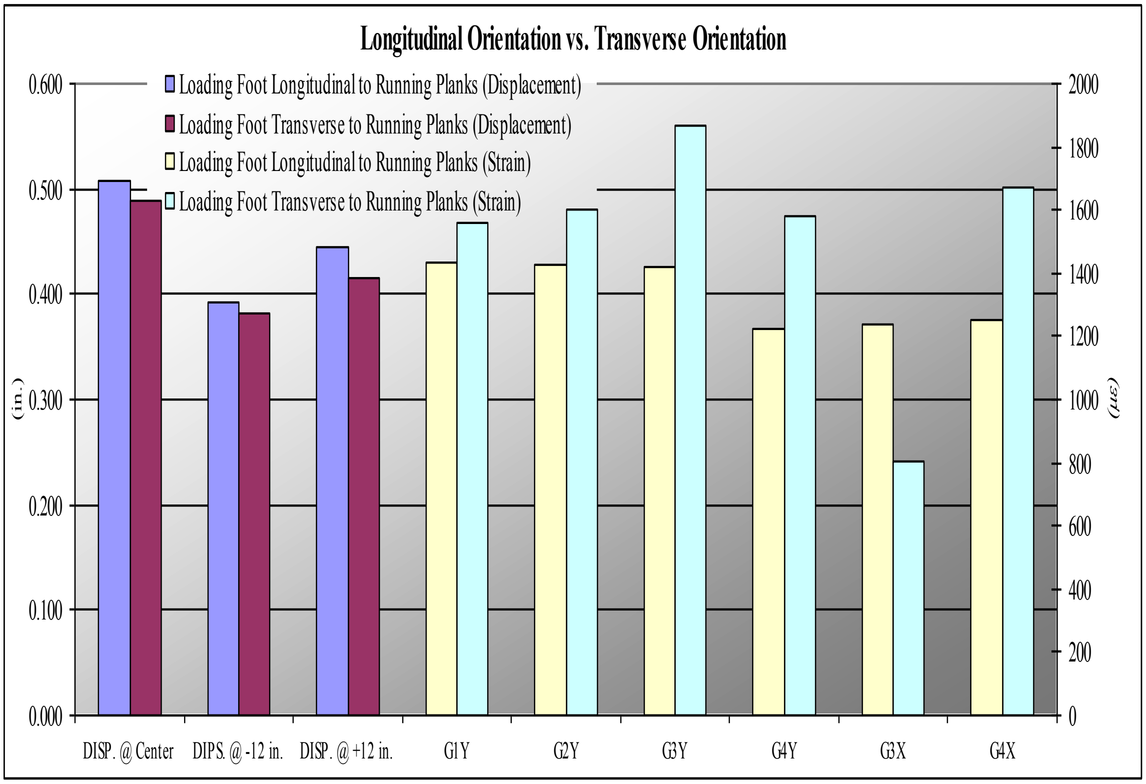

Figure 6.3 Timber/timber: Orientation of load foot, longitudinal vs. transverse.

Displacements averaged 4% higher when the load foot was longitudinal versus transverse to the running planks. This small increase in displacement was not significant. Orientation of the loading foot did not affect the behavior of the panel. Figure 6.3 shows the strain for six strain gages located along the *x*-axis of the timber/timber panel. Maximum displacement for this simply supported two-way composite plate was about 0.5 in., and the largest strain was about 1864 micro-strains. Additional details are available in Jerla (2008).

Test results for the room-temperature and cold-temperature tests for the timber/timber panel show similar behavior between room temperature and at -11°F. Results from the temperature tests are shown in the chart in Figure 6.4.

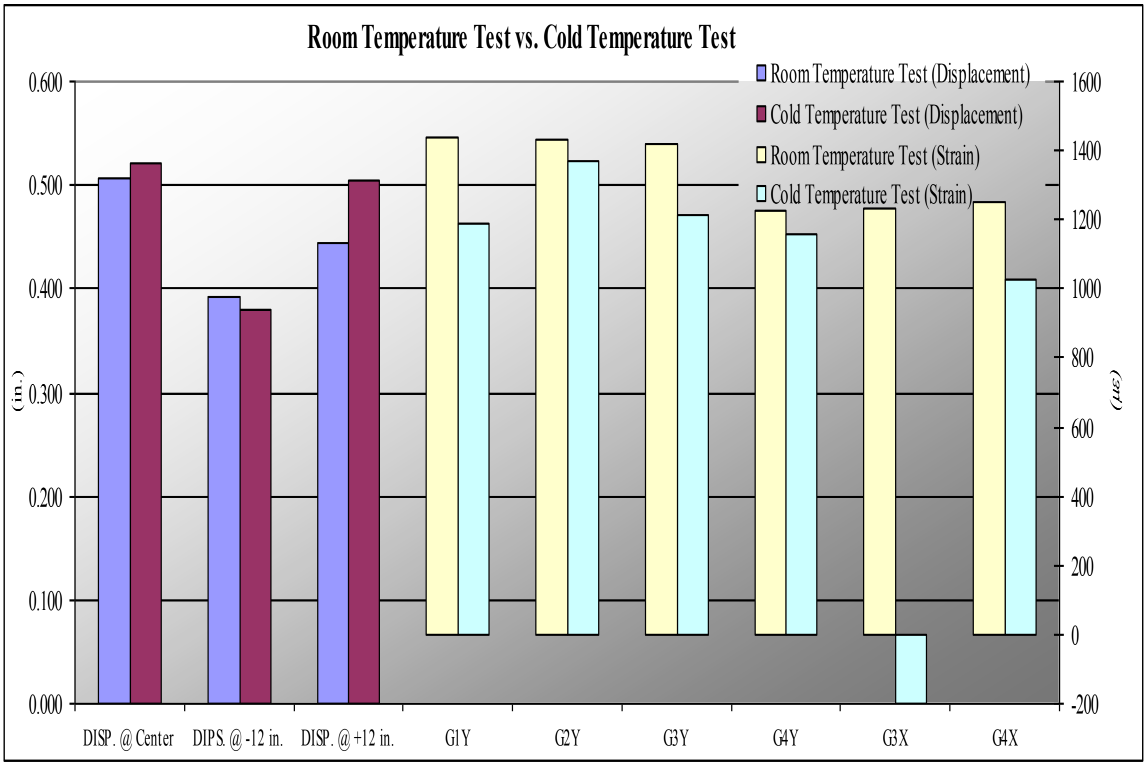

Figure 6.4 Timber/timber: Tests at room temperature vs. cold temperature.

Strains for cold-temperature tests were compared with room-temperature tests. Cold-temperature strains averaged 11% lower, indicating an increase in panel stiffness. The strain measured at gage G3X during the cold-temperature test was -198 micro-strains. We believed that this gage was damaged during panel transportation; thus, the strain value was considered invalid. Maximum displacement values showed a 3% increase in center-point displacement and a 12% increase at +12 in. from the center point along the *y*-axis during the cold-temperature test. Although the strain data support increasing panel stiffness at cold temperature, the displacement data do not. Stiffness determined from load displacement data are provided in the summary of this section.

Transonite Panel

The complex structure of the Transonite panel was acknowledged, in part, based on the sounds produced by the panel as it began to take load. During initial loading, the panel produced snapping and cracking noises, indicating that the structural members of the panel were undergoing stress and possibly failing. The panel only produced noise during the first test, when the load on the panel was greater than any previous loading condition. Figure 6.5 shows the load versus deflection diagram of all five tests for the Transonite panel during the room-temperature test, with the loading foot oriented longitudinal to the direction of traffic.

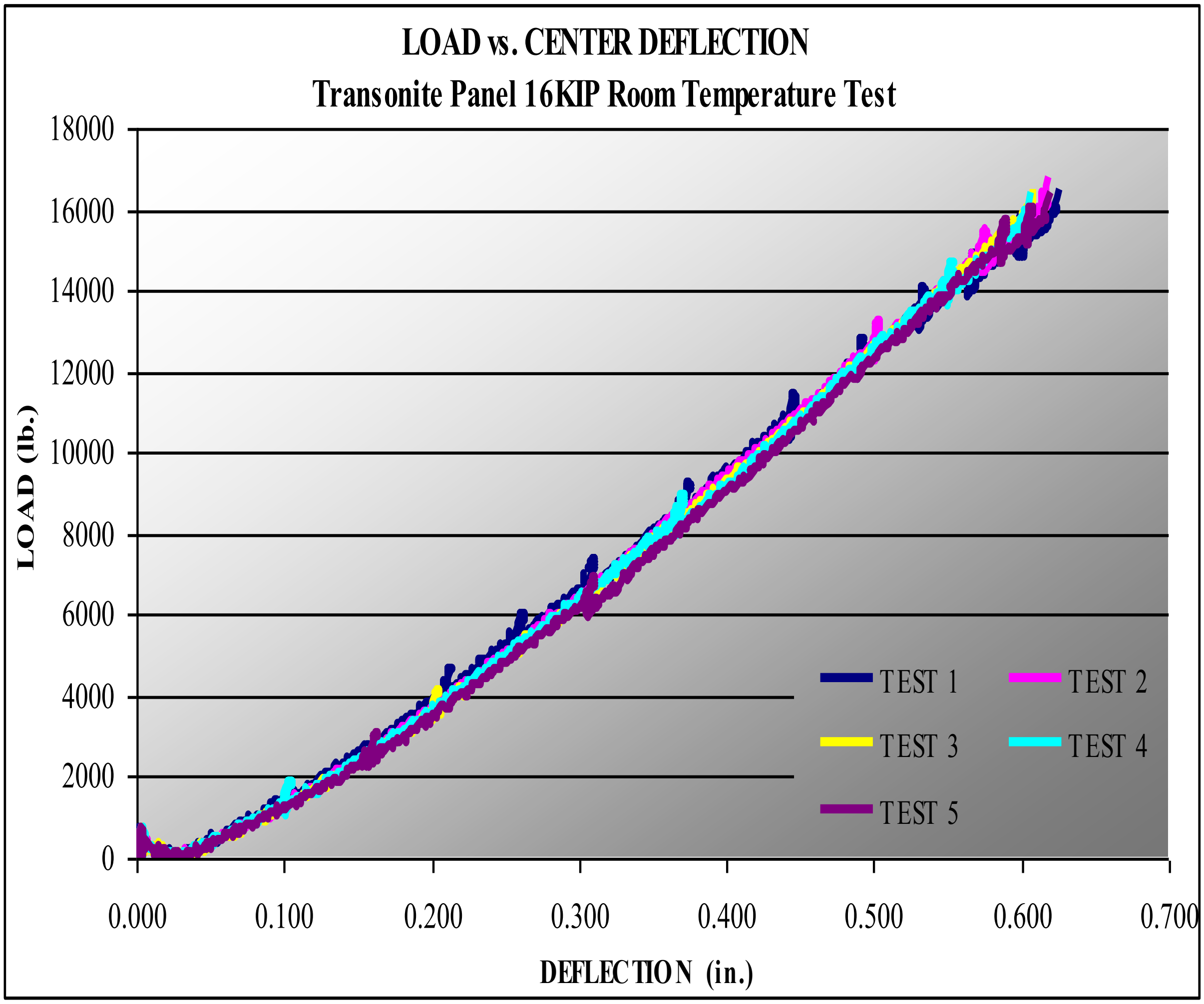

Figure 6.5 Transonite panel: Load vs. center deflection.

The diagram shows (despite the initial noise in readings) that all tests performed approximately the same as the first test; no change in stiffness was seen.

Displacement and strain readings recorded at 16,000 lb, with the loading foot in the longitudinal and transverse positions, are displayed in Figure 6.6.

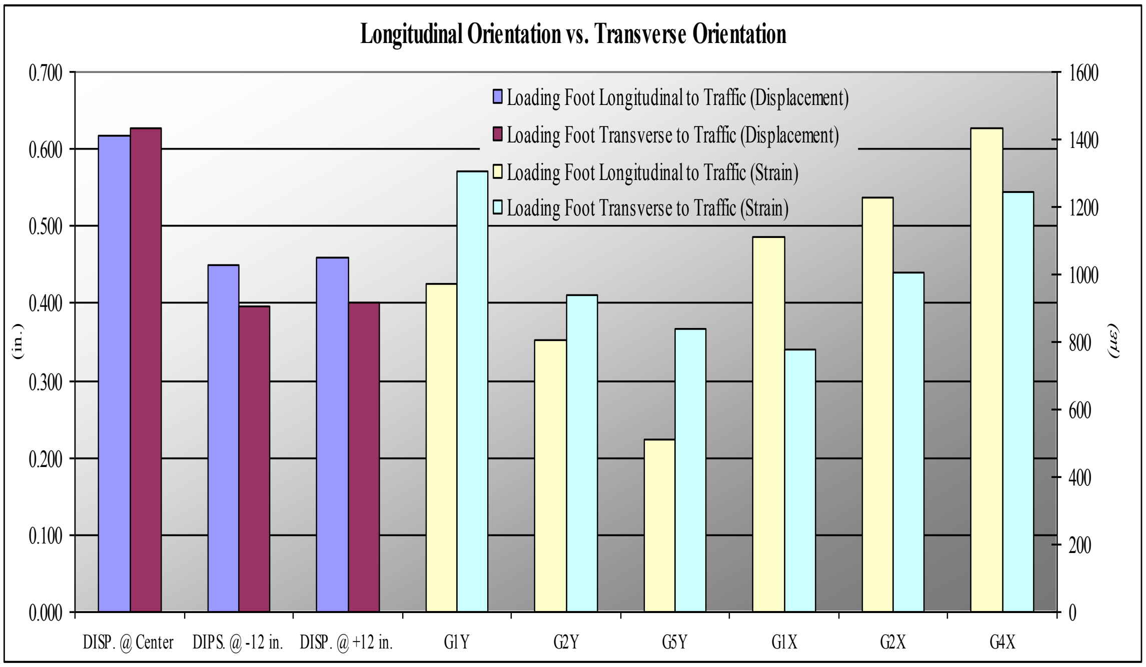

Figure 6.6 Transonite panel: Longitudinal orientation vs. transverse orientation.

A 1.4% increase in center displacement occurred when the loading foot was rotated, but *y*-axis displacements decreased 12% to 13%. The decrease occurred because, as the loading foot was rotated into the transverse position, the load became centered about the *x*-axis, moving the force away from the measured displacements. Only small changes in displacements occurred due to direction change of the load footprint. The strain gage data also support this finding. Larger strains were present along the *y*-axis when the load footprint was transverse, and higher along the *x*-axis when it was longitudinal (Jerla, 2008).

Both centerline displacements and strain gage measurements decreased for the cold-temperature test (see Figure 6.7). The center displacement decreased 6%, and strains decreased from 8% to 18%.

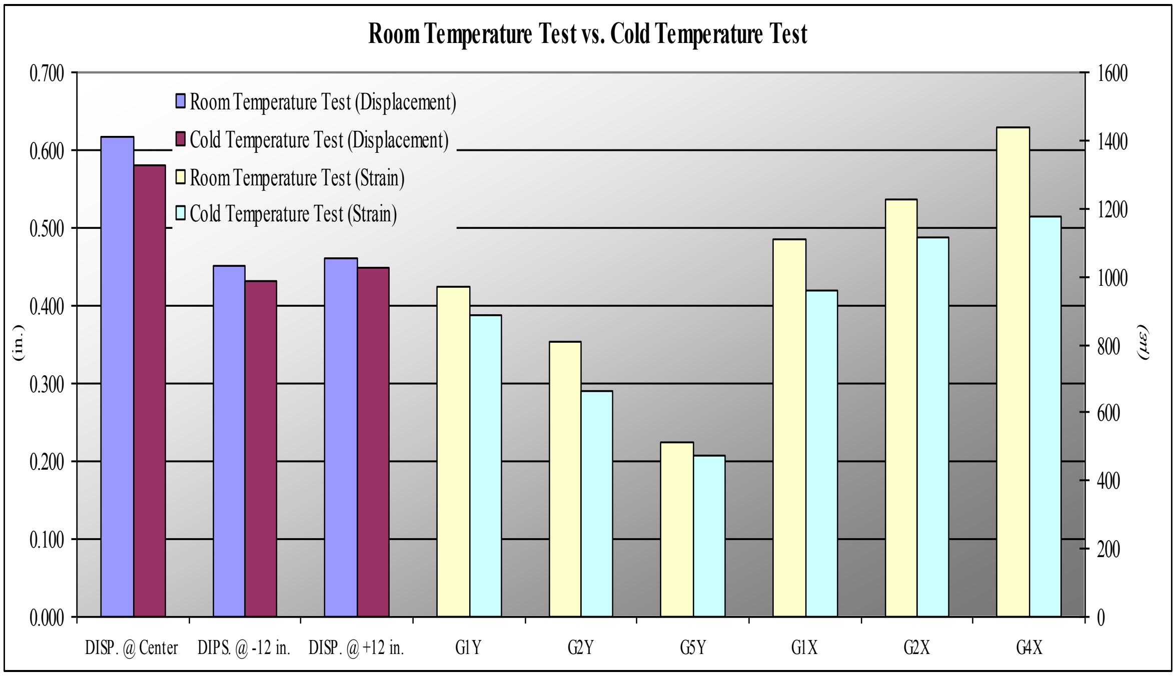

Figure 6.7 Transonite panel: Room temperature vs. cold temperature.

Super Panel

The load-versus-deflection diagram shown in Figure 6.8 illustrates that the Super Panel behaves nearly identically for all five tests conducted at room temperature with the loading foot oriented longitudinal to the direction of traffic.

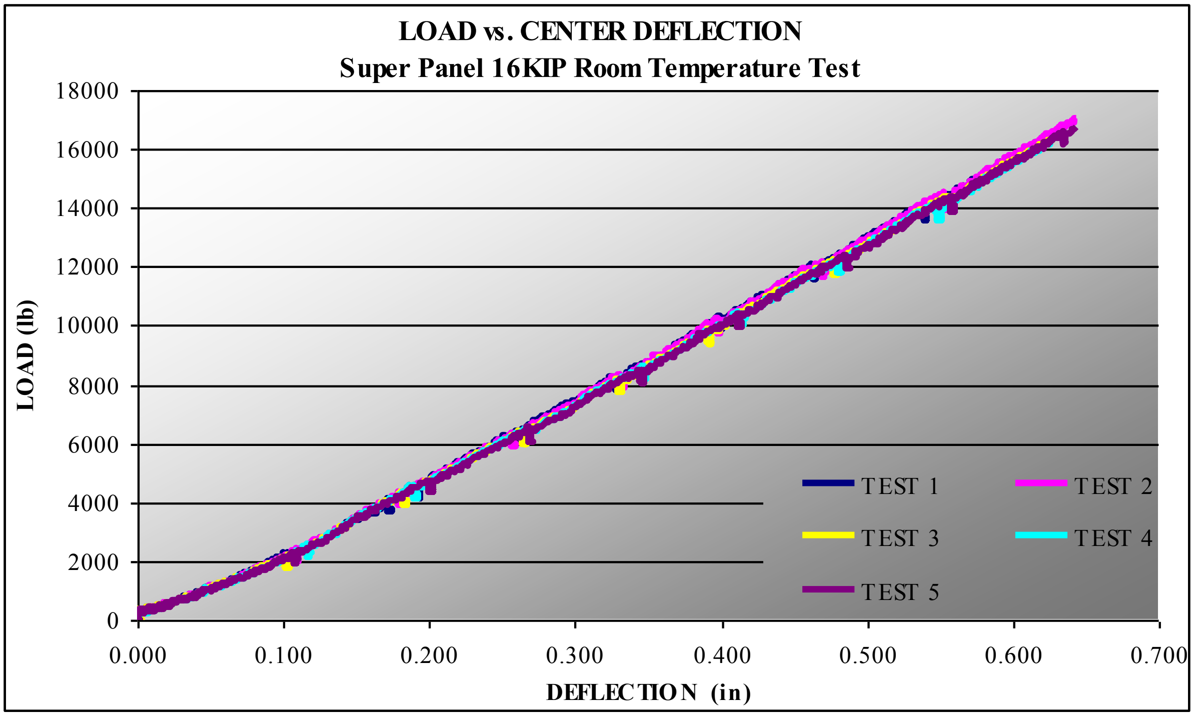

Figure 6.8 Super Panel: Load vs. center deflection.

No visual changes in behavior of the panel other than some minor deflection were detected during testing. The deflected shape of the panel fully recovered after testing, and the load-versus-deflection diagram shows that the stiffness did not change for the five repeated load tests.

The structural behavior of the Super Panel's hollow box-core system was evident upon comparing the displacement and strain readings when 16,000 lb was applied. Unlike other tests, this panel was simply supported on two edges (one-way plate action). Therefore, displacement and strain values are not comparable to the other four experimental bridge-deck panels. Figure 6.9 provides a comparison of results at 16,000 lb force for the Super Panel during the two room-temperature tests.

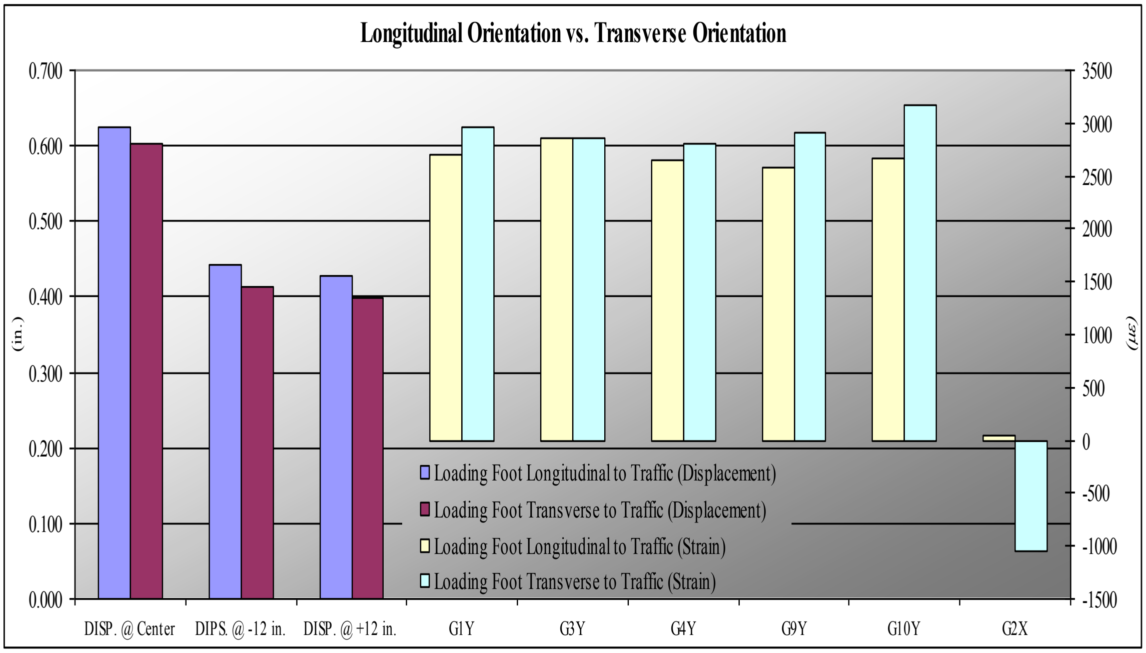

Figure 6.9 Super Panel: Longitudinal orientation vs. transverse orientation.

Decreases of 4%, 7%, and 6% were recorded at the center of the panel, -12 in. from center and +12 in. from center, respectively. The decrease in displacement was not unexpected as the force was moved away from the -12 in. and +12 in. measurement locations. Strain gage data show that when the loading foot was orientated longitudinal to the direction of traffic, there was no strain present in the *x*-direction at the center of the panel. As the loading foot was rotated, strain readings in the *y*-direction were small, while strains in the *x*-direction increased up to 105%. It is important to note that a significant amount of bending occurred along the weaker *x*-axis, even though the panel was supported on two edges and was designed to take bending along the *y*-axis. The Super Panel was initially thought to bend only along the *y*-axis, but with strains present along the *x*-axis, the panel demonstrated plate behavior. This plate behavior indicates that the Super Panel is a very stiff system even when only supported on two edges.

Displacements and strains decreased for the cold temperature (see Figure 6.10).

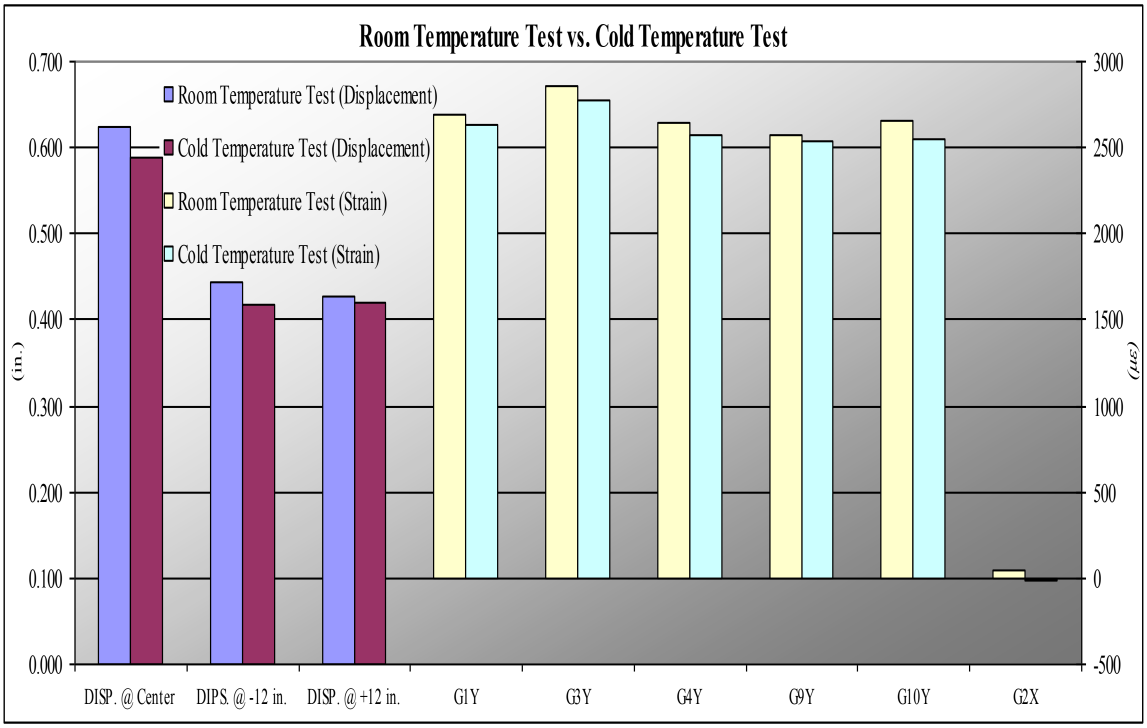

Figure 6.10 Super Panel: Room-temperature test vs. cold-temperature test.

A comparison between room-temperature and cold-temperature tests shows that the displacements at three different locations experienced a 1% to 6% decrease, and strains decreased from 1% to 2%.

Timber on Solid UHMW Panel

Each of the five room-temperature tests that we conducted on the panel showed minor timber on UHMW adjustments during the tests. During Test 1, any gaps between the timber and UHMW polyethylene that could not be removed during construction were removed once the testing load exceeded 6200 lb. Initially, there is the potential for slippage and movement between materials. After some load is applied, slippages and movements between these layers are minimized, and the panel acts as a system. These slippages and movements between the timber layer and the UHMW layer resulted in more flexibility the first time we tested the panel. In the four remaining tests, many of these movements appeared to be minimized. Figure 6.11 shows the load-versus-deflection diagram for the panel when the loading foot was oriented longitudinal to the running planks.

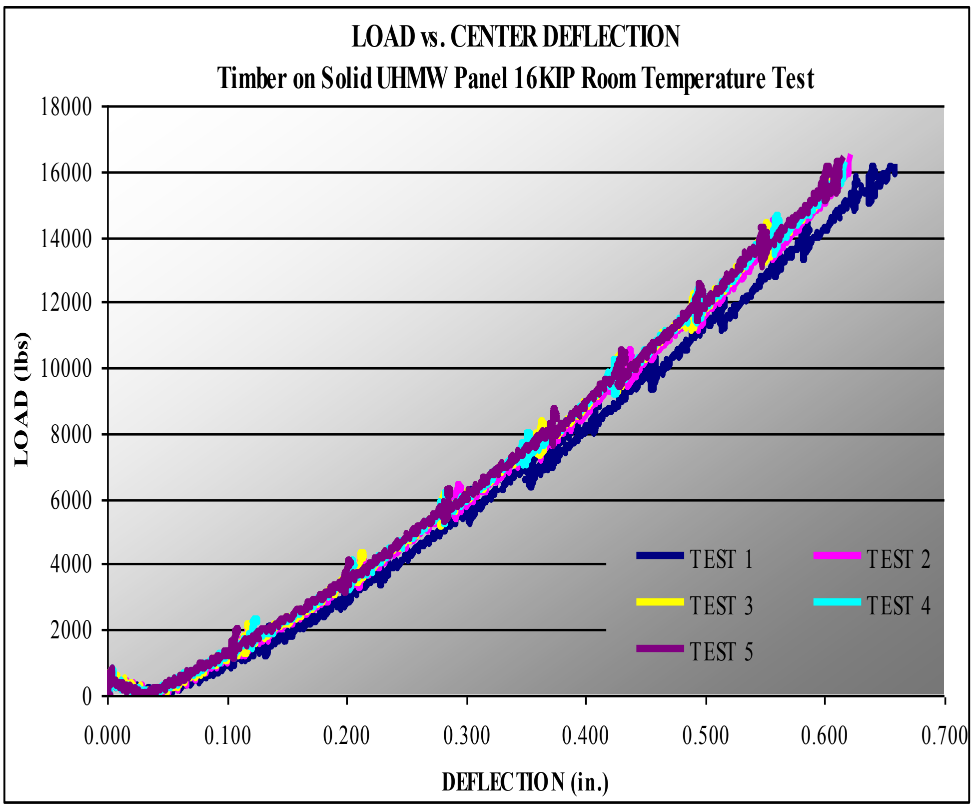

Figure 6.11 Timber on solid UHMW panel: Load vs. center deflection.

Test 1 was more flexible than the remaining tests, while Tests 2–4 appeared to have the same stiffness (see Figure 6.11). A toe region (also seen in the figure) was a direct effect of the timber running planks adjusting and settling into the solid UHMW panel.

Comparative test results at room temperature show that the loading foot orientation significantly affected both magnitude and location of the principle strains. Displacement values tend to remain equal for both tests, with only a 6% and 2% change recorded at three locations along the *y*-axis of the timber on solid UHMW panel (see Figure 6.12).

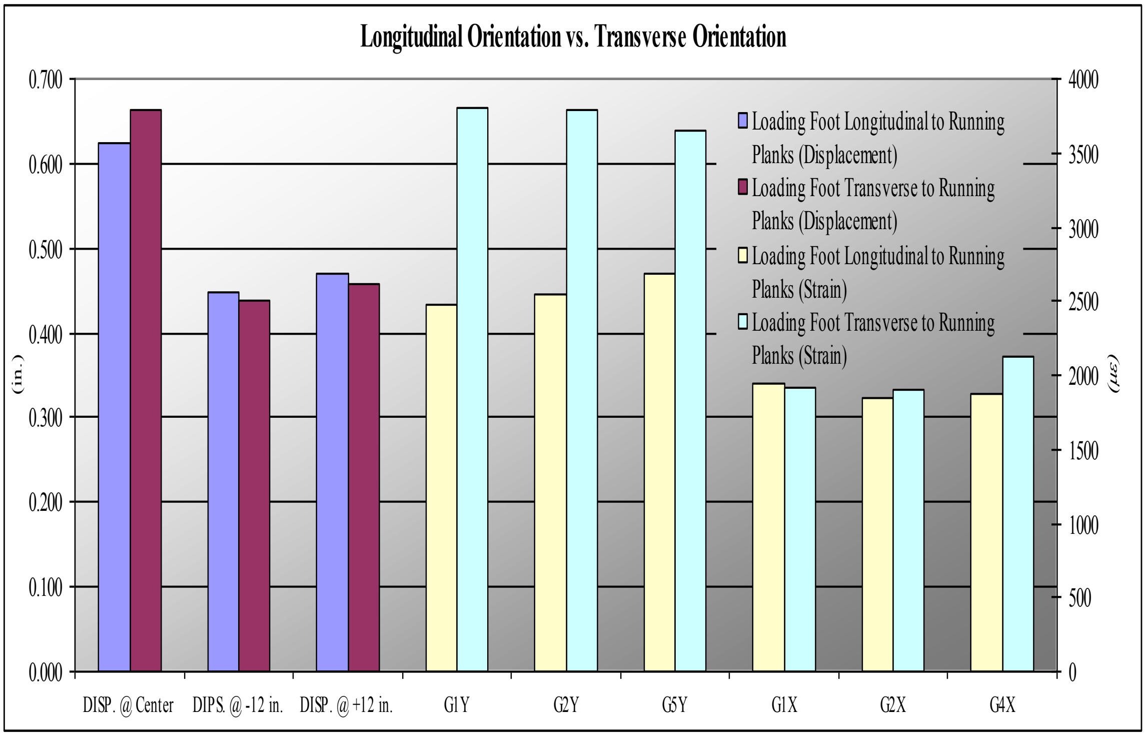

Figure 6.12 Timber on solid UHMW: Longitudinal vs. transverse.

Figure 6.12 illustrates that strains remain virtually unchanged along the *x*-axis, as the loading foot was positioned longitudinal and transverse to the running planks. However, strain values along the *y*-axis increased from 26% to 35%. These strain increases emphasize the possible influence of running-plank orientation. A much stiffer panel was observed when the loading foot was placed longitudinal to the running planks, causing the 16,000 lb force to take a more evenly distributed load path into the UHMW polyethylene panel. With the loading foot transverse to the running planks, the 16,000 lb force provided a more direct path into the panel, causing higher strains.

Panels tested near -11°F were stiffer. Because the timber/timber panel showed very little change in behavior between room-temperature tests and cold-temperature tests, it is believed that the UHMW polyethylene component of the timber on solid UHMW panel stiffened due to cold temperatures. Figure 6.13 shows the data recorded from the displacement and strain gages at 16,000 lb for both the room-temperature test and cold-temperature test.

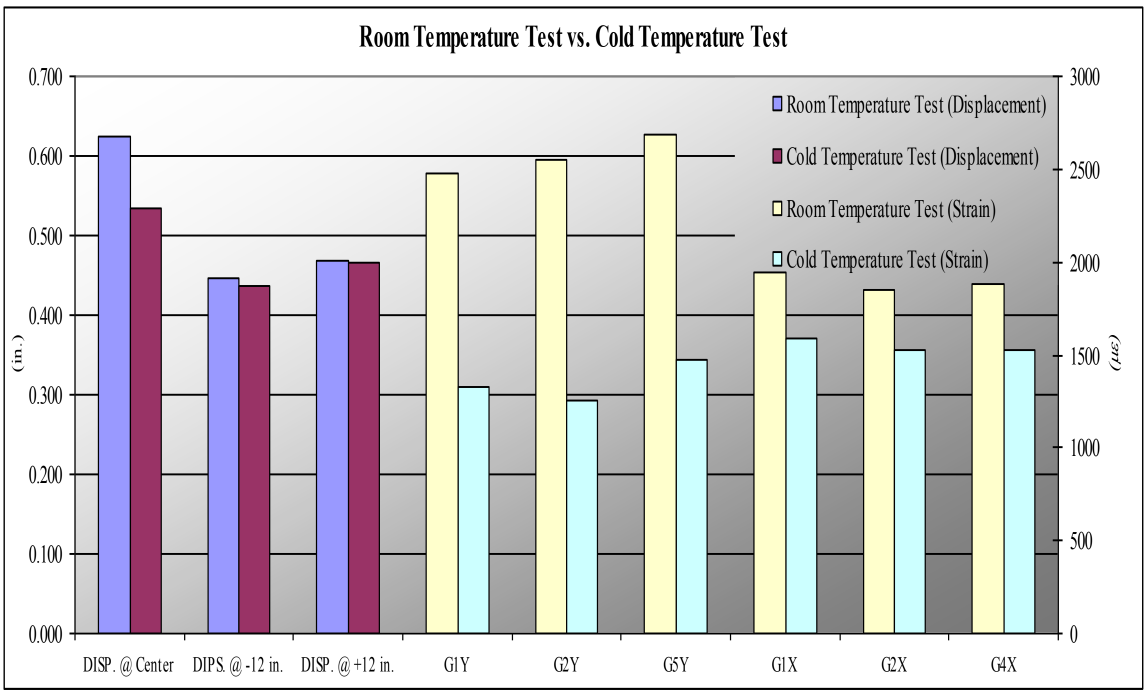

Figure 6.13 Timber on solid UHMW: Tests at room temperature vs. cold.

The center displacements reduced 15% and remained constant along the *y*-axis. Strains decreased in both *x*- and *y*-directions. Strains reduced 17% to 19% in the *x*-direction and 45% to 51% in the *y*-direction (see Figure 6.13).

Timber on M-Shaped UHMW Panel

The M-shaped UHMW panel behaved similar to the solid UHMW panel, where the first test showed a more flexible bridge-deck system than the remaining four tests. As with the solid UHMW panel, this was due to spaces between timbers. At initial loading, gaps between the two materials abruptly closed, causing a spike in deflection and loss of stiffness. A spike in deflection occurred at approximately 8200 lb, and it was believed that one of the lag bolts sheared, as a sharp metallic breaking sound was heard. Figure 6.14 shows the load-versus-deflection curve generated from the room-temperature tests.

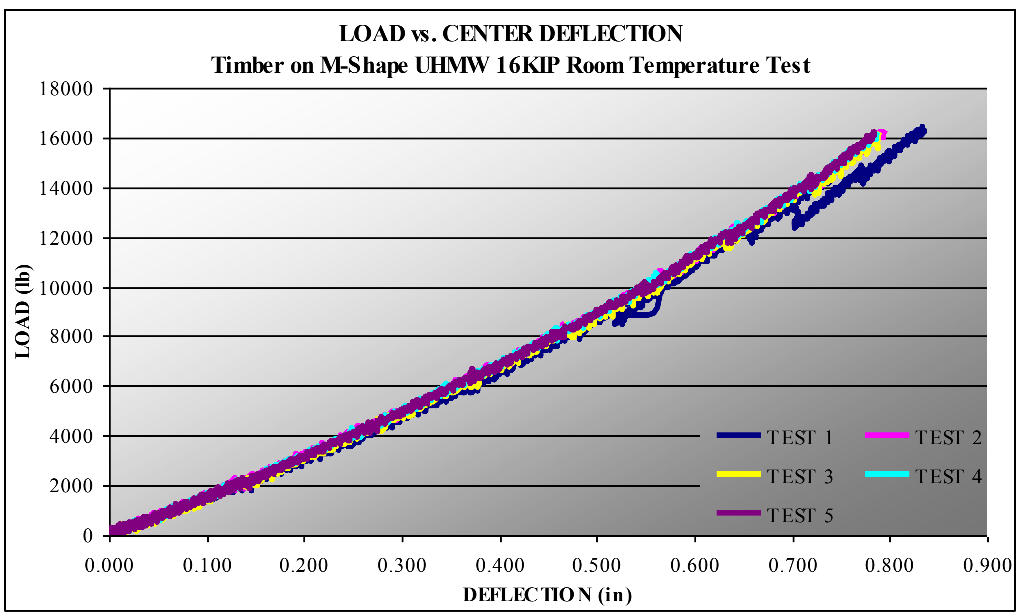

Figure 6.14 Timber on M-shaped UHMW: Load vs. center deflection.

Although the M-shaped UHMW panel and the solid UHMW panel show similar progression of stiffness during testing, they did not exhibit a similar toe region in the load-versus-deflection curve. Figure 6.14 illustrates that the M-shaped UHMW panel immediately begins to take load with the loading foot oriented longitudinal to the direction of the running planks.

Comparative results of the longitudinal orientation versus the transverse orientation of the loading foot are provided in Figure 6.15. This figure shows that both center-point displacement and strain increased with the loading foot in the transverse position. Results also display a stiffer system when the loading foot was placed transverse to the running planks.

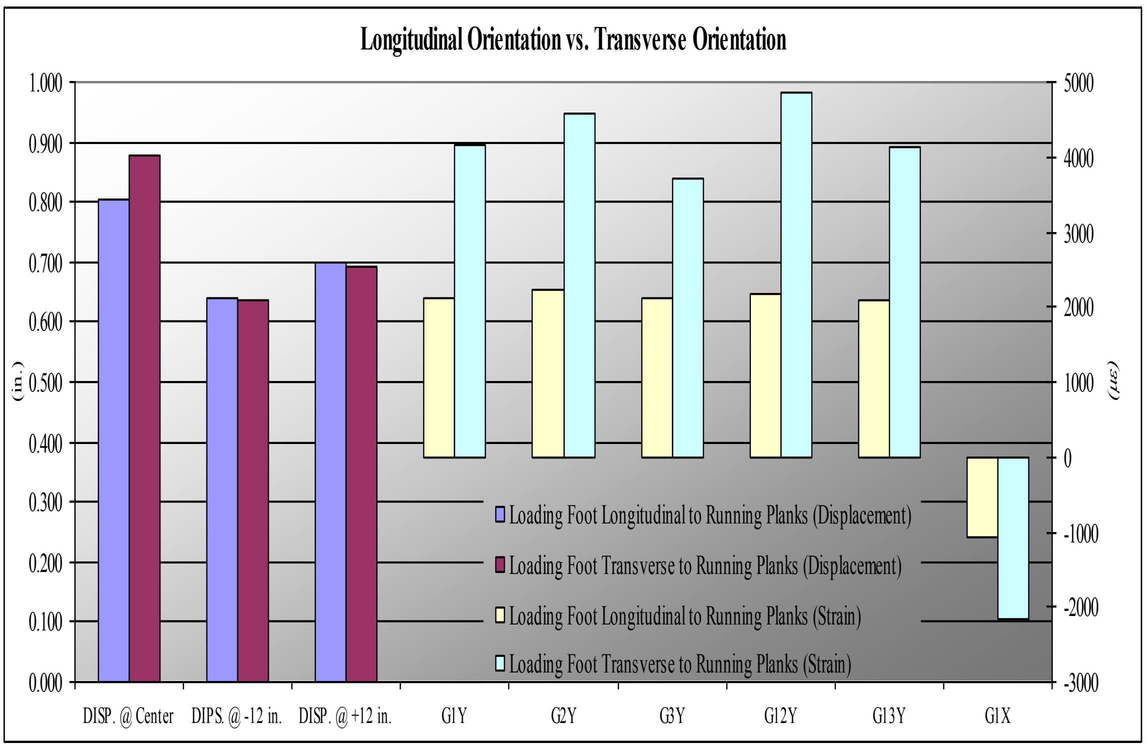

Figure 6.15 Timber on M-shaped UHMW: Longitudinal vs. transverse orientation.

Center displacement increased 8% when the load foot was longitudinal versus transverse. We believe that the increase in displacement was due to the placement of the sensors on the center ridge. Recall that the M-shaped UHMW panel was designed with ridges molded into one side of the panel to reduce weight and create an orthotropic panel. With the loading foot in a longitudinal position, the ridges of the panel run transverse to the foot. A lesser amount of force appeared too distributed to the ridges, resulting in less displacement and less strain at the center of the panel. When the loading foot was in the transverse position, the ridges were longitudinal and the load was distributed so more load went to the ridges. This caused a higher center-point displacement and higher strains. Strain readings averaged 50% greater when the loading foot was in the transverse position. Note that even though the system was believed to behave highly orthotropic, an *x*-axis strain of 2169 micro-strains was recorded at the center of the panel. The importance of the *x*-axis strain indicates that the panel bends along the *x*-axis, and the strain was shown to increase from one test to another. This effect was most likely due to the addition of the timber running planks, causing the system to bend as a plate.

As with the timber on solid UHMW panel, the stiffness of the M-shaped UHMW panel increased as temperatures decreased. Results from the room-temperature test versus cold-temperature test are provided in Figure 6.16.

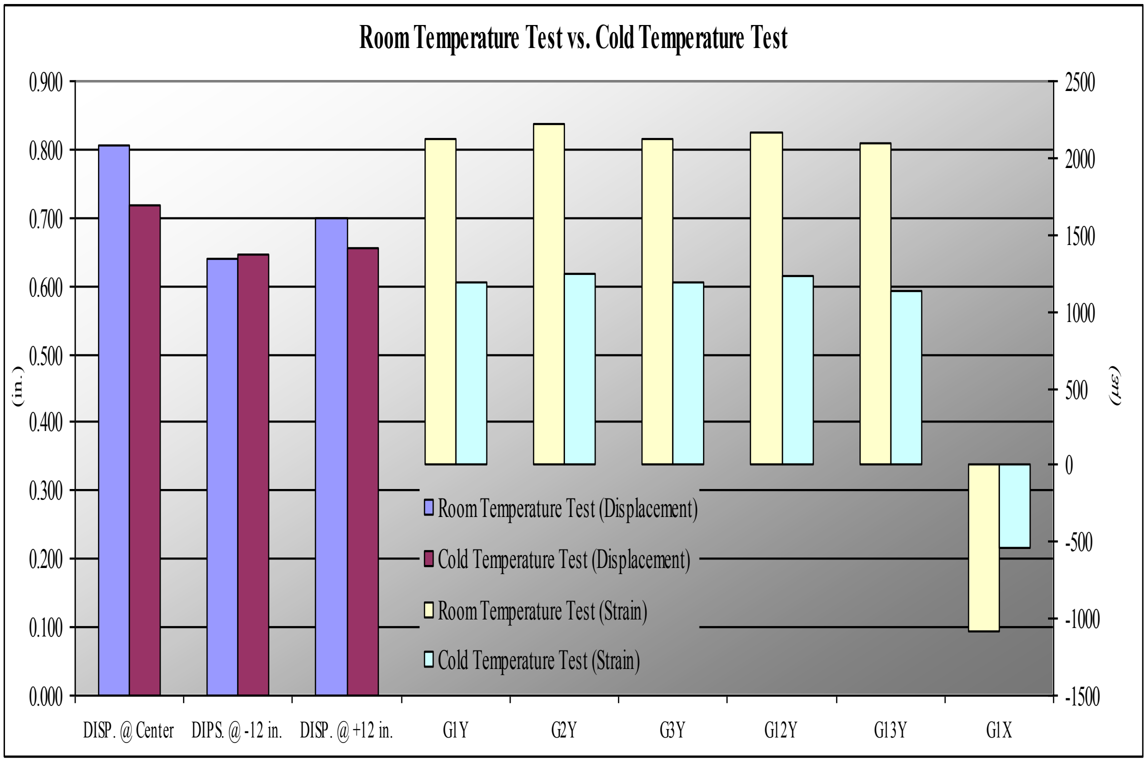

Figure 6.16 Timber on M-shaped UHMW: Room temperature vs. cold.

Displacement decreased as much as 11% at the center of the panel, while strains decreased an average of 45%. The system clearly stiffened as temperatures decreased.

Panel Comparison

Figure 6.17 provides a center-displacement comparison for 16,000 lb load tests at room temperature and cold temperature.

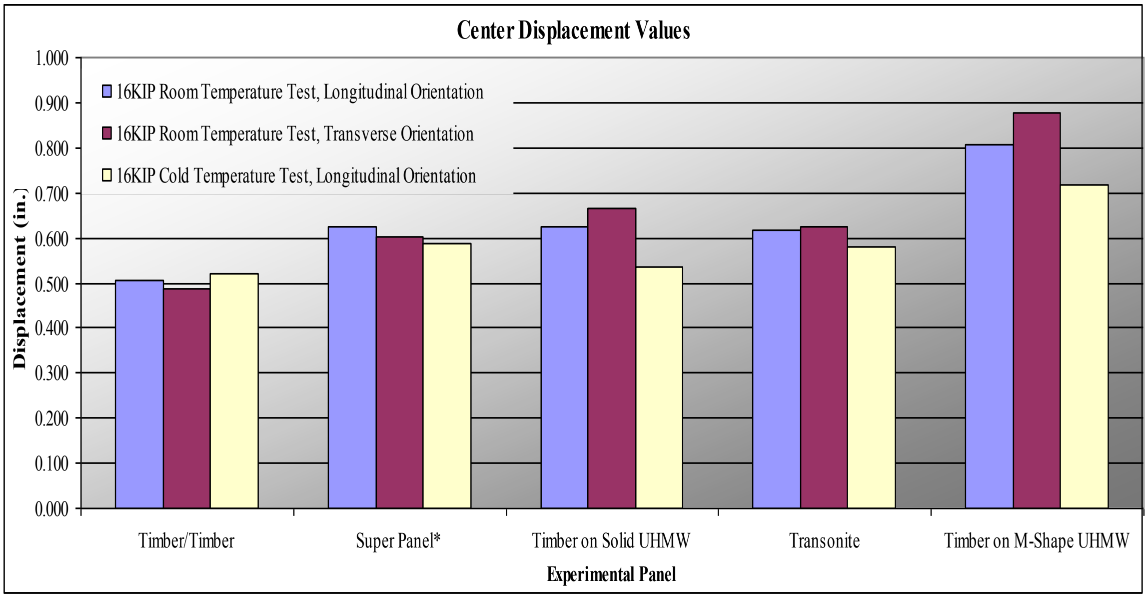

Figure 6.17 Center displacement for all five panels.

Only marginal change in center displacement was observed at room temperature, and the load foot orientation was changed (see Figure 6.17). All panels, with the exception of the timber/timber panel, experienced a decrease in displacement for the cold-temperature test. This change in displacement indicates that panels began to stiffen when subjected to cold temperatures. The timber on solid UHMW and timber on M-shaped UHMW panels showed the greatest change in displacement under cold-temperature testing, with values decreasing from 15% to 11%, respectively. Strains showed similar trends.

Figure 6.18 provides a comparison (at the 16,000 lb load) between strains at gage G1Y for all five experimental panels.

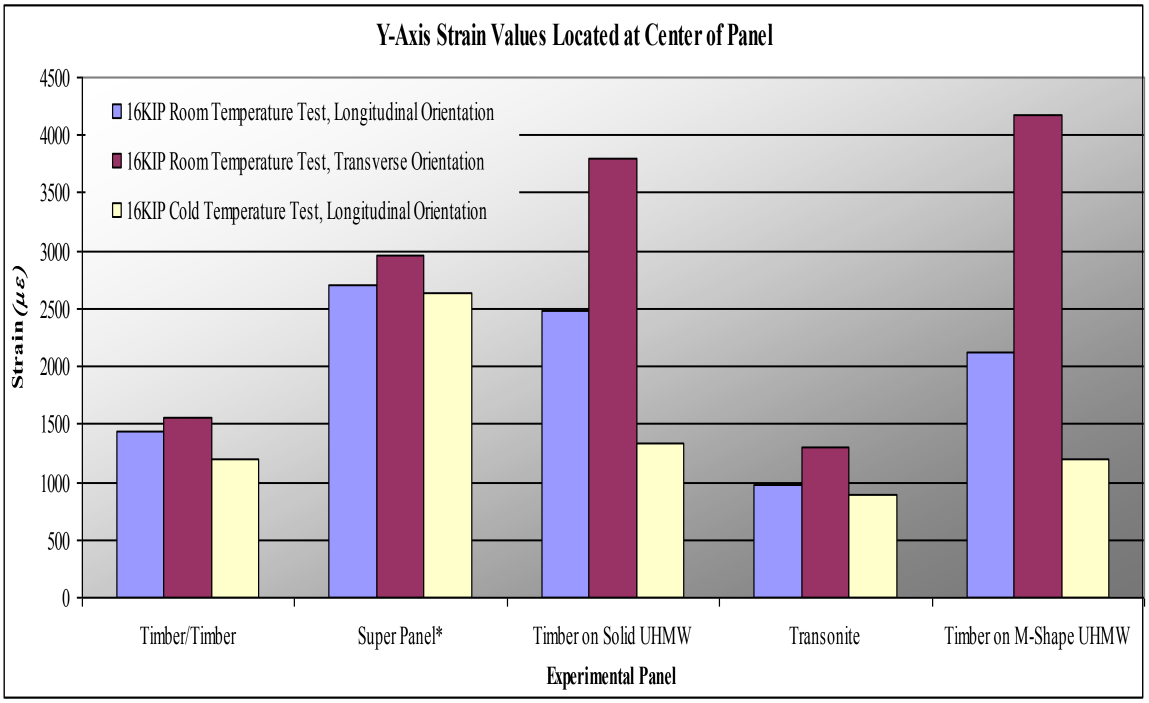

Figure 6.18 *Y*-axis strain for all five panels.

We chose Gage G1Y as an effective comparative gage because its location was common to all panels, and significant readings were always recorded regardless of the test. G1Y was located in the *y*-direction at the panel centerline. The chart shows that as the orientation of the loading foot was altered from the longitudinal position to the transverse position, strain increased for all five panels. An opposite but similar trend was seen as the strain decreased for all five panels when tested at cold temperatures. Strain values decreased as temperature decreased; that is, panels stiffen as temperature drops.

The timber on solid UHMW panel and timber on M-shaped UHMW panel show the greatest increase in strain between the two room-temperature tests. Strains were seen to increase by 35% for the timber on solid UHMW panel as the orientation of the loading foot was altered. The timber on M-shaped UHMW displayed strain increases of 49% between the two room-temperature tests. The two panels also showed the greatest decrease in strain from the room-temperature test to the cold-temperature test. A strain decrease of 46% was recorded for the timber on solid UHMW panel, and a decrease of 44% was recorded for the timber on M-shaped UHMW. The timber on solid UHMW panel and the timber on M-shaped UHMW panel both appear to be highly sensitive to the orientation of the loading foot and cold temperatures.

This abrupt change in strain indicates that the majority of the load was being taken by timber running planks for the panels constructed of UHMW and timber. Material tests discussed later in this section show that timber running planks had a flexural modulus of elasticity thirteen times that of the UHMW polyethylene. Creating a system with these two materials, with equal thicknesses, allows the neutral axis of bending to shift from the center of the section into the timber running planks. With the section no longer symmetric about the neutral axis, the bending curvature of the section creates greater strain values in the UHMW polyethylene layer. Laboratory tests confirmed that the timber running planks were taking the majority of the load as the planks began to crack. Figure 6.19 shows cracked running planks for the timber on M-shaped UHMW panel during the room-temperature tests.

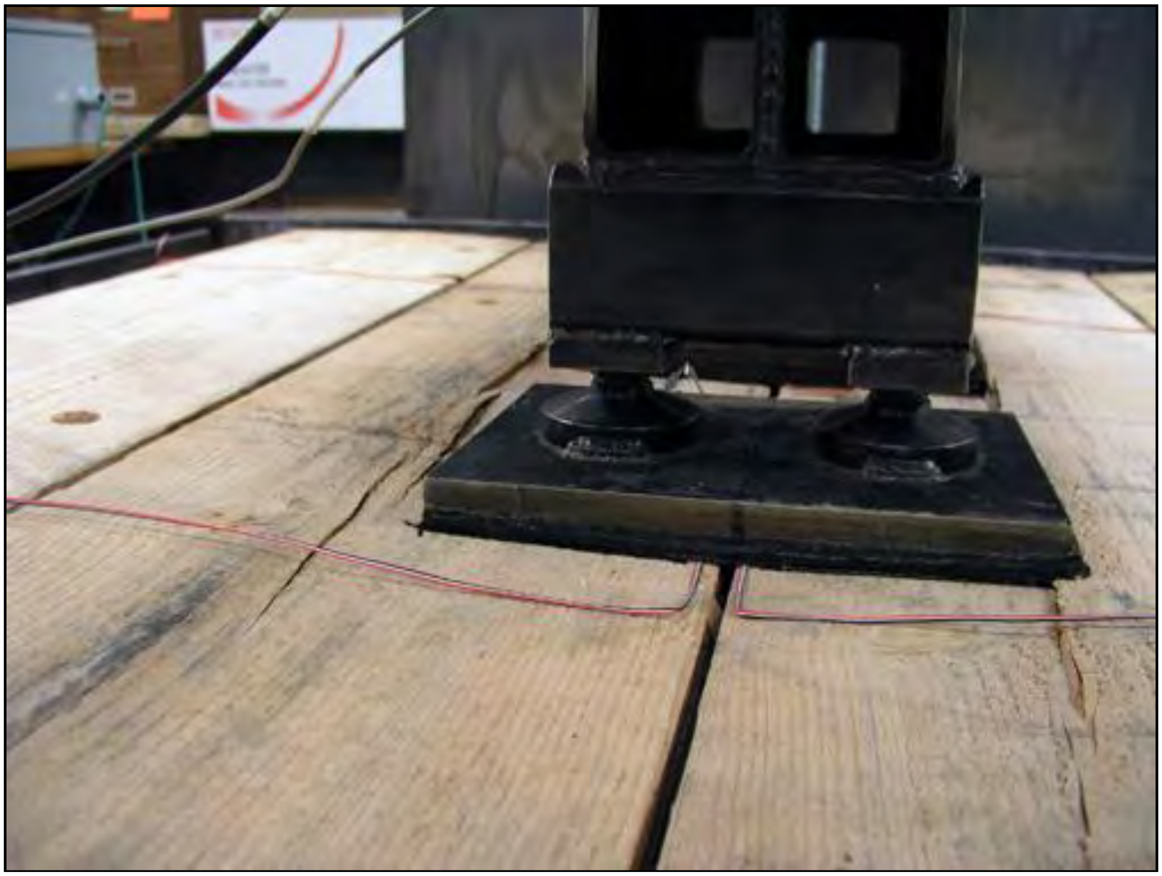

Figure 6.19 Timber on M-shaped panel with running planks cracking.

Stiffness for room-temperature tests was compared with the cold-temperature tests. This was done by determining the slope of the load-deflection curve. The slope is the effectiveness, and is reported in lb/in. Slope for the load-deflection curve was calculated using a secant line that passed through values at 25% and 75% of the maximum load. The maximum load for all tests was 16,000 lb; therefore, displacement values at 4,000 lb and 12,000 lb were used in the secant-line slope equation. Values of 25% and 75% were used because inspection of all load-deflection curves showed a linear region between these two values. Stiffness values for all five panels under three testing conditions are provided in Table 6.1.

Table 6.1 Stiffness Comparisons for All Five Panels

Experimental Panel	Room-Temperature Test, Longitudinal Orientation, k_{room} (lb/in.)	Room-Temperature Test, Transverse Orientation, k (lb/in.)	Cold-Temperature Test, Longitudinal Orientation, k_{cold} (lb/in.)	k_{cold} / k_{room}
Timber/Timber	44,422	46,420	48,439	1.09
Transonite	29,657	28,519	30,691	1.03
Super Panel	26,634	27,922	28,989	1.09
Timber on Solid UHMW	28,256	26,455	34,816	1.23
Timber on M-shaped UHMW	20,520	18,490	22,861	1.11

Table 6.1 shows that during the cold-temperature test, all panels demonstrated an increase in stiffness, and the timber/timber panel was the only panel to show an increase in stiffness as the orientation of the loading foot was changed.

Panel Failure Tests

In an attempt to reach the ultimate load-carrying capacity of the experimental bridge-deck panels, failure tests were conducted. Load was increased until the panel failed or the 35 k ram limit was reached. The details are explained in Jerla (2008). All failure tests were carried out at room temperature, with the load foot in the longitudinal direction.

Except for the Super Panel, none of the panels failed. The tests were terminated at the load limit of the testing frame. The load-displacement behavior of each panel is shown in Figure 6.20.

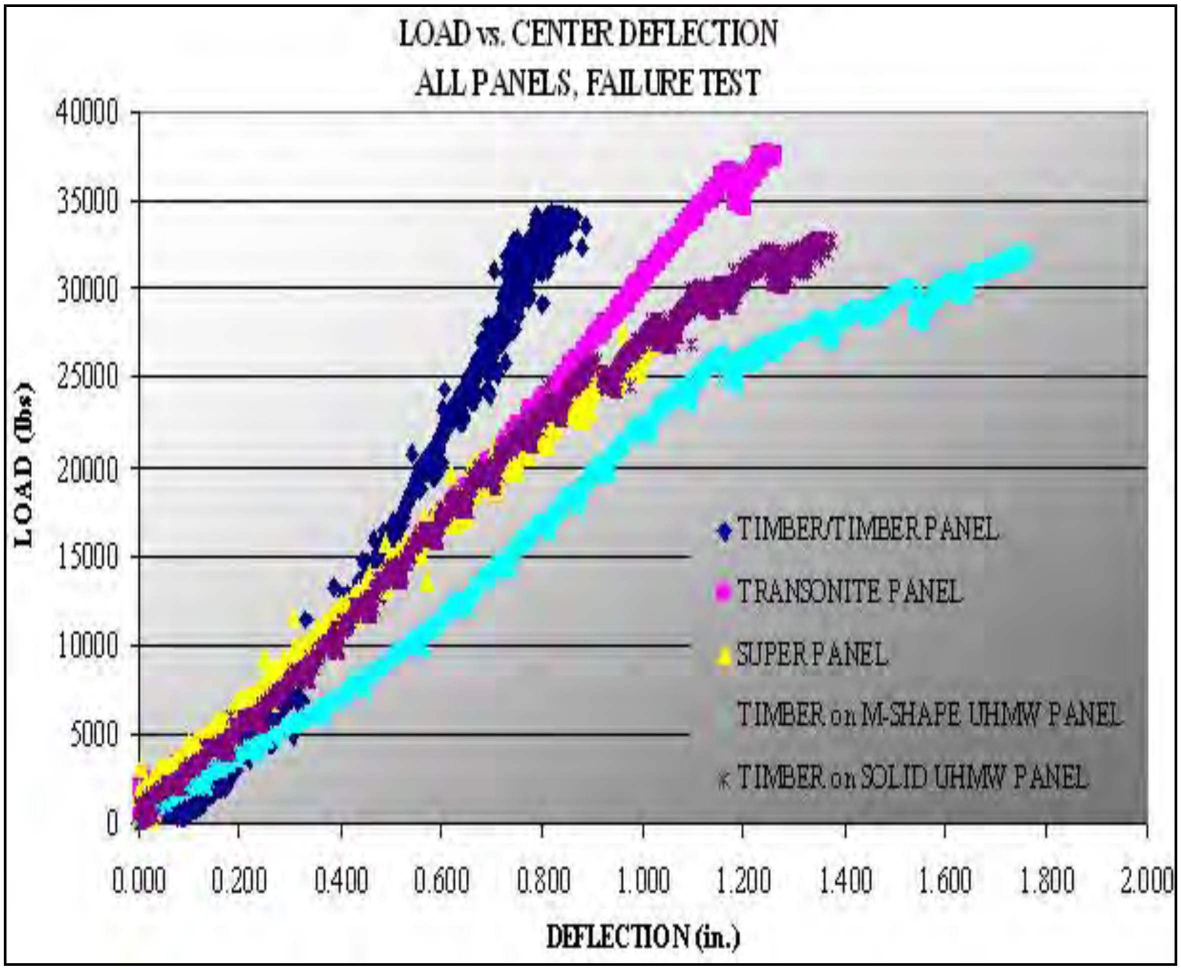

Figure 6.20 Failure test, load-deflection curve for all panels.

The stiff behavior of the timber/timber panel became more evident after the applied load passed 15,000 lb and the slope steepened. Except for the timber on M-shaped on UHMW, all panels showed similar behavior. Flexibility of the timber on M-shaped UHMW panel increases with load once the applied load is over 25,000 lb. This panel nearly reached 2 in. of deflection for an applied load near the 35,000 lb limit.

The Super Panel was supported on two edges; it acts as a stiffened one-way plate. This panel failed at 27,753 lb. We observed the first signs of failure at the lower intersection of the web and flange at the middle of the panel. As this failure progressed, the webs of the box-shape panel began to buckle. Post failure inspection of the panel revealed that several webs had buckled directly under the loading foot. We observed another mode of failure as the flanges sheared from the webs on the edges of the panel. Both of these modes of failure were seen during the material tests. Figure 6.21 shows the initial signs of failure observed during the Super Panel failure test.

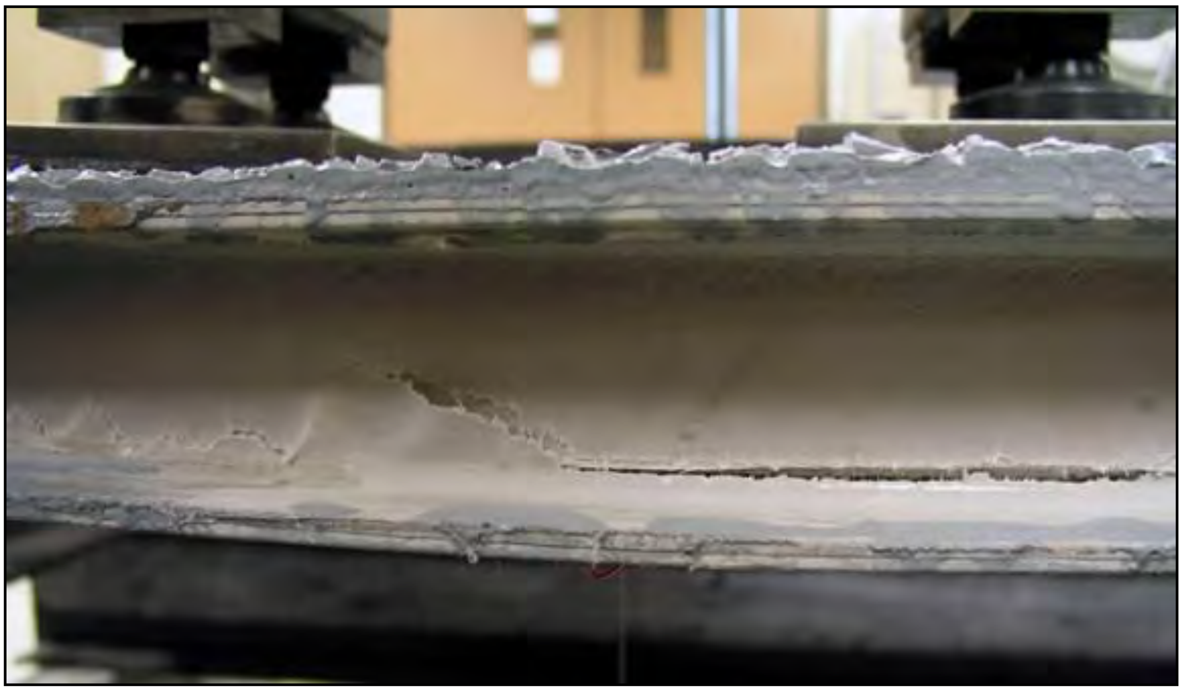

Figure 6.21 Super Panel at ultimate load-carrying capacity.

A load-strain curve for all five panels during the failure test is provided in Figure 6.22. The load-strain curve illustrates that the timber/timber and the Transonite panels demonstrate analogous behaviors in the presence of high loads. The additional panels demonstrated a similar load-strain curve, though different from the timber/timber and Transonite panels. The maximum load reached for the four full-size bridge-deck panels was around 35,000 lb. All panels supported load without failure, but timber began to exhibit signs of failure in the final stages of testing.

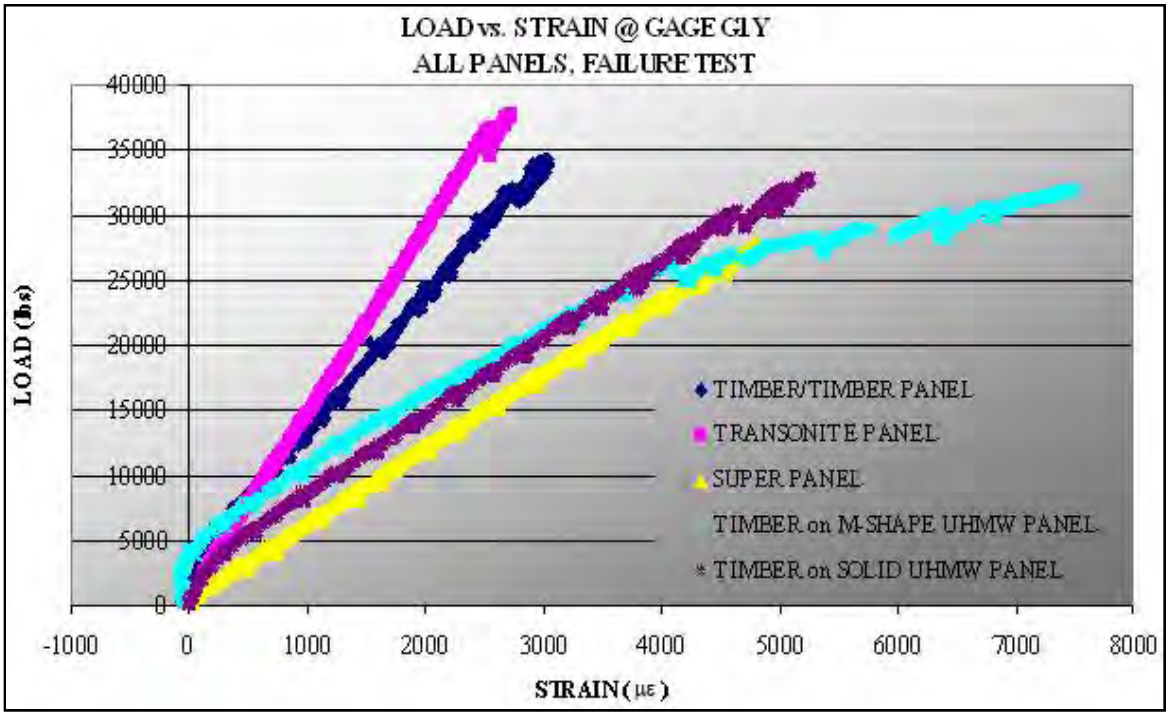

Figure 6.22 Failure test, load-strain curve for all panels.

On the timber/timber panel, large cracks developed in the bottom layer of the panel, as shown in Figure 6.23.

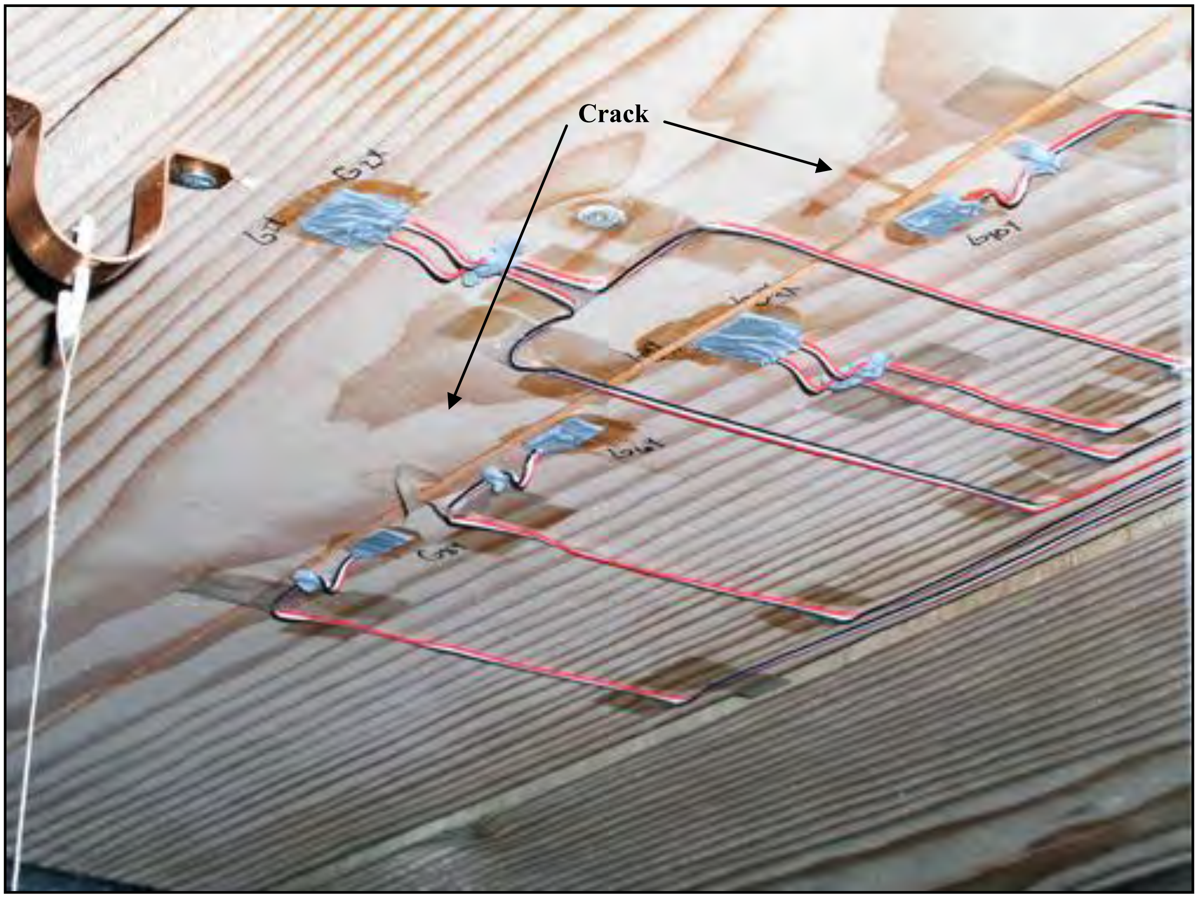

Figure 6.23 Timber/timber panel failure cracks.

CHAPTER 7 – MATERIAL TESTS

Material mechanical properties were determined through standardized ASTM material testing. Test procedures are outlined in detail by Jerla (2008). Tests were conducted to determine service load behavior and strengths for compression, tension, and flexure. Stress-strain curves for each test were evaluated and graphed. The unloading portion of the stress-strain graph is provided.

Transonite

Compressive tests for twelve different test specimens are provided in Table 7.1 and presented in Figure 7.1.

Table 7.1 Transonite Compression Specimens with Steel-Bearing Plate

Beam No.	Cross-Sectional Area (in.^{2})	Maximum Compressive Stress (psi)	Compressive Strain at Max. Stress (με)	Compressive Modulus of Elasticity (psi)
1	16.28	393	10975	24300
2	16.23	375	13040	18800
3	16.03	375	9924	33900
4	16.40	400	11648	15700
5	15.86	384	11192	25200
6	14.59	334	8812	33600
7	15.95	334	8387	32200
8	16.17	335	11878	19000
9	16.19	342	10025	21600
10	16.43	349	13786	15500
11	16.16	316	10232	27100
12	13.51	324	7105	55200
Average Strengths		**333**	**10032**	**29171**
Standard Deviation		**11**	**2247**	**13281**

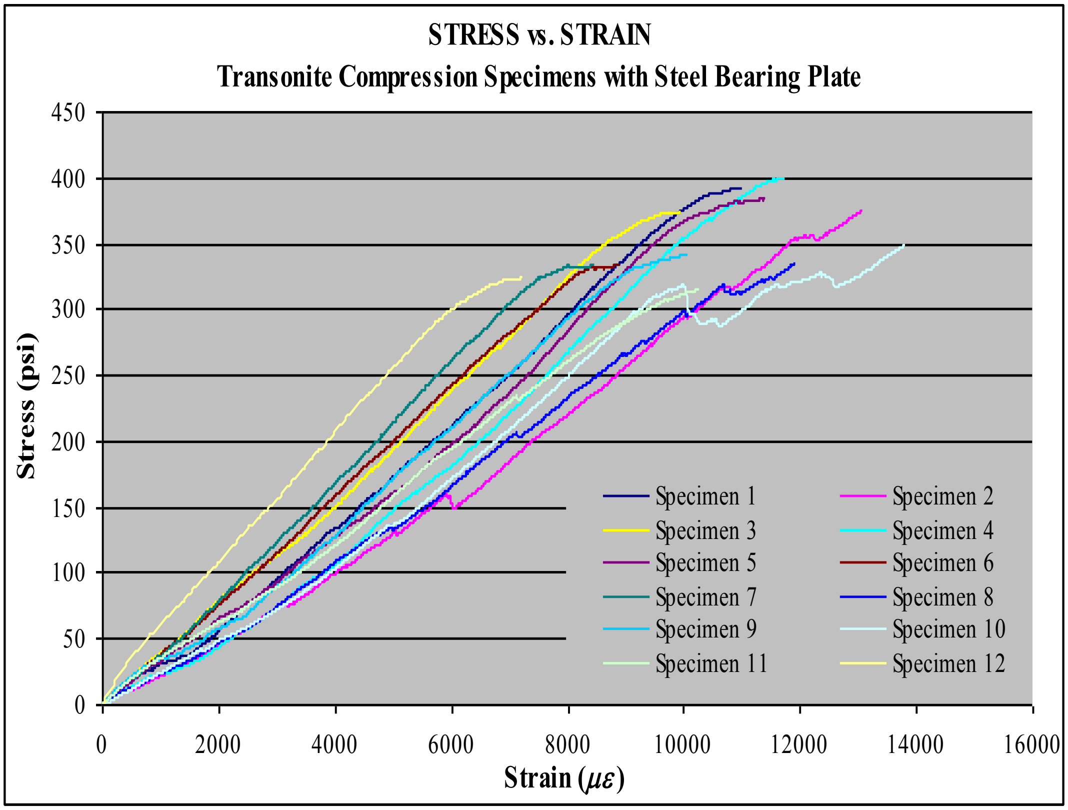

Figure 7.1 Compression stress-strain for Transonite.

Only two of the twelve specimens failed by crushing. The remaining ten specimens failed due to lateral instability. The two modes of failure are captured in the photographs presented in Figure 7.2.

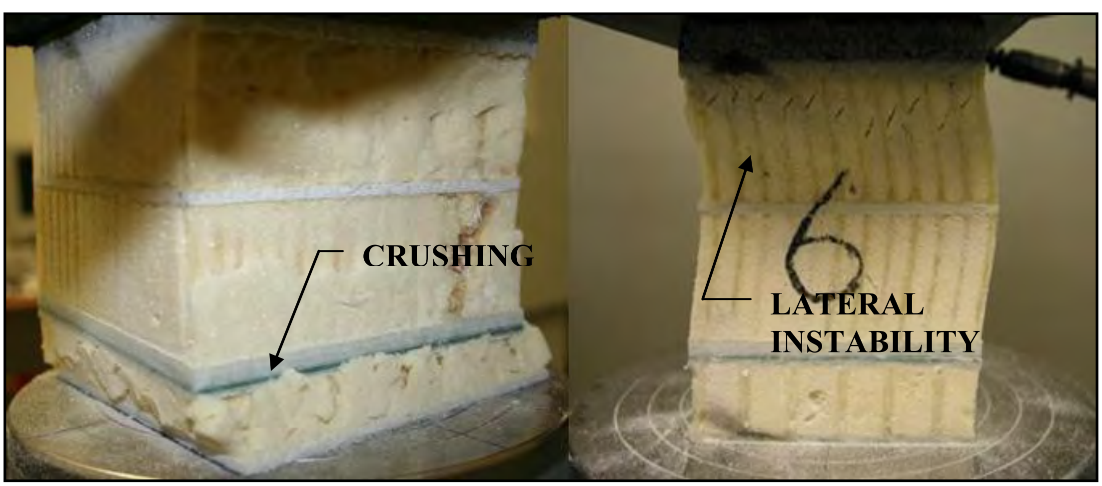

Figure 7.2 Failure of Transonite compression specimens.

When the specimens failed due to lateral instability, a secondary buckling failure occurred. The buckling failure became evident as the 3-D fiber insertions began to buckle on one side of the specimen due to eccentric loading in the system. The buckling of one fiber triggered a chain reaction in the neighboring fibers, resulting in the inability of the specimen to withstand the load.

A four-point bending test was performed to evaluate the material behavior of the Transonite material. Test beams cut from the Transonite panel were too large for the MTS, and the four-point bending test was performed using the load frame (Jerla, 2008). Experimental results from the four-point bending test are provided in Table 7.2.

Table 7.2 Transonite Four-Point Bending Specimens

Beam No.	**Cross-Sectional Area (in.^{2})**	**Moment of Inertia, I (in.^{4})**	**Maximum Flexural Stress (psi)**	**Flexural Strain at Max. Stress (με)**	**Flexural Modulus of Elasticity (psi)**
1	31.125	69.798	664	3373	236300
2	31.125	69.798	638	3821	216600
3	31.125	69.798	626	3296	236400
4	31.125	69.798	651	3184	298200
5	31.125	69.798	647	3278	275800
Average Strengths			**645**	**3390**	**252660**
Standard Deviation			**14**	**250**	**33323**

Stress was calculated using the flexure formula, and strain was measured (see Figure 7.3).

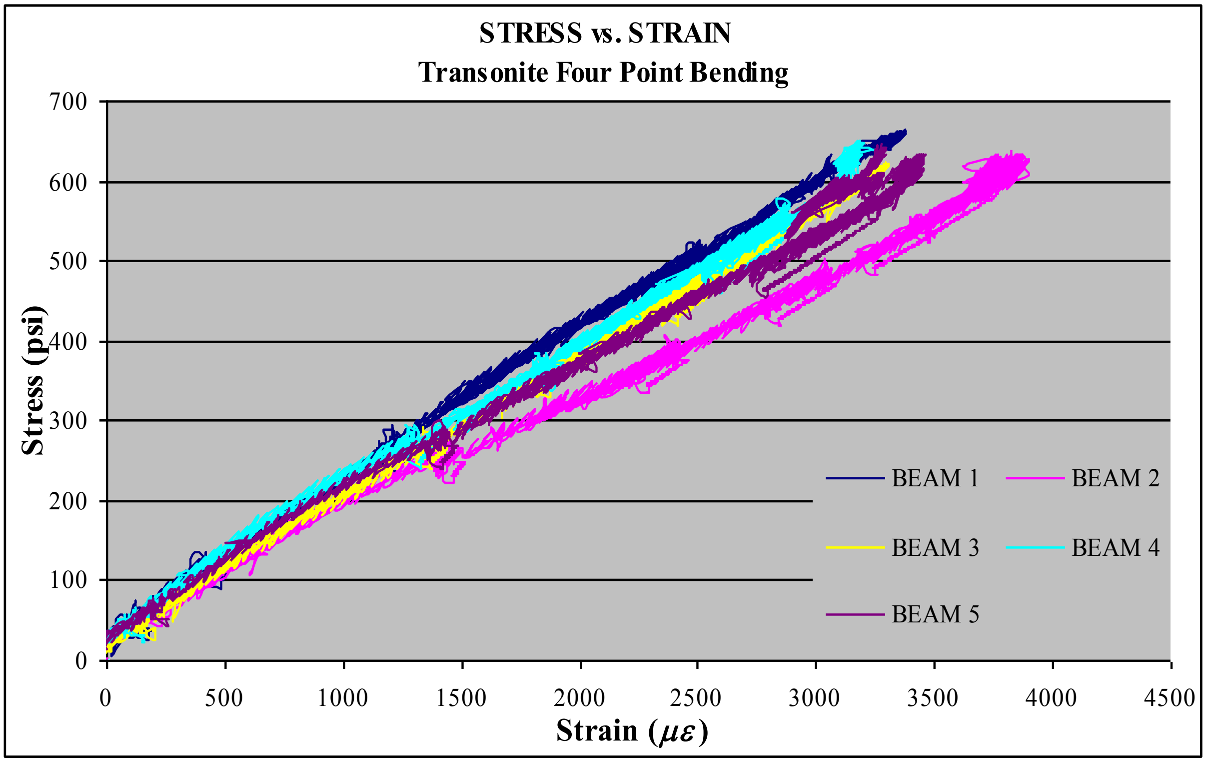

Figure 7.3 Stress-strain for Transonite under four-point bending.

Strain values for the five different tests were repeatable; that is, there was a low standard deviation of 14 at maximum flexural stress. As with the compression specimens, the modulus of elasticity was determined using the tangent line slope at zero strain.

During the test, all beams displayed an area of zero shear and pure bending. Forty-five degree shear cracks began to develop in the foam, as shown in Figure 7.4. Shear cracks became distinguishable in all five beams when the applied load was between 1000 lb and 1500 lb.

Figure 7.4 Transonite 45° shear cracks.

Based on the visual signs of shear, we speculated that the beam would have failed in shear if the bottom layer of the panel had not crushed at the supporting edges. All beams failed due to the bottom layer crushing at the supports; this failure potentially could have been avoided if the beam was placed on rollers. It is important to note that as the upper surface of the beam began to undergo large deflections, the traction surface cracked and could be peeled from the upper layer of Transonite with a small amount of pressure. Cracks in the traction surfaces formed immediately above the crushing of the lower layer, as illustrated in Figure 7.5.

Figure 7.5 Transonite four-point bending failures.

Douglas Fir

Douglas Fir compression parallel-to-grain tests were conducted in accordance with ATM standards (Jerla, 2008). Ten clear specimens were used in the test, and the average results are presented in Table 7.3.

Table 7.3 Douglas Fir Parallel-to-Grain Compression Specimens

Beam No.	Cross-Sectional Area (in.^{2})	Maximum Compressive Stress (psi)	Compressive Strain at Max. Stress (με)	Compressive Modulus of Elasticity (psi)
1	4.055	6557	8367	915200
2	4.088	7992	9424	979100
3	4.013	7885	8873	833800
4	4.021	7812	8746	861300
5	4.016	7925	9310	811300
6	4.015	8700	9326	897200
7	4.017	7545	8683	882600
8	4.017	8149	8567	863300
9	4.022	7875	9671	802100
10	4.024	6284	7176	717900
Average Strengths		**7672**	**8814**	**856380**
Standard Deviation		**726**	**713**	**71189**

The tested average maximum compressive stress was 7672 psi. This value is significantly higher than the clear wood Douglas Fir strength of 3610 psi that is published in ASTM D 2555-06, Table 3. Strength values for Douglas Fir tend to vary due to moisture content, age of wood, and the purity of the specimen. All these factors may have contributed to the 72% difference in strength values. Stress-strain curves for parallel-to-grain tests were linear and similar for stresses 4000 psi (see Figure 7.6). Maximum compressive stresses were between 6500 psi and 8900 psi. The maximum compressive stress between specimens varied by 2416 psi. The average compressive modulus of elasticity for these specimens is 856,380 psi.

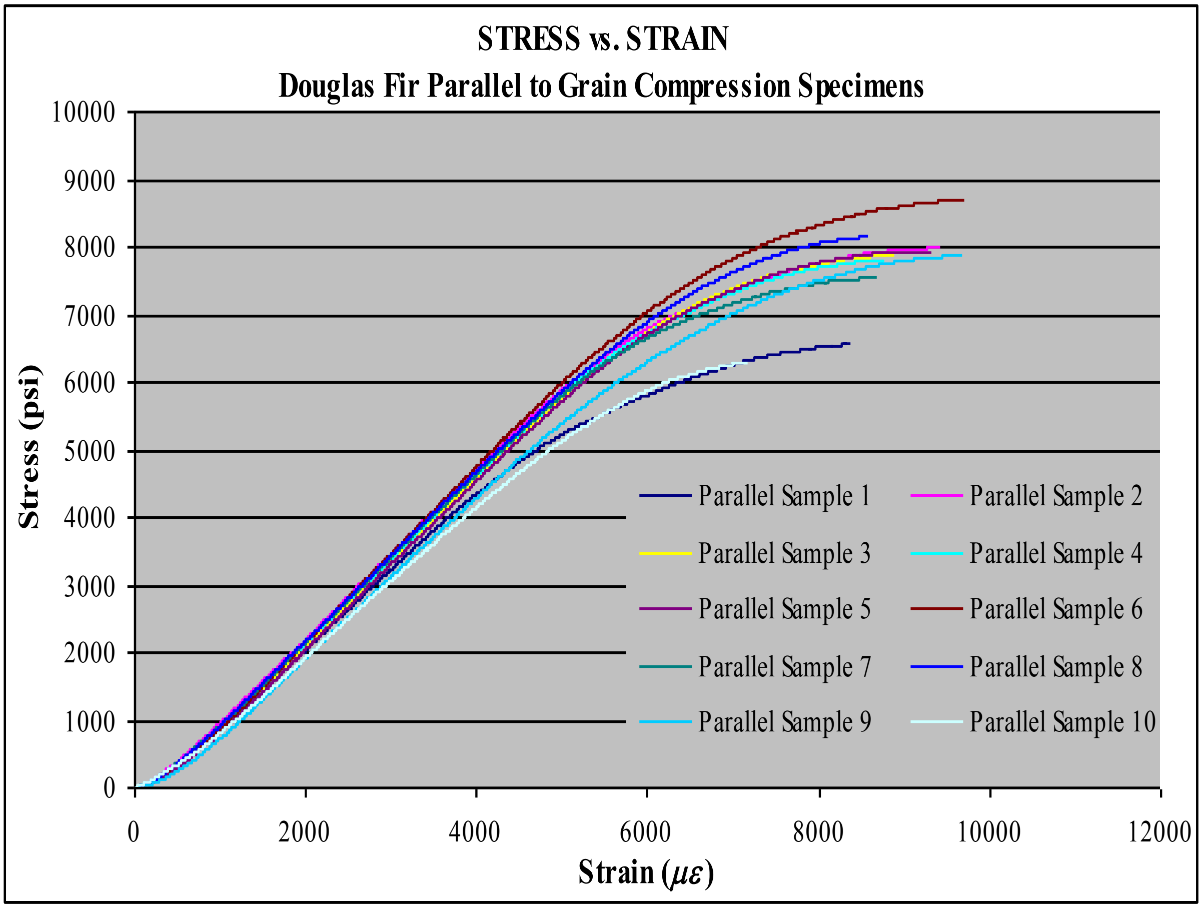

Figure 7.6 Stress-strain Douglas Fir parallel-to-grain compression specimens.

The cause of failure for all ten specimens was a combination of shearing or compression and shearing parallel to the grain. Specimen 3 (see Figure 7.7) showed signs of compression and shearing as horizontal cracks started to form parallel to the grain in conjunction with the shearing cracks. The second specimen in Figure 7.7 experienced a shear failure. The plane of rupture made an angle of roughly 45° with the top of the specimen. The cracks are outlined in the photograph to provide clarity.

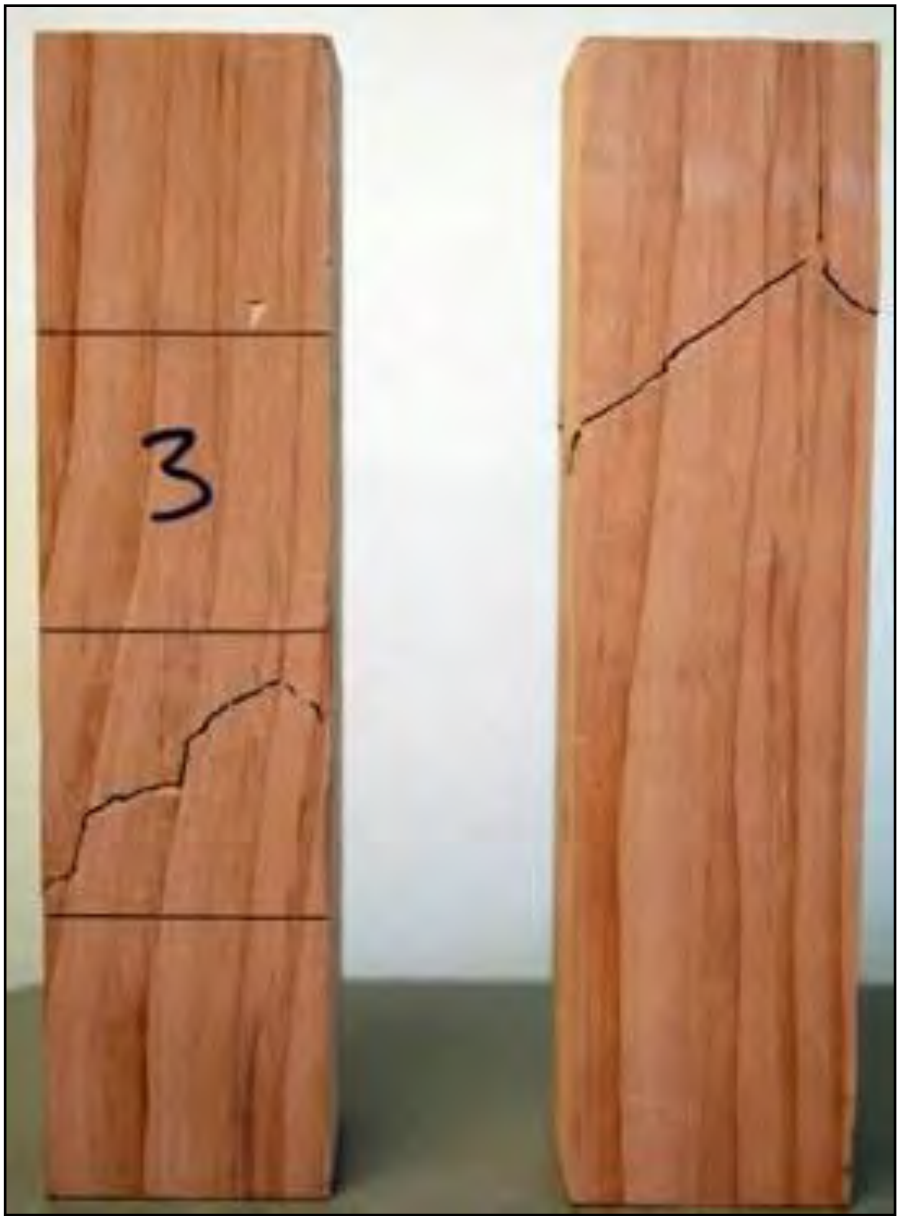

Figure 7.7 Compression parallel-to-grain failure.

Compression perpendicular-to-grain tests were also conducted for Douglas Fir, and these test results are presented in Table 7.4.

Table 7.4 Douglas Fir Perpendicular-to-Grain Compression Specimens

Specimen No.	Cross-Sectional Area (in.^{2})	Maximum Compressive Stress (psi)	Compressive Strain at Max. Stress (με)	Compressive Modulus of Elasticity (psi)
1	4.041	618	23146	53900
2	4.020	625	23996	57800
3	4.023	608	26420	44400
4	4.055	572	22268	57500
5	4.059	628	26475	55100
6	4.019	525	24725	54600
7	4.045	657	29060	53000
8	3.996	581	25764	52000
9	4.041	620	24882	47000
10	4.031	633	29026	51300
Average Strengths		**607**	**25576**	**52660**
Standard Deviation		**38**	**2264**	**4266**

As with the parallel-to-grain specimens, the perpendicular-to-grain specimens exhibited a higher compressive stress than the published ASTM values. The average compressive stress reported by ASTM D 2555-06 is 460 psi, 27% less than the average stress of 607 psi recorded in the laboratory. Stress and strain were calculated at all force and deflection intervals until the maximum compressive load was attained (see Figure 7.8).

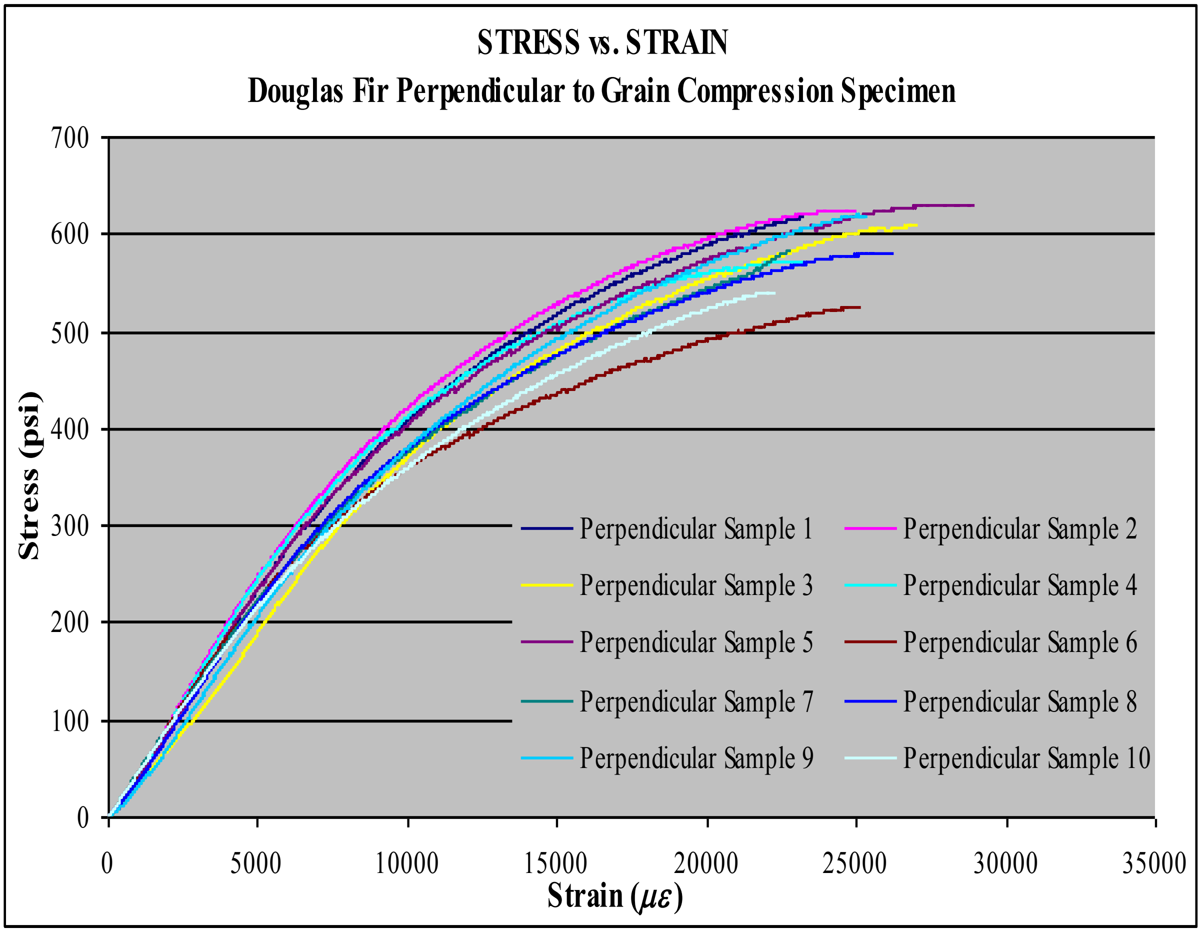

Figure 7.8 Compression: Stress-strain, Douglas Fir, perpendicular to grain.

Below 350 psi, specimens experienced approximate linear behavior. Above 350 psi, compressive stress varied between samples. However, the variation in maximum compressive strength was minor; the standard deviation was 38. The majority of specimens failed in crushing, as the plane of rupture was approximately horizontal with the compression platens (see Figure 7.9).
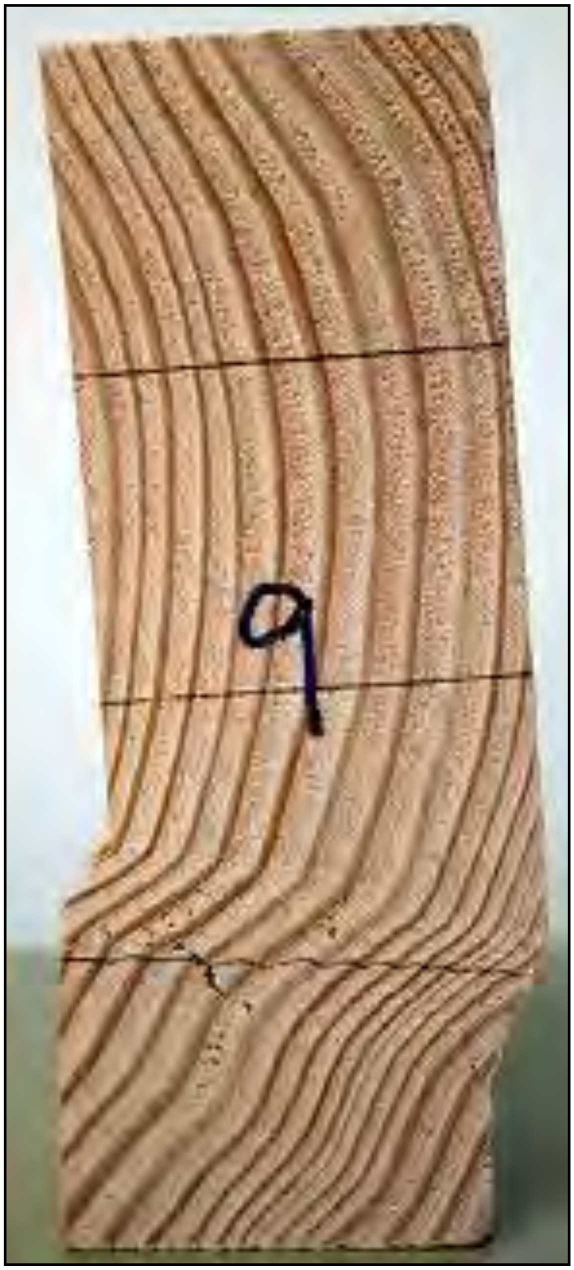
Figure 7.9 Compression perpendicular-to-grain failure.

Flexural properties for the Douglas Fir were determined using a three-point bending test. Specimens were ½ in. by 2 in. by 12 in., and had a span-to-depth ratio of 16 (Jerla, 2008). See Table 7.5 for the results, and Figure 7.10.

Table 7.5 Douglas Fir Three-Point Bending Specimens

Beam No.	Cross-Sectional Area (in.^{2})	Moment of Inertia, I (in.^{4})	Maximum Flexural Stress (psi)	Flexural Strain at Max. Stress (με)	Flexural Modulus of Elasticity (psi)
1	1.020	0.023	14801	11325	1916900
2	1.008	0.022	14092	11427	1902700
3	1.041	0.024	15140	10829	2256000
4	1.019	0.023	12229	10230	2180500
5	1.013	0.022	10976	9685	2028900
6	1.046	0.024	12696	11537	2226300
7	1.034	0.023	8586	8847	1834700
8	1.017	0.023	8588	7971	1980500
9	1.048	0.024	7874	9308	1959600
10	1.022	0.022	5677	5809	1924200
Average Strengths			**11066**	**9697**	**2021030**
Standard Deviation			**3253**	**1812**	**148022**

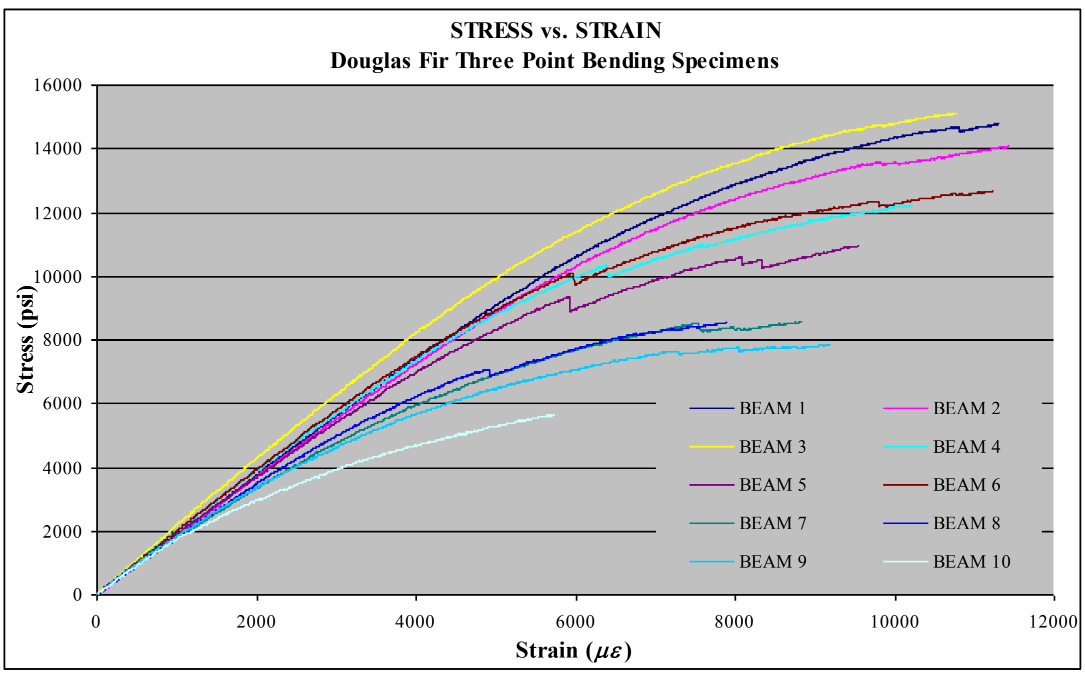

Figure 7.10 Douglas Fir: Flexural stress-strain, three-point bending.

The average flexural modulus for the ten specimens is 2,021,030 psi. The value published in ASTM D 2555-06, Table 3, is approximately 22% lower at 1,613,000 psi. The bending failure seen in all the beam specimens was a splintering tension. The early wood showed a brash failure as the late wood displayed a fibrous failure. Figure 7.11 shows the bending failure.

Figure 7.11 Douglas Fir three-point bending splintering tension.

Results for material tests indicate that the overall strength of the Douglas Fir used in the makeup of the experimental panels was higher than ASTM published values. The flexural modulus of elasticity was determined to be approximately 22% greater than the published ASTM value. Tension and compression material test results were also higher than published values. For example, parallel-to-grain maximum compressive stress was 72% higher, and perpendicular-to-grain maximum compressive stress was 27% higher.

UHMW Polyethylene

Stress-strain for tension, compression, and bending were determined through testing. Test procedures for these tests were described by Jerla (2008). Stress-strain results for eleven dumbbell-shaped tension specimens are presented in Table 7.6.

Table 7.6 UHMW Polyethylene Tension Specimens

Specimen No.	Cross-Sectional Area (in.^{2})	Maximum Tensile Stress (lb/in.^{2})	Tensile Strain at Max. Stress (με)	Tensile Modulus of Elasticity (psi)
1	0.56	3725	149395	105768
2	0.56	3851	146964	119174
3	0.56	3903	142326	113989
4	0.56	3964	143541	110369
5	0.56	4025	149750	126060
6	0.56	4125	144709	125829
7	0.56	4149	151988	119500
8	0.56	4214	148163	120625
9	0.56	4270	147583	125017
10	0.57	4344	151839	108361
11	0.56	4398	160267	107522
Average Strengths		**4250**	**150758**	**117809**
Standard Deviation		**108**	**5413**	**8027**

Maximum tensile stress was calculated by dividing maximum tensile force by average cross-sectional area within the gage-length segment of the specimen. Average tensile strength for these specimens was 4250 psi, with a standard deviation of 108 psi. Ultra Poly, the producer of the UHMW polyethylene, posted a tensile break stress between 4200 psi and 5000 psi for the product. By comparison, published values for the UHMW polyethylene and the tested values were nearly equal.

Strain was recorded instantaneously using a MTS model 632.25B-20 extensometer. The relationship between stress and strain was nonlinear (see Figure 7.12). Therefore, modulus was based on a secant calculation between 25% and 50% of the maximum stress.

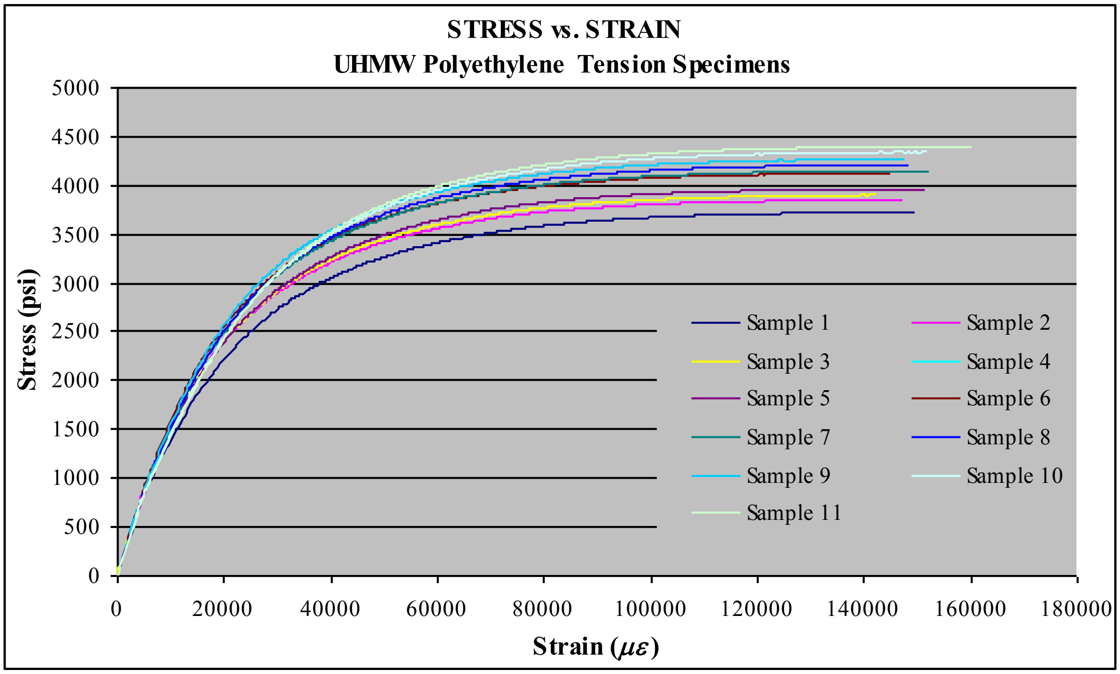

Figure 7.12 Stress vs. strain UHMW polyethylene tension specimens.

Compression specimens were loaded at two different load rates to verify yield (see Table 7.7).

Table 7.7 UHMW Polyethylene Compression Specimens

Specimen No.	Loading Rate (in./min)	Cross-Sectional Area (in.^{2})	Maximum Compressive Stress (psi)	Compressive Strain at Max. Stress (με)	Compressive Modulus of Elasticity (psi)
1	0.05	1.00	5213	278887	41303
2	0.05	1.00	4847	259111	45855
3	0.05	1.00	4627	267192	41430
4	0.05	1.00	3969	211565	46206
5	0.05	1.00	4457	259318	35733
Average Strengths			**4623**	**255214**	**42105**
Standard Deviation			**462**	**25696**	**4260**
7	0.25	1.00	4773	250548	50176
8	0.25	1.00	4759	234475	59955
9	0.25	0.99	4339	211646	55495
10	0.25	1.00	4852	223992	59556
11	0.25	0.98	4746	229498	52115
12	0.25	1.00	4511	217049	52874
13	0.25	1.00	4675	211849	65725
Average Strengths			**4665**	**225580**	**56556**
Standard Deviation			**179**	**13999**	**5473**

Results show that average maximum compressive stress was nearly the same for the two loading rates. The average modulus values differed by 29%, however, with the higher loading rate resulting in a stiffer modulus. The stiffer modulus for specimens loaded at a faster rate was not unexpected, as strain values for these specimens are lower. Ultra Poly does not report a compressive stress for its product. Stress-strain curves for all specimens are displayed in Figure 7.13.

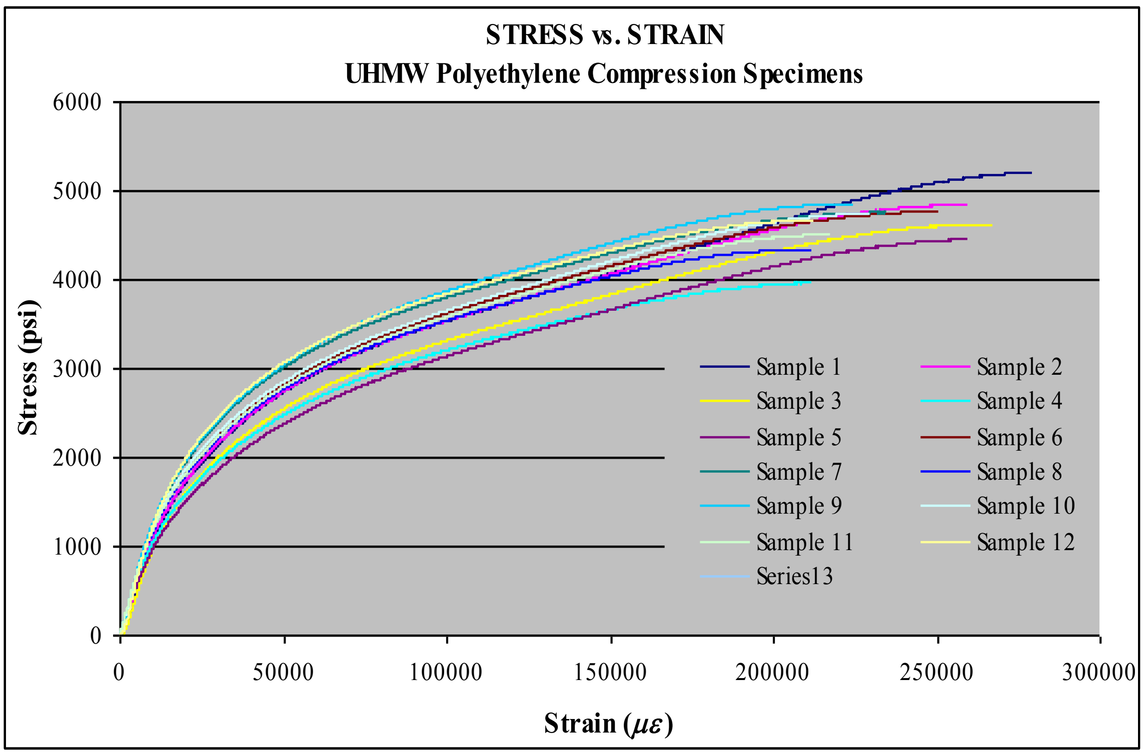

Figure 7.13 Stress vs. strain UHMW polyethylene compression specimens.

As with tension, a secant calculation was used to determine the modulus. Failure of the compression specimens was not observed during testing. Instead, the specimen developed excessive deformation. Figure 7.14 shows a specimen prior to testing (Specimen 6) and another specimen after testing (Specimen 12).

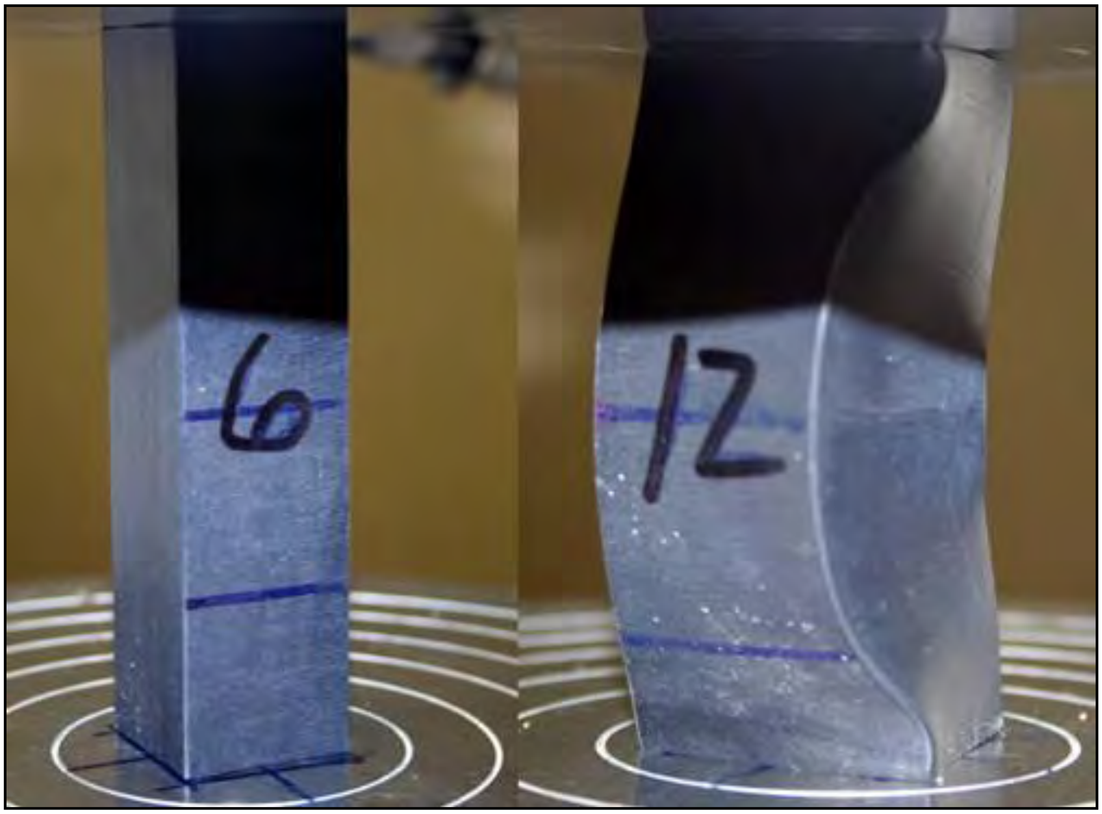

Figure 7.14 UHMW polyethylene compression failure.

Material bending properties were determined using a three-point bending test. Experimental results for nine specimens are provided in Table 7.8.

Table 7.8 UHMW Polyethylene Three-Point Bending Specimens

Beam No.	**Cross-Sectional Area (in.^{2})**	**Moment of Inertia, I (in.^{4})**	**Maximum Flexural Stress (psi)**	**Flexural Strain at Max. Stress (με)**	**Flexural Modulus of Elasticity (psi)**
2	0.930	0.011	4651	47821	152900
3	0.930	0.011	4948	50725	164700
4	0.935	0.011	4618	48652	147200
5	0.930	0.011	4553	48302	145300
6	0.936	0.011	4772	52438	145600
7	0.943	0.011	4934	55069	158600
8	0.936	0.011	4904	52078	160400
9	0.936	0.011	4876	53836	148100
10	0.930	0.011	4568	47901	140500
Average Strengths			**4758**	**50758**	**151478**
Standard Deviation			**163**	**2736**	**8140**

Flexural modulus of elasticity was computed by determining the slope of a third-order polynomial best-fit line for the stress-strain values. Stress versus strain for the bending tests is shown in Figure 7.15.

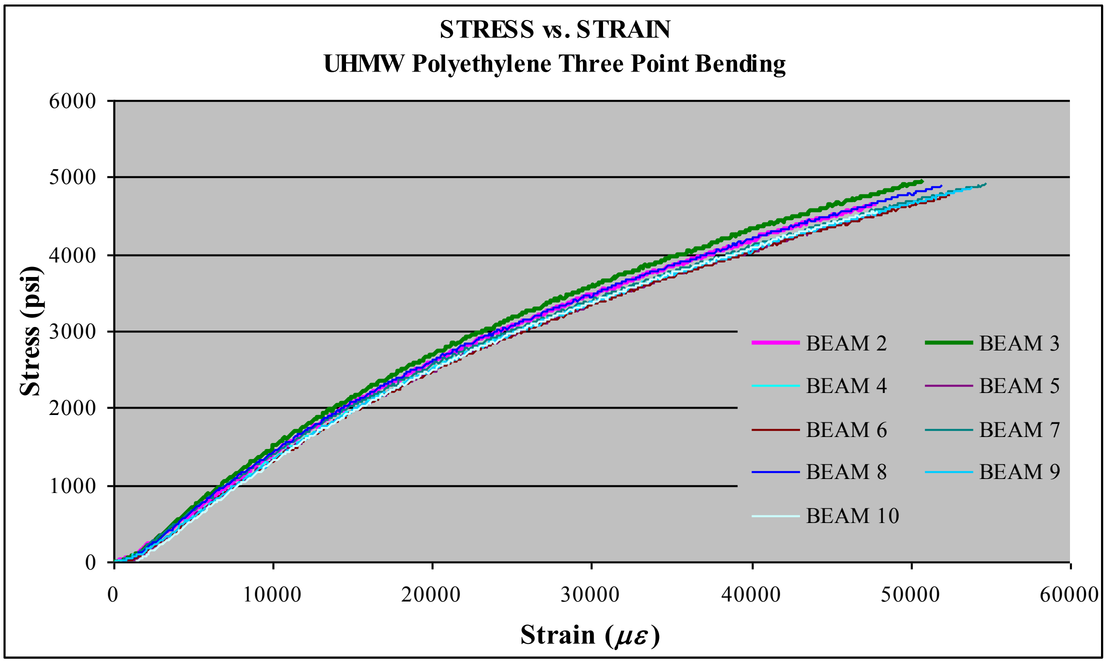

Figure 7.15 UHMW: Flexural stress-strain three-point bending.

The average flexural modulus for the UHMW polyethylene was 151,478 psi. Ultra Poly reports a flexural modulus between 111,000 psi and 140,000 psi. The slightly higher modulus was expected because the span-to-depth ratio was 10.6. This is less than the recommended 16 to 32 value. A smaller ratio resulted in a stiffer test and did not compromise the integrity of the results.

It is evident from the stress-strain graph that the nine beams tested exhibited the same behavior. Again, failure was not achieved, as the specimens were very ductile and continued to deform with increased load. This ductility, illustrated in Figure 7.16, shows a specimen near its maximum flexural stress.

Figure 7.16 UHWM polyethylene three-point bending failure.

Super Panel

Compression and three-point bending tests were performed to evaluate the material property makeup of the Super Panel. The full-size Super Panel was destroyed during the failure test. Subsequently, only a limited number of specimens were available for material tests. Eight compression specimens and three bending specimens were tested. Compression test results are presented in Table 7.9.

Table 7.9 Super Panel Compression Specimens

Specimen No.	Cross-Sectional Area (in.^{2})	Maximum Compressive Stress (psi)	Compressive Strain at Max. Stress (με)	Compressive Modulus of Elasticity (psi)
1	0.495	15845	56345	31300
2	0.461	17706	58444	190900
3	0.459	10829	49174	86800
4	0.493	14064	50654	171300
5	0.518	17882	61395	96200
6	0.536	17581	50039	87300
7	0.491	15152	39852	170400
8	0.451	17023	50175	293000
Average Strengths		**15760**	**52010**	**140900**
Standard Deviation		**2413**	**6689**	**82149**

Maximum compressive stress was calculated by dividing the maximum load by the original minimum cross-sectional area of the specimen's web. Compressive strain was calculated by dividing change in the specimen's height by the original measured specimen height. Compressive modulus of elasticity was determined by the slope-of-the-line tangent to the stress-strain curves. Super Panel compressive stress-strain is shown in Figure 7.17.

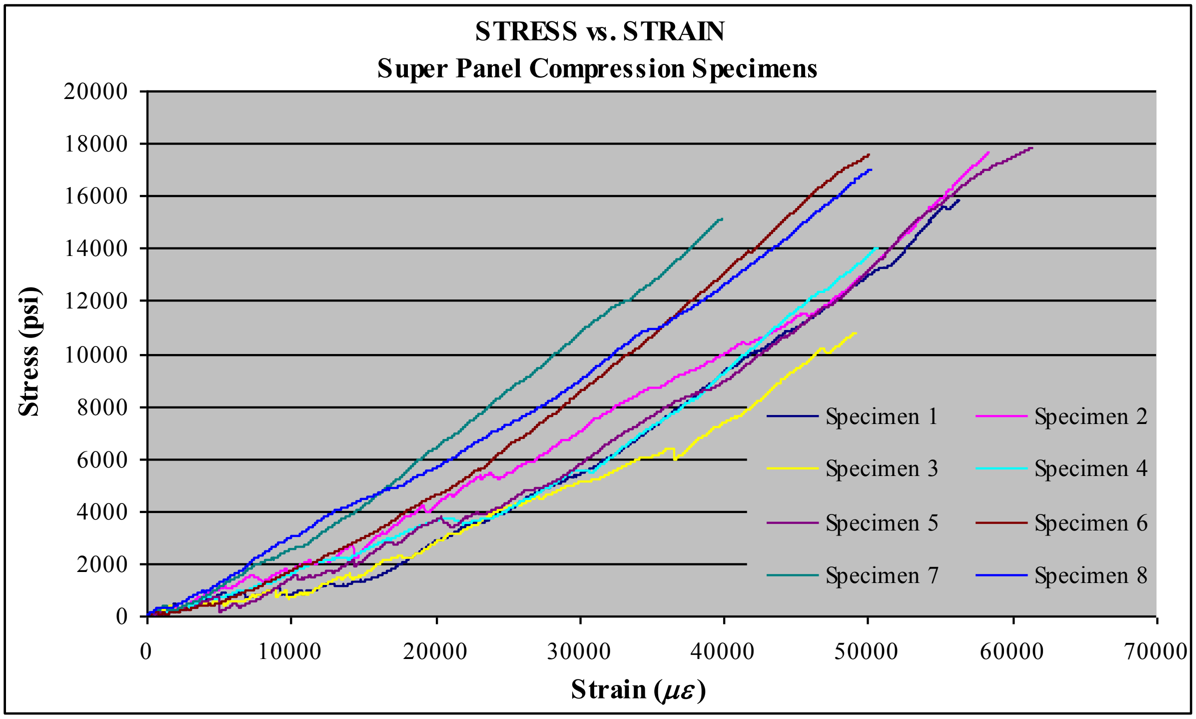

Figure 7.17 Stress vs. strain, Super Panel compression specimens.

Variation in maximum compressive stress was 7053 psi. Modulus varied by 261,700 psi. Variation-in-strength values likely occurred due to irregularities in the traction surface; this affected height-measurement accuracy. These irregularities occurred during manufacturing. Recall that the Super Panel was created using a pultrusion process that resulted in a fiber-reinforced polymer profile. Schedule and orientation of the reinforcement lay-up can change from one set to another, also causing the ultimate strength of the material to change. Although there is variation in the compressive strength values, the failure modes were the same. All specimens failed in compression due to a shattering facture. This mode of failure is characteristic of low-ductility materials such as the Super Panel. When a shattering

fracture occurs, the maximum strength threshold can be identified more easily. Figure 7.18 shows examples of web failure observed in all specimens.

Figure 7.18 Super Panel compression specimens.

Super Panel's flexural strength was tested using a three-point bending test. Three beams were tested with a support-to-span ratio of 5.6. Results are provided in Table 7.10. Stress-strain curves for the three beams are provided in Figure 7.19.

Table 7.10 Super Panel Three-Point Bending

Beam No.	Cross-Sectional Area (in.^{2})	Moment of Inertia, I (in.^{4})	Maximum Flexural Stress (psi)	Flexural Strain at Max. Stress (με)	Flexural Modulus of Elasticity (psi)
1	2.894	3.0426	12599	29517	407700
2	2.894	3.0426	12967	28436	338400
3	2.894	3.0426	12836	24620	349300
Average Strengths			**12801**	**27524**	**365133**
Standard Deviation			**187**	**2572**	**37265**

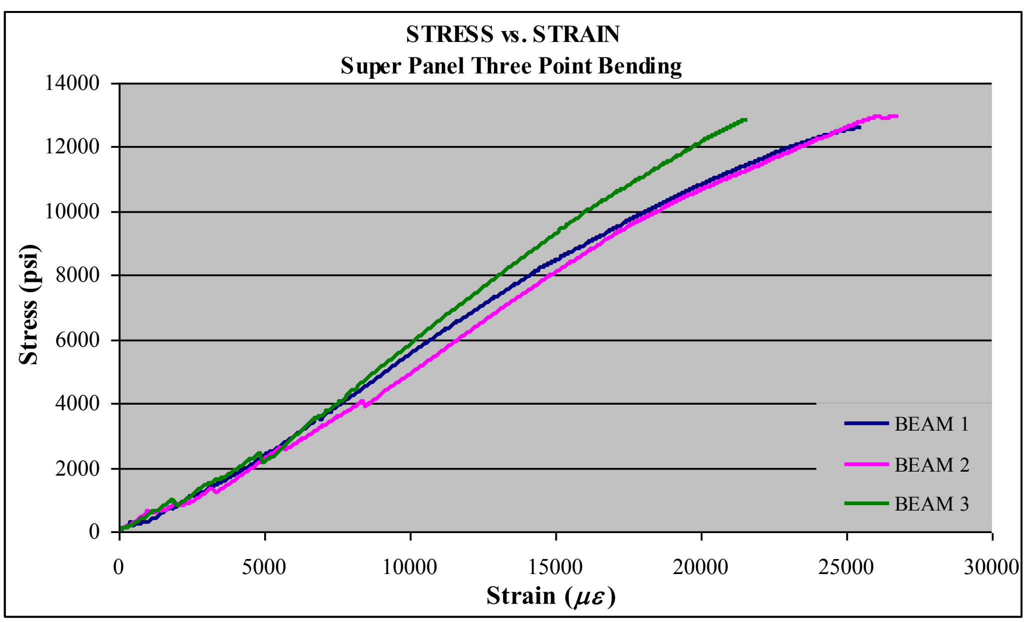

Figure 7.19 Stress vs. strain, Super Panel, three-point bending specimens.

A clear failure point in the load-deflection curve was observed in all three beams; this was similar to the compression specimens. Sudden failures in the beams indicate how the low-ductile material behaves under load. The stress-strain curve remained linear until failure, and the flexural modulus of elasticity was computed as the slope of the tangent line. Although the beam stress-strain curves are similar, there were two different modes of failure. In Beams 1 and 3, failure started by the upper flange, shearing from the web. Shortly thereafter, the web buckled directly under the loading point. Figure 7.20 depicts shear failure at the ends of the beams and the buckling of the web that occurred after the shear failure.

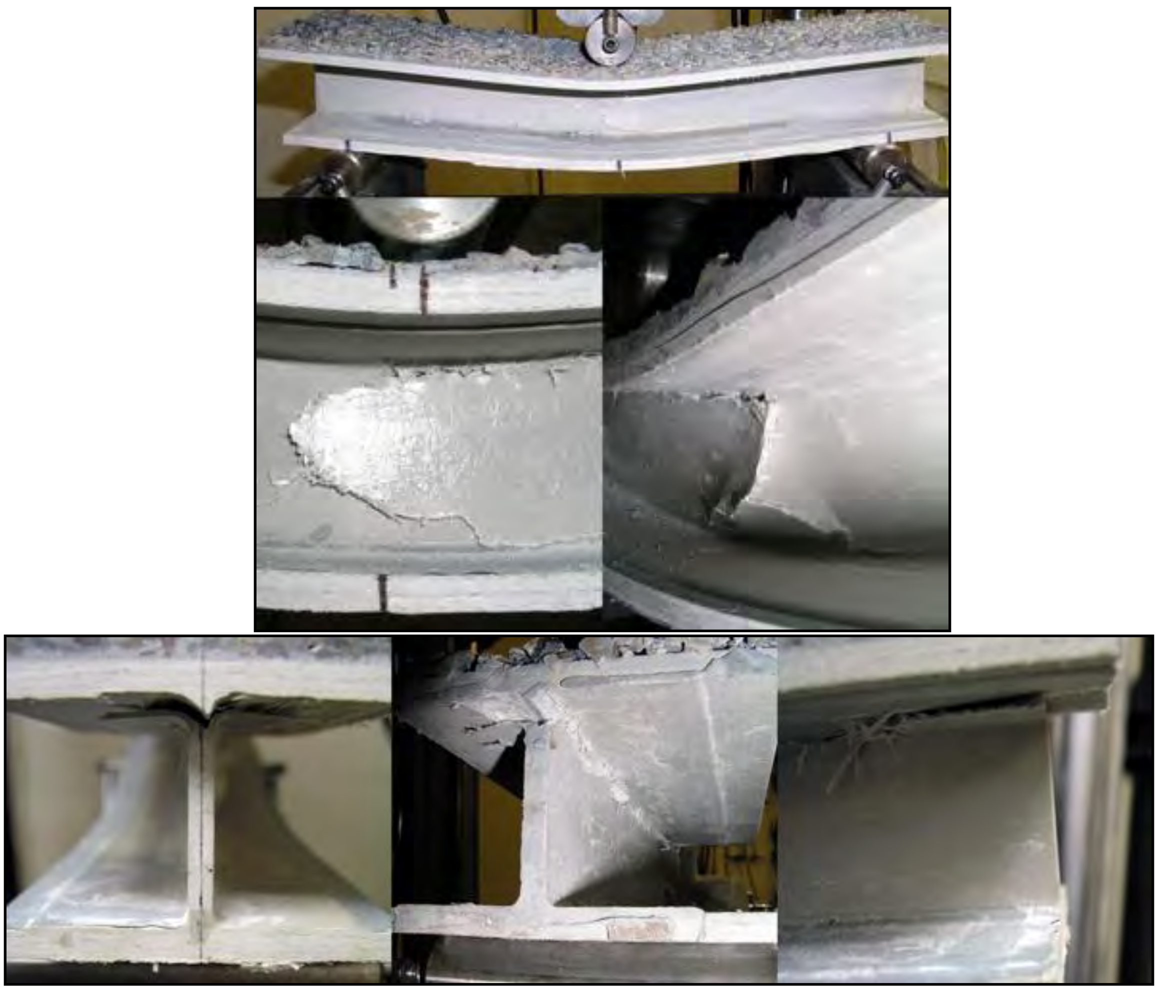

Figure 7.20 Super Panel web buckling and flange shear in Beams 1 and 3.

Beam 2 failed in a completely different manner than Beams 1 and 3. In this beam, a local crushing failure occurred in the upper flange and area of the web directly below the point of load. At the point of rupture, the web crushed and the reinforcement layer in the flange began to separate. Continuous loading of the beam caused separation in the flange layer to become more pronounced, and the web continued to crush. Figure 7.21 shows the local failure of Beam 2.

Figure 7.21 Super Panel local crushing failure in Beam 2.

Panel Material Comparisons

Tables 7.11 through 7.13 present summaries of material test findings for all four materials. The tables provide the strength values for each structural property (flexural, compressive, and tensile). Table 7.11 shows the flexural properties, Table 7.12 provides the compressive properties, and Table 7.13 shows the tensile properties for UHMW polyethylene.

Table 7.11 Material Test Flexural Properties

Material	Flexural Properties		
	Maximum Flexural Stress (psi)	**Flexural Strain at Max. Stress (με)**	**Flexural Modulus of Elasticity (ksi)**
Transonite	645	3,390	253
Douglas Fir	11,066	9,697	2,021
UHMW Polyethylene	4,758	50,758	151
Super Panel	12,801	27,524	365

Table 7.12 Material Test Compressive Properties

Material	Compressive Properties		
	Maximum Compressive Stress (psi)	**Compressive Strain at Max. Stress (με)**	**Compressive Modulus of Elasticity (psi)**
Transonite	355	10,584	26,842
Douglas Fir Perpendicular to Grain	607	25,576	52,660
Douglas Fir Parallel to Grain	7,672	8,814	856,380
UHMW Polyethylene (Loading Rate 0.05 in./min.)	1,457	30,750	54,147
UHMW Polyethylene (Loading Rate 0.25 in./min.)	3,469	135,506	63,345
Super Panel	15,760	52,010	140,900

Table 7.13 Material Test Tensile Properties

Material	**Tensile Properties**		
	Maximum Tensile Stress (psi)	**Tensile Strain at Max. Stress (με)**	**Tensile Modulus of Elasticity (psi)**
UHMW Polyethylene	4,250	150,758	118,000

CHAPTER 8 – TRACTION AND DAMAGE TESTS

Four new and two old wearing-surface materials were laboratory tested. The four new wearing surfaces were:

- Transonite
    - This product was supplied by Martin Marietta, Inc. at no cost to the research project. Transonite was installed on the bridge as an experimental feature in the summer of 2005.
    - Martin Marietta provided one 4 ft × 4 ft panel for use in testing structural integrity, and five 18 in. wide × 24 in. long × 5 in. thick samples for use in testing traction and damage caused by tire chains.
- Timber
    - This product was supplied by AKDOT&PF at no cost to the project.
    - AKDOT&PF provided five 2½ in. × 12 in. × 12 ft Douglas Fir #2 boards for testing structural integrity, traction, and damage caused by tire chains.
    - These timbers represent the type of product that has been used repeatedly as a temporary wearing surface since 1976.
- UHMW
    - Ultra Poly, Inc. provided a ultra high-density polyethylene at no cost to the research project.
    - Two types of 5-in.-thick 4 ft × 4 ft panels were provided for study. One was solid and the other was M-shaped, the bottom being corrugated to save weight and material.

    - Five 18 in. × 24 in. solid panels were supplied for testing traction and damage caused by tire chains.
- Super Panel
    - Compositech, Inc. in cooperation with Creative Pultrusions, Inc. supplied a sample at no cost to the research project.
    - This product is a fiber-reinforced panel that was manufactured by Creative Pultrusions, Inc. for floors in well-drilling housings on the North Slope, and adapted for this test by Compositech by providing a local aggregate wear surface that was applied with methyl methacrylate.

Two old wearing surfaces were tested for traction to provide a baseline for comparison:

- Cobra X (age 14 years)
    - In 1992, AKDOT&PF took the initiative and installed an experimental wearing surface on the Yukon River Bridge, using a 2½ in. deep lightweight high-density polyethylene (HDPE) grade-crossing module created by Railroad Friction Products. This product was used extensively at railroad crossings throughout Alaska. The skid surface for the Cobra X module used as a bridge-deck panel was improved by the addition of quartz particles embedded in an epoxy coating. A section was removed from the bridge and supplied by AKDOT&PF for study. Traction was tested in the laboratory, and in 2007, the traction was tested in the field and compared with the laboratory values.
- Asphalt concrete (age 9 years).

- This section of asphalt pavement was removed from a Tudor Road intersection in the summer of 2005, before which it had been in service since 1996. This test was conducted to provide a baseline for comparison between products.

Five 18 in. by 24 in. structural plastic panels from each manufacturer and five 24 in. long timbers were tested for traction and damage by tire chains. Tests included:

1. Surface traction of new wearing surfaces for the following conditions:
    - Dry coefficient of friction.
    - Wet coefficient of friction
    - Coefficient of friction for an icy surface
    - Coefficient of friction for a surface with snow
2. Surface wear by rolling tire chains
    - An 8000 lb vertically loaded wheel with carbide chains was rotated for a given number of cycles at -20°F. After a given number of rotations, surface wear was measured.
3. Surface wear caused by dragging the tire chains
    - An 8000 lb vertically loaded wheel with carbide chains was locked and dragged across the wearing surface a given number of times at -20°F. After a given number of passes, surface wear was measured.
4. Surface damage caused by a loose tire chain
    - A wheel with loose carbide chains was rotated with respect to a wearing surface at a -20°F temperature exposure. The number of rotations was counted, and surface damage was measured after a given number of rotations.

Traction Test Equipment

Initially, we conducted a literature search to determine a reliable laboratory method for evaluating surface traction and surface damage caused by tire chains. The literature did not reveal equipment or available test methods.

Since no known laboratory test could be found to determine wearing-surface wear due to tire chains, we developed test equipment and a testing procedure. The testing apparatus consisted of a tray containing the sample to be tested. This tray could be moved horizontally by use of a hydraulic ram over a distance of 7.875 in. (20 cm). We located a 14-ply 235/85R16 tire over the tray through which downward force could be applied to the sample by means of a second hydraulic ram. The tire was located on an axle that rotated in the direction of the motion of the sample or locked, depending on the requirements of a given test. Electric load cells were provided to measure vertical and horizontal force on the tire in the direction of the sample's motion. The size of test samples was limited to 18 in. (45 cm) wide by 24 in. (61 cm) long by 6 in. (15 cm) thick. The entire apparatus was approximately 23.6 in. (60 cm) wide and 91 in. (230 cm) long, and weighed around 1000 lb (4500 N). We selected the size of the equipment to fit within the UAF low-temperature (cold) testing room (see Figure 8.1).

The equipment could be used to apply different vertical loads. measure static friction and dynamic friction, and simulate braking. Mr. Muench designed another piece of equipment to provide an accurate assessment of surface damage on a test panel after it was subjected to rolling-tire chain action, lashing tests, and dragging tests (see Figures 8.2 and 8.3). Accurate vertical (z) measurements (using an LVDT) as a function of x–y position are available.

Figure 8.1 Test equipment: to measure traction and apply chain damage.

We hypothesized that wear of the wearing surface due to tire chains is caused by three mechanisms as vehicles drive over the bridge. The types of damage are:

- Lashing – As the chain strikes the surface there is an impact that causes some damage;
- Rolling – As the tire rolls over the chain, it causes the chain to place load over a small contact area on the surface; and
- Dragging – While on the bridge, the chain slips or drags due to a vehicle either climbing or braking.

Figure 8.2 Travel arm measures x, y position; LVDT measures z position.

Figure 8.3 Recording surface wear for a test panel.

Since it is nearly impossible to conduct a test featuring all three types of damage in a small area in a laboratory setting, damage was tested and analyzed separately. We measured impact damage by rotating a tire with chains over the sample. The speed of rotation was equivalent to a vehicle moving at 40 mph (65 kph). Links of chain were allowed to impact the surface for several seconds. The amount of material removed was measured by profiling the surface before and after the test; this provided a measure of the damage by lashing.

We tested rolling damage by placing a tire with chains on the test sample. A vertical load, equivalent to an axle load of 80 kN (18,000 lb), was applied to the wheel. The tire was free to rotate as the test sample was moved under the tire for a given number of cycles. We measured the depth of indentation formed by the chains.

We measured slipping or dragging damage caused by tire chains by placing a vertical load on the wheel, which imposed load to the test sample. This was similar to the rolling test. In this case, however, the wheel was prevented from rotating while the sample was moved under the tire and chain. This test was developed to measure damage caused by drag between a tire chain and the wearing surface. The amount of material removed was measured by profiling the surface before and after the test.

In addition to tests for surface damage, we tested samples for traction. This was done by loading the tire, without chains but with rotation of the tire prevented. A vertical load was applied to the wheel. With vertical load acting on the wheel, we measured the force required to move the sample (this was the friction force). Normal force was measured indirectly, and friction force was measured directly. We then calculated the coefficient of friction. Traction tests were conducted to evaluate various surface conditions, including dry, wet, and icy.

Traction Tests

Traction was tested for three surface conditions—dry, wet, and icy—and three temperatures: 70°F, 20°F, and -20°F. Due to the freezing temperature of water, the wet surface condition was only tested at 70°F, and the icy surface condition, at 20°F and -20°F. We tested the following traction surfaces:

- Transonite (sample size: 18 in. wide × 24 in. long × 4½ in. thick).
- UHMW (sample size: 18 in. wide × 24 in. long × 5 in. thick).
- Super Panel (sample size: 18 in. wide × 24 in. long × 2½ in. thick).
    - This sample was similar to the Bedford Plastics Prodeck 4, an experimental feature installed on the Yukon River Bridge in the summer of 2005.
- Asphalt concrete (sample size: 18 in. wide × 24 in. long × about 4 in. thick).
    - This sample provided a baseline of comparison with conventional pavements.
    - The sample was from a Tudor Road intersection in Anchorage, where it had been subjected to Anchorage traffic for about 9 years.
- Cobra X (sample size: 18 in. wide × 24 in. long × 2½ in. thick).
    - This sample was installed on the Yukon River Bridge in 1992 as an experimental feature. At the time of testing, it had been subjected to Yukon River Bridge traffic for about 14 years.

An 18,000 lb equivalent single axle load (ESAL) acting on a 14-ply 235/85R16 tire, with and without chains, was used for the study. A normal force of 4500 lb and tire air pressure of 110 psi were used for all tests, representing conditions related to trucks crossing the bridge.

Temperature had relatively little effect on dry static friction for any particular panel type (see Figure 8.4). With the exception of the uncoated UHMW panel, samples had a dry static friction coefficient that was equal to or higher than that found for used asphalt concrete pavements.

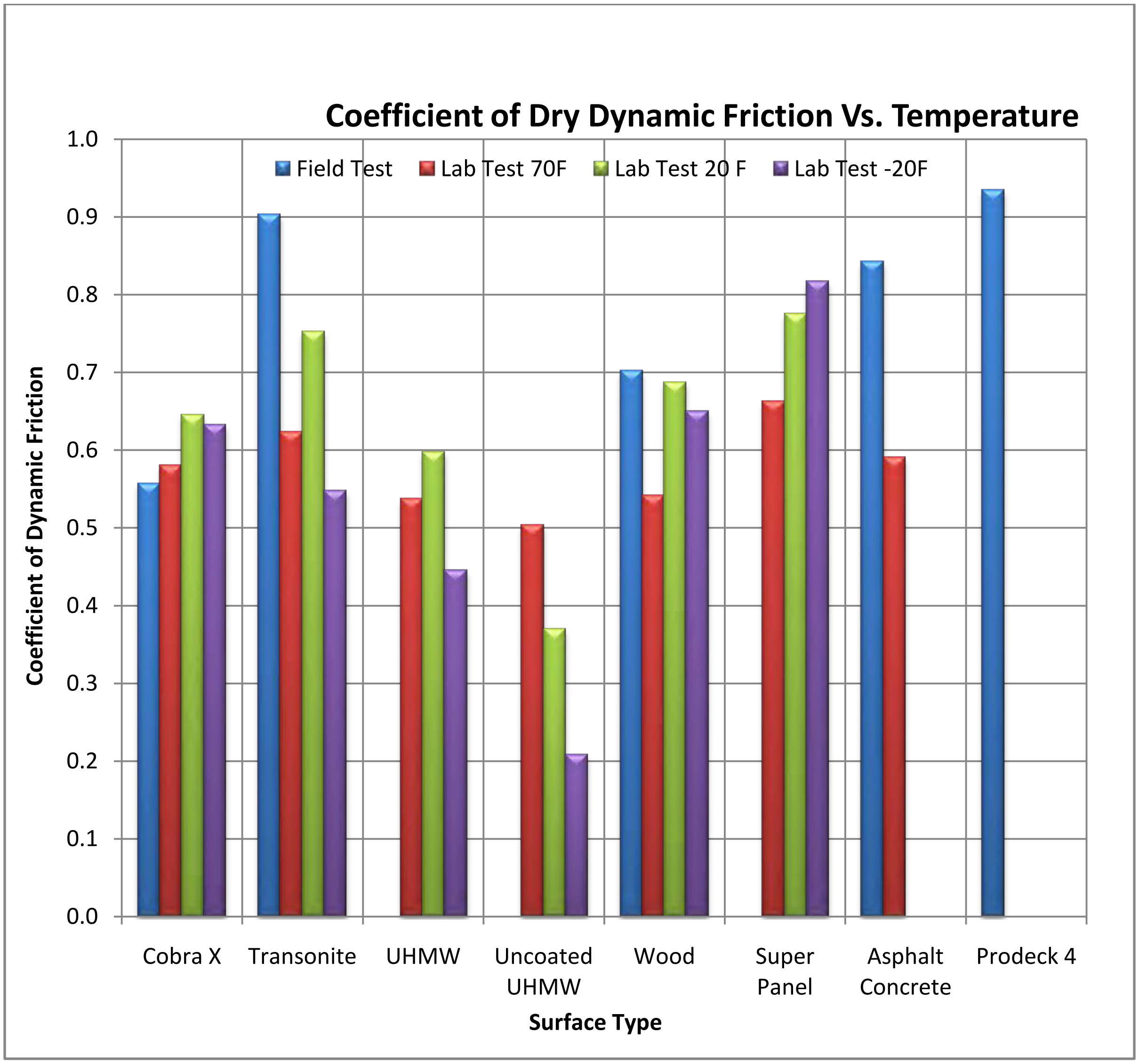

Figure 8.4 Wearing surface dry static friction vs. temperature.

In the laboratory, we measured the dynamic traction coefficients for the seven wearing surfaces. Field traction measurements were measured on June 22, 2007, at the bridge site with a Findley Irvine Grip Tester. Laboratory tests showed that temperature had relatively little effect on dry dynamic friction on the coefficient of dynamic friction (see Figure 8.5). It is clear from the field data that the Transonite (Martin Marietta), the Prodeck 4 (Bedford panel), and the asphalt concrete outperformed all of the other products. In the laboratory, the better performers were Transonite, Super Panel, wood, and Cobra X, in that order.

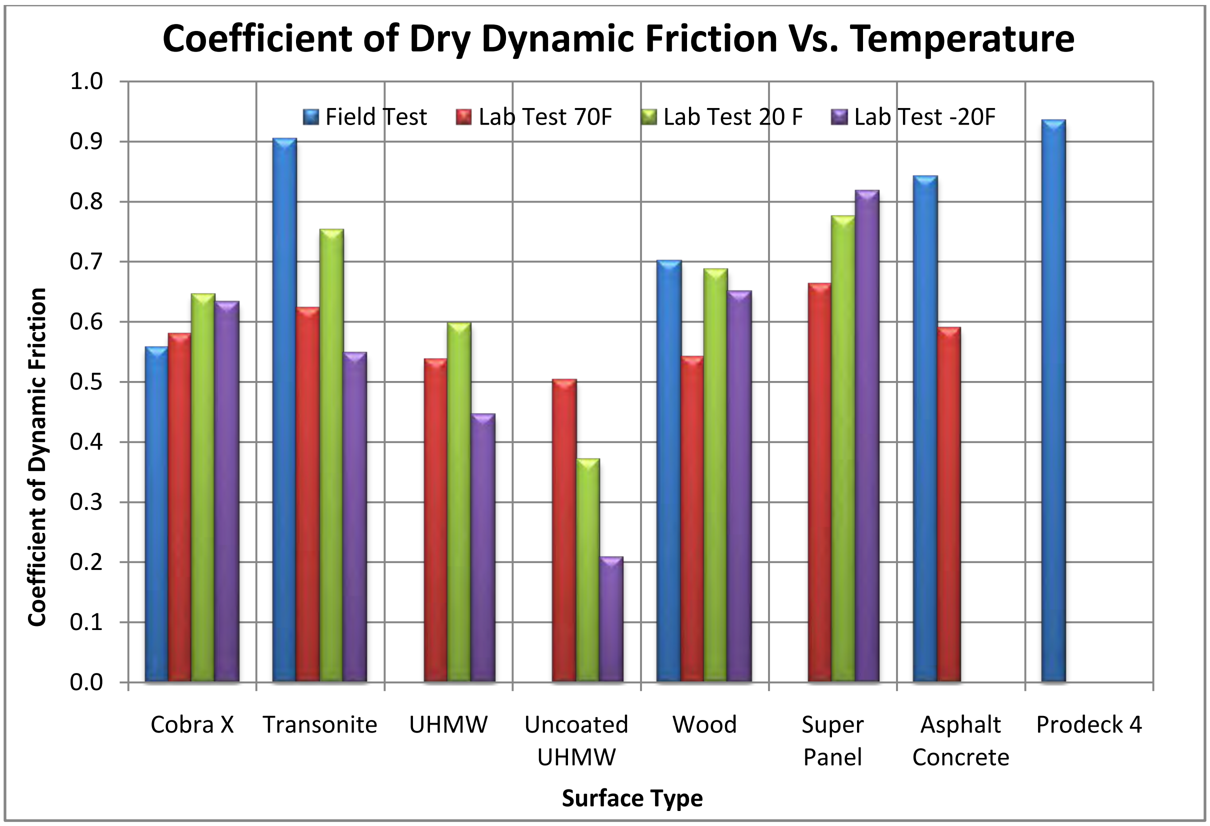

Figure 8.5 Coefficient of dynamic friction (laboratory and field) vs. temperature.

Except for the uncoated UHMW, we found that static friction in a dry condition was roughly equal to or higher than the used asphalt concrete. Static friction in wet conditions showed little change between types. According to AKDOT&PF, Cobra X was reported to be very slick. Laboratory test results show that the static friction of wet Cobra X compared favorably to static friction for wet wood (see Figure 8.6).

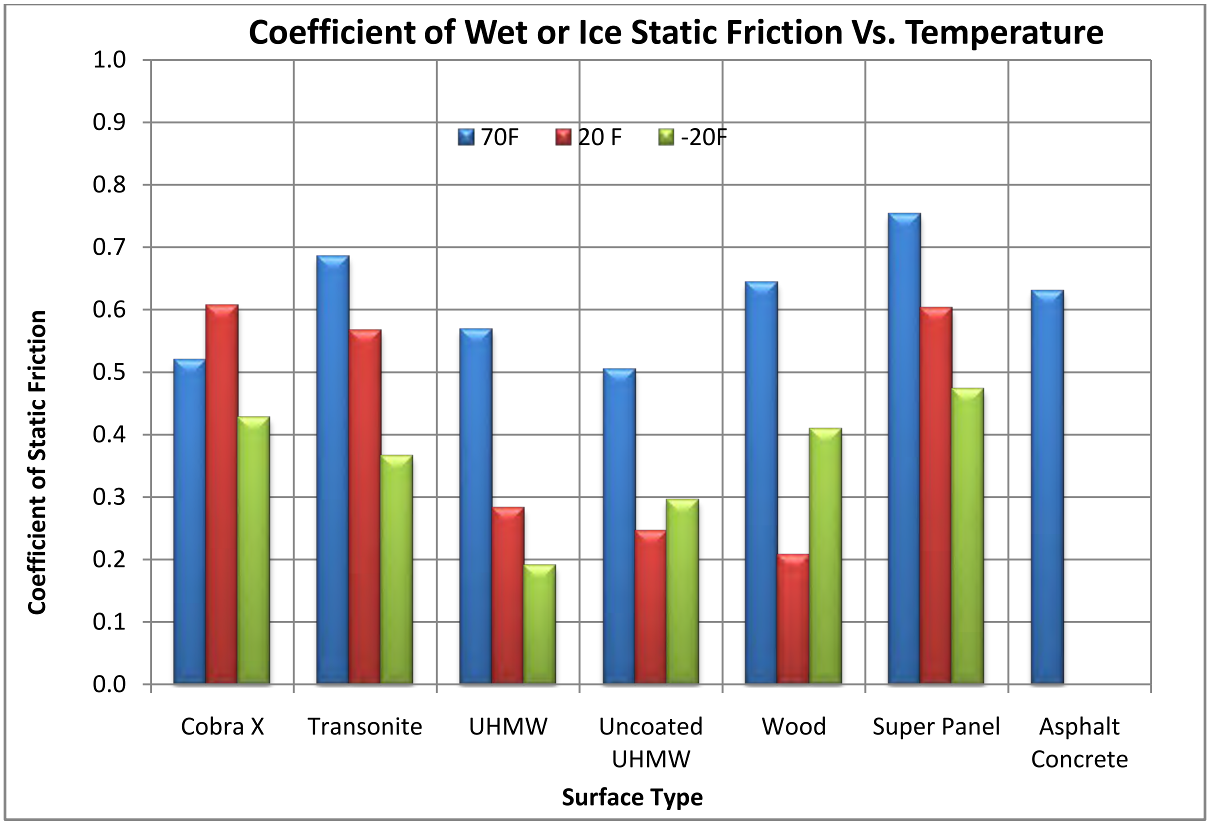

Figure 8.6 Wet static friction vs. temperature.

Static and dynamic friction in icy conditions varied considerably by panel type (see Figures 8.6 and 8.7). Panels with a relatively smooth surface texture, such as wood, UHMW, and uncoated UHMW, showed large reductions in static and dynamic coefficients of friction. Panels with an extremely uneven surface texture, such as the Super Panel and Cobra X, had little change between static and dynamic coefficients of friction between wet and icy conditions. The Transonite panel, with a surface texture falling between smooth and rough, showed a moderate drop in coefficients of friction when icy. It is worth noting that the dynamic coefficient of friction is about 0.05 when the wood is wet or has a thin coat of ice at 20°F. If it is colder or warmer, these coefficients increase dramatically: 0.61 at 70°F and 0.38 at -20°F.

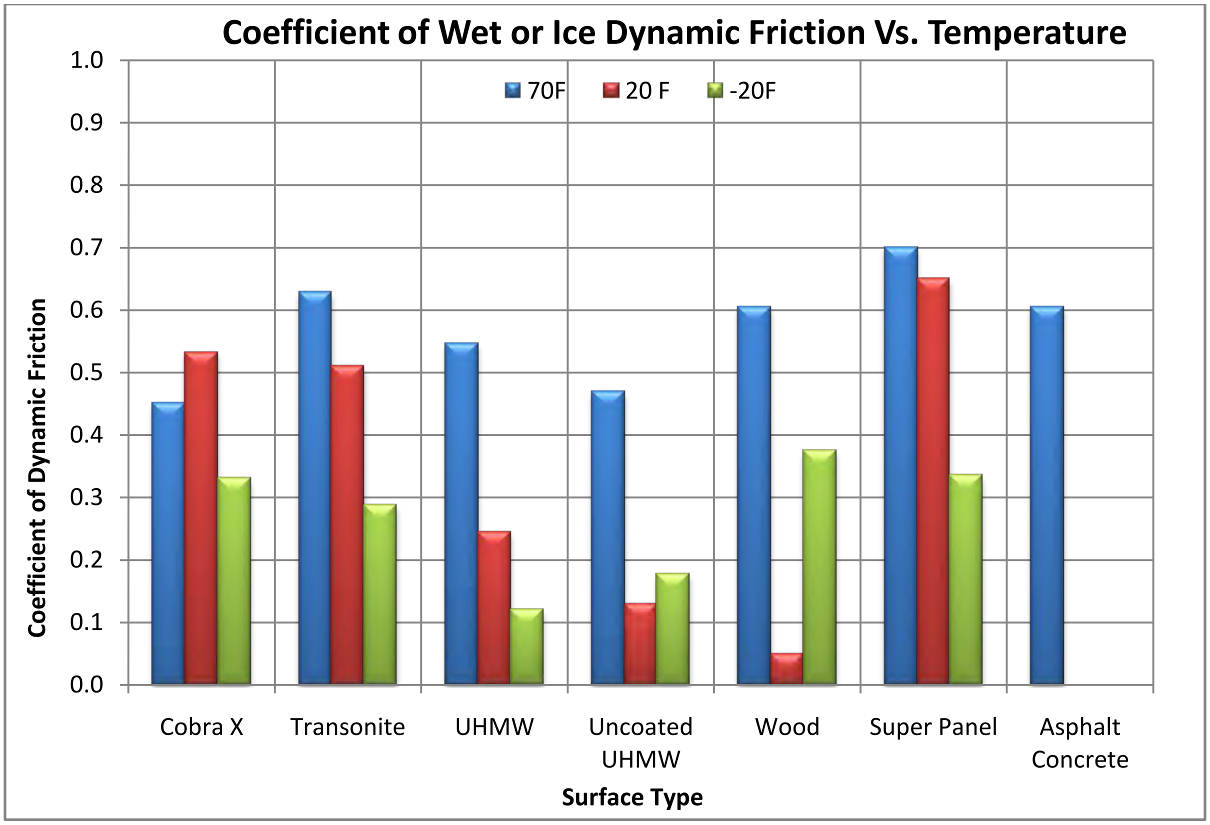

Figure 8.7 Wet or ice dynamic friction vs. temperature.

In summary, dynamic frictional resistance of the various wearing surfaces were sorted for icy conditions at -20°F. The highest coefficients are listed at the top of the table. The results illustrate which wearing surface will likely be the best choice for the traveling public (see Tables 8.1 and 8.2).

Table 8.1 Sorted Dynamic Friction at -20°F and Icy

	70°F		20°F		-20°F	
Sample	Dry	Wet	Dry	Icy	Dry	Icy
Wood	0.54	0.61	0.69	0.05	0.47	0.38
Super Panel	0.66	0.70	0.78	0.65	0.70	0.34
Cobra X	0.58	0.45	0.65	0.53	0.55	0.33
Transonite	0.62	0.63	0.75	0.51	0.63	0.29
Uncoated UHMW	0.50	0.47	0.37	0.13	0.37	0.18
UHMW	0.54	0.55	0.60	0.25	0.48	0.12
Asphalt Concrete	0.59	0.61	NT	NT	NT	NT

NT - Not tested

Table 8.2 Sorted Dynamic Friction at -20°F and Dry

Sample	70°F		20°F		-20°F	
	Dry	Wet	Dry	Icy	Dry	Icy
Super Panel	0.66	0.70	0.78	0.65	0.70	0.34
Transonite	0.62	0.63	0.75	0.51	0.63	0.29
Cobra X	0.58	0.45	0.65	0.53	0.55	0.33
UHMW	0.54	0.55	0.60	0.25	0.48	0.12
Wood	0.54	0.61	0.69	0.05	0.47	0.38
Uncoated UHMW	0.50	0.47	0.37	0.13	0.37	0.18
Asphalt Concrete	0.59	0.61	NT	NT	NT	NT

NT - Not tested

We also carried out studies to simulate the friction coefficient of smaller vehicles. In order to approximate this condition, tire air pressure and applied load were reduced to approximate the wheel conditions that may be expected for a lighter vehicle. Resulting traction coefficients are shown in Figures 8.8 and 8.9.

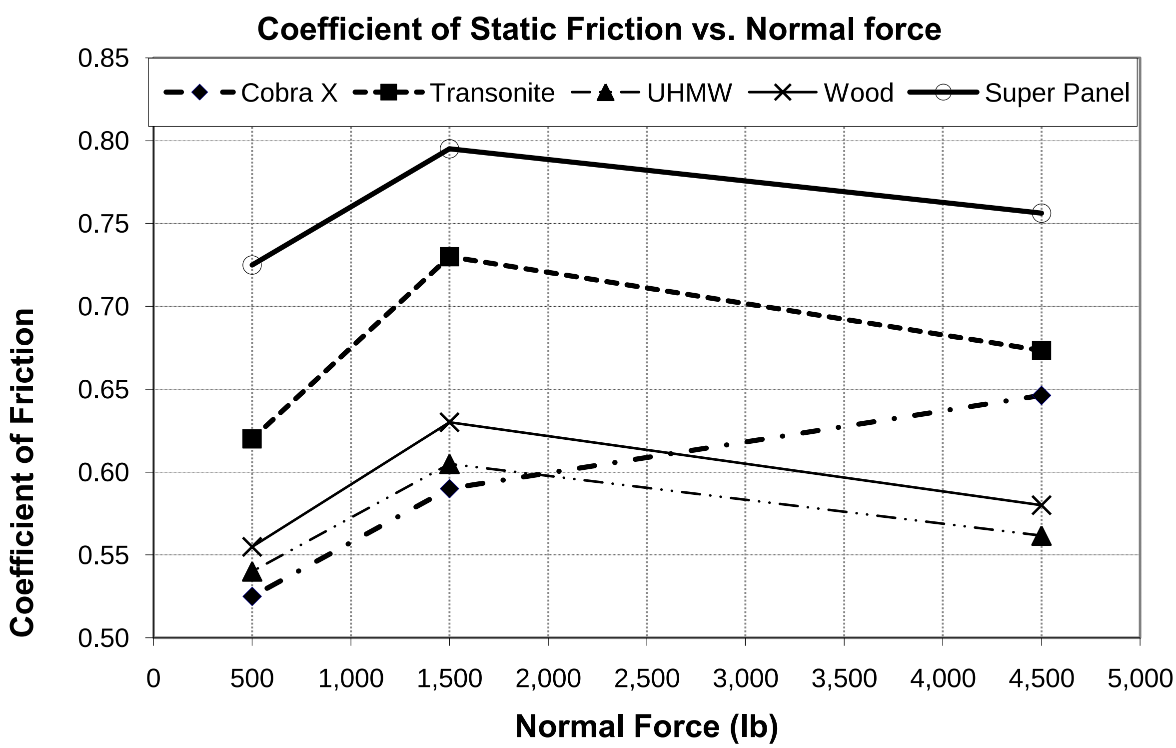

Figure 8.8 Dry static friction vs. normal force.

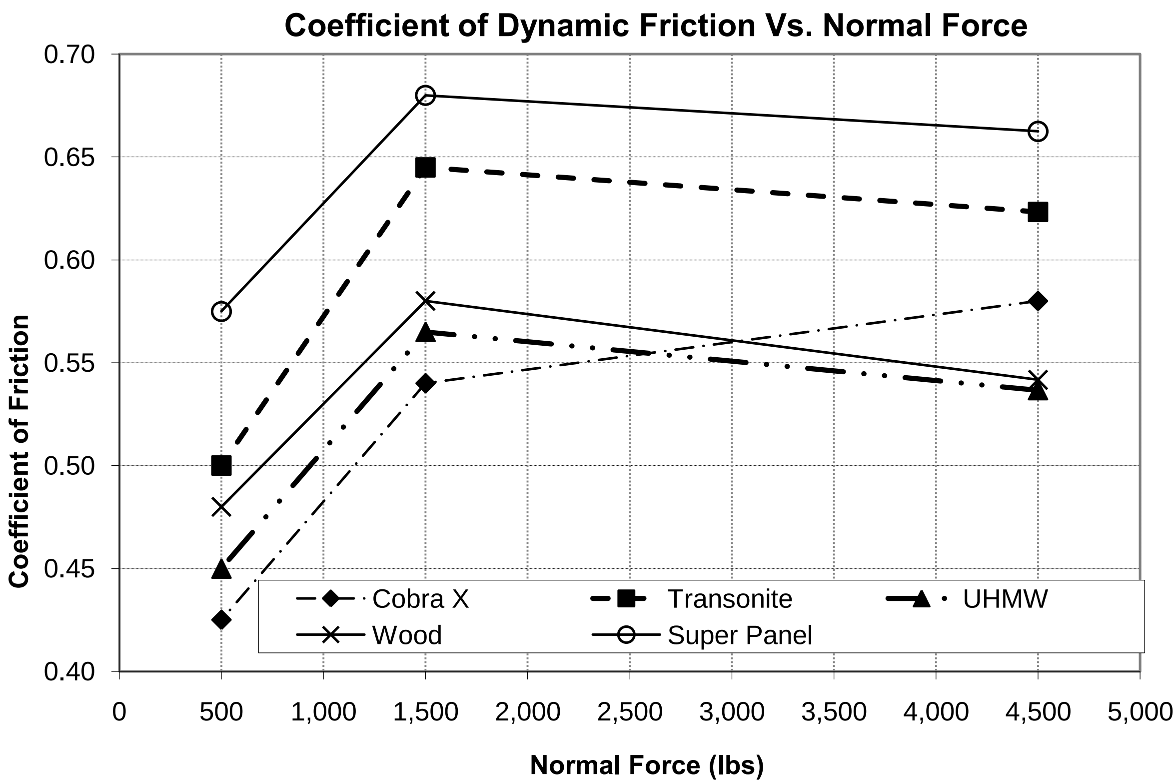

Figure 8.9 Dry dynamic friction vs. normal force.

The test results shown in Figures 8.8 and 8.9 illustrate that the tractability on this bridge for lighter vehicles will be worse than the heavily loaded trucks. Further, we can expect that most of the truck traffic driving south is unloaded, and that is when they must climb the 6% grade.

Procedures for Measuring Surface Damage

Prior to testing, the sample surface was defined using a rolling LVDT. This procedure was used to define the surface topography (*z* height) with respect to an *x*–*y* position. Once the topography was defined, the sample was placed under the wheel, and either dragging, rolling, or lashing was implemented for a given number of cycles. After a number of cycles, the sample was removed from the test frame, and the surface and the surface topography were again measured. The difference between the initial topography and after-test topography was used to define the level of damage. These beginning and ending conditions were used to evaluate surface damage.

Surface Damage Tests

In an attempt to determine damage caused by tire chains, we tested damage by three different methods: rolling, lashing, and dragging. Lashing and dragging damage were measured from a surface before and after testing. The average depth of material removed during testing was calculated.

We used a 14-ply 235/85R16 tire to simulate truck traffic. A vertical load equivalent to the force of a standard axle of 18,000 lb (80 kN) was applied to the wheel. The tire with chains was free to rotate as the test sample was moved under the tire for a given number of cycles. The cycle speed approximated 40 mph (65 kph) (see Figure 8.10). We determined the amount of damage caused by a rolling tire by measuring the depth of penetration of the panel surface. We then recorded the depth of penetration caused by the tire chains.

We conducted lashing tests by spinning a tire with a chain at approximately 40 mph (65 kph) (see Figure 8.10). The tire and tire chain were located 1 in. above the surface, and the tire spun for 2 sec. We determined the number of cycles for each type of test from annual truck counts that were recorded by the AKDOT&PF weigh station at Fox, Alaska.

Figure 8.10 Equipment for traction, applying rolling, lashing, and drag forces.

In this test, the objective was to evaluate damage that may be caused by loose links of chain that strike the wearing surface.

We tested dragging damage by cyclically moving the test panel 11 cycles under a chained tire. The tire was subjected to a normal force of 4500 lb while the tire was locked and prevented from rotating (a drag condition). The normal force of 4500 lb was used to approximate the force on a single tire in an 18,000 ESAL. We used two seconds of lashing time and 11 cycles of dragging as an approximation of one year of damage.

Rolling Damage

We measured rolling damage by moving a normally loaded (4500 lb) test panel under the tire. During this test, the tire was allowed to rotate. Figure 8.11 is a measure of the damage after one pass. Figure 8.12 shows the level of damage after 32 passes. When subjected to rolling damage, wood experienced considerably more damage than other panel types (see Figures 8.11 and 8.12).

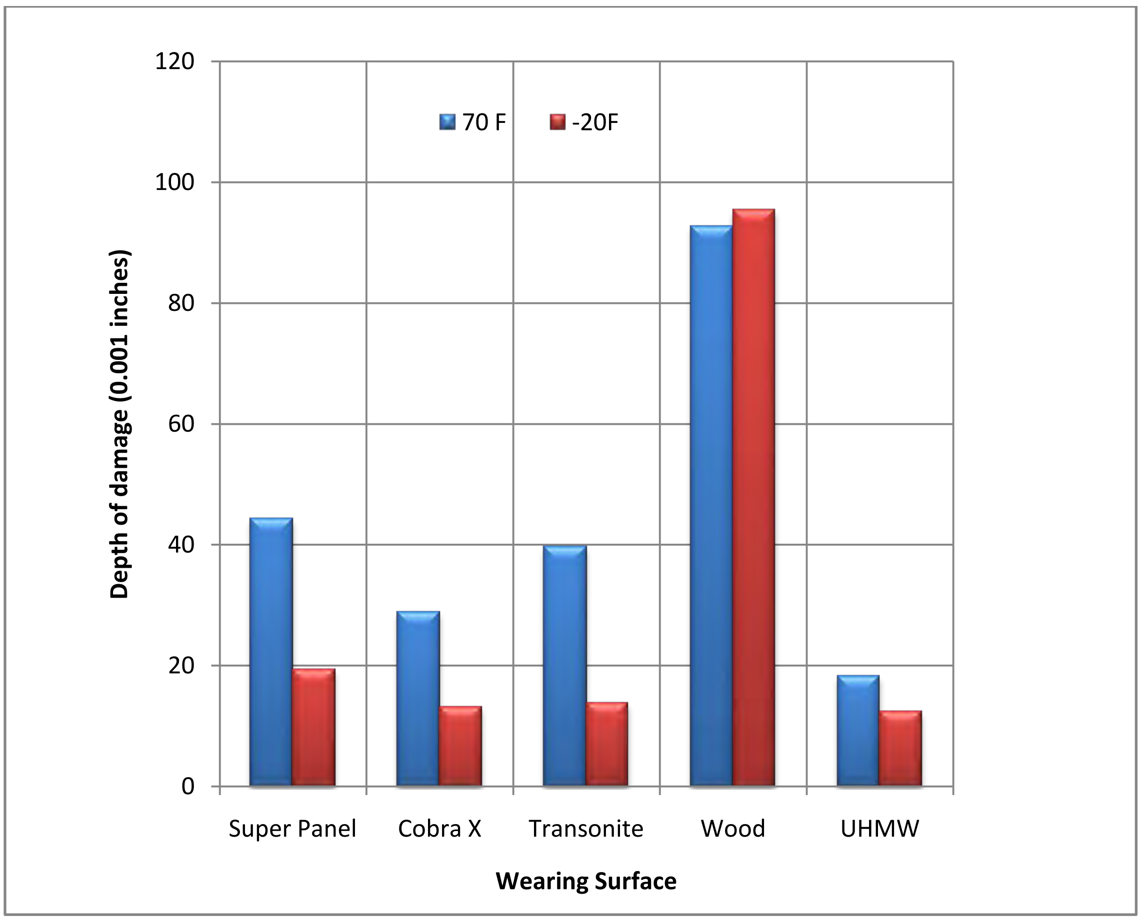

Figure 8.11 Depth of rolling damage after one pass.

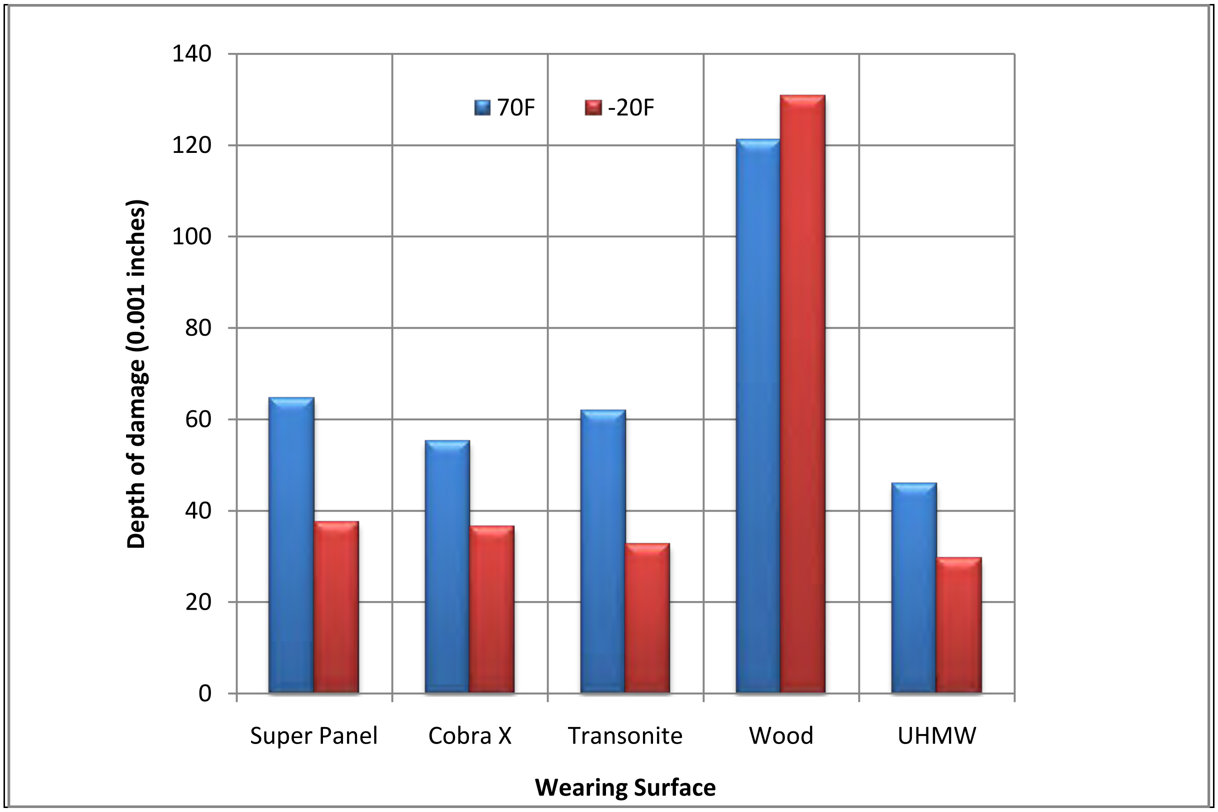

Figure 8.12 Rolling damage after 32 to 36 passes.

Surface damage caused by tire chains rolling over the wearing surface is estimated by measuring depth of damage after a given number of passes. Table 8.3 shows how each wearing surface resisted rolling tire chain damage for two different temperature conditions. Each wearing surface is ranked for its ability to resist rolling damage at -20°F. Wood suffered the most damage under this type of action.

Table 8.3 Wearing Surfaces Ranked by the Least Rolling Damage

		Damage Depth (0.001 in.)		
Ranking	Surface	-20°F	20°F	70°F
1	UHMW	29.49	NT	45.85
2	Transonite	32.63	NT	61.99
3	Cobra X	36.59	NT	55.27
4	Super Panel	37.56	NT	64.69
5	Wood	130.70	NT	121.10

NT = Not tested

Lashing and Dragging Damage

Lashing and dragging damage results varied considerably between panel types. Panels with epoxy and aggregate surfaces, such as the Super Panel and Transonite, showed considerably more damage as temperature decreased, while those with polymer surfaces, such as UHMW and Cobra X, showed much less damage at lower temperature (see Figures 8.13 and 8.14 and Tables 8.4 and 8.5). Wood performance was relatively unchanged with respect to temperature for lashing and dragging.

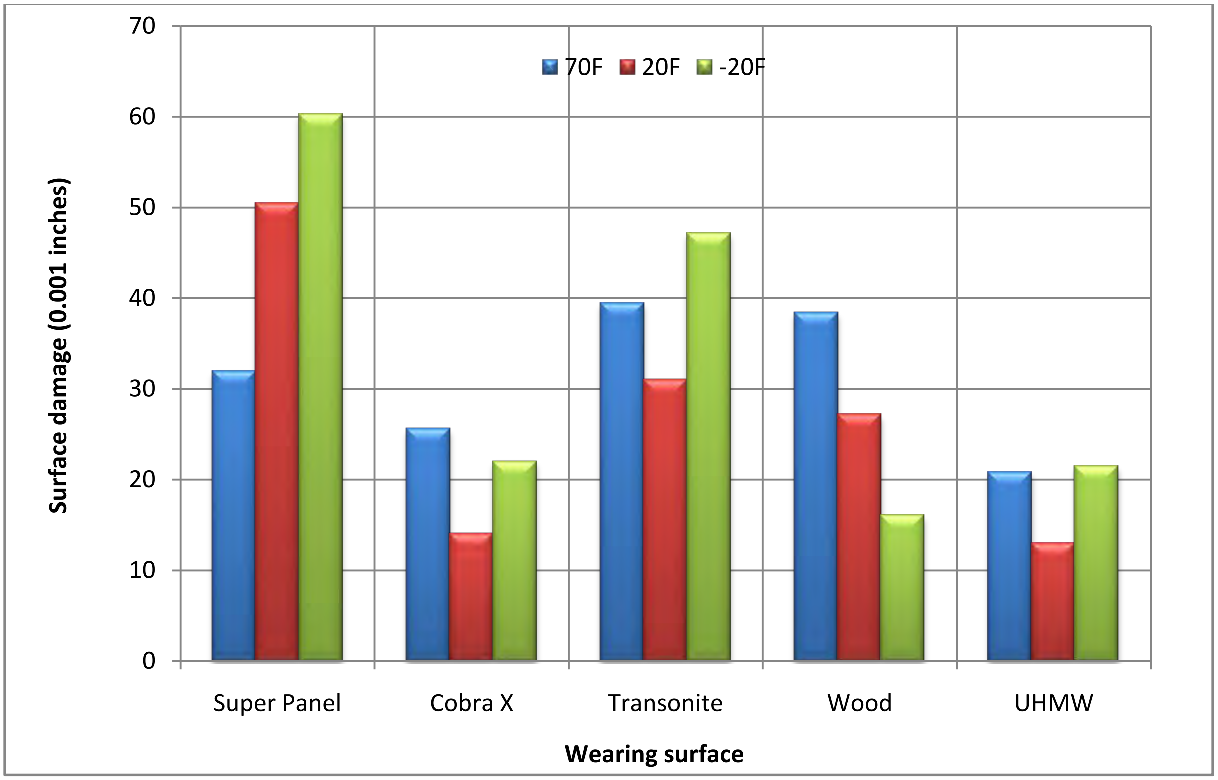

Figure 8.13 Lashing damage.

Table 8.4 Wearing Surfaces Ranked for Lashing Damage (0.001)

Ranking	Surface	Damage (in.)
1	Wood	16
2	UHMW	21
3	Cobra X	22
4	Transonite	47
5	Super Panel	60

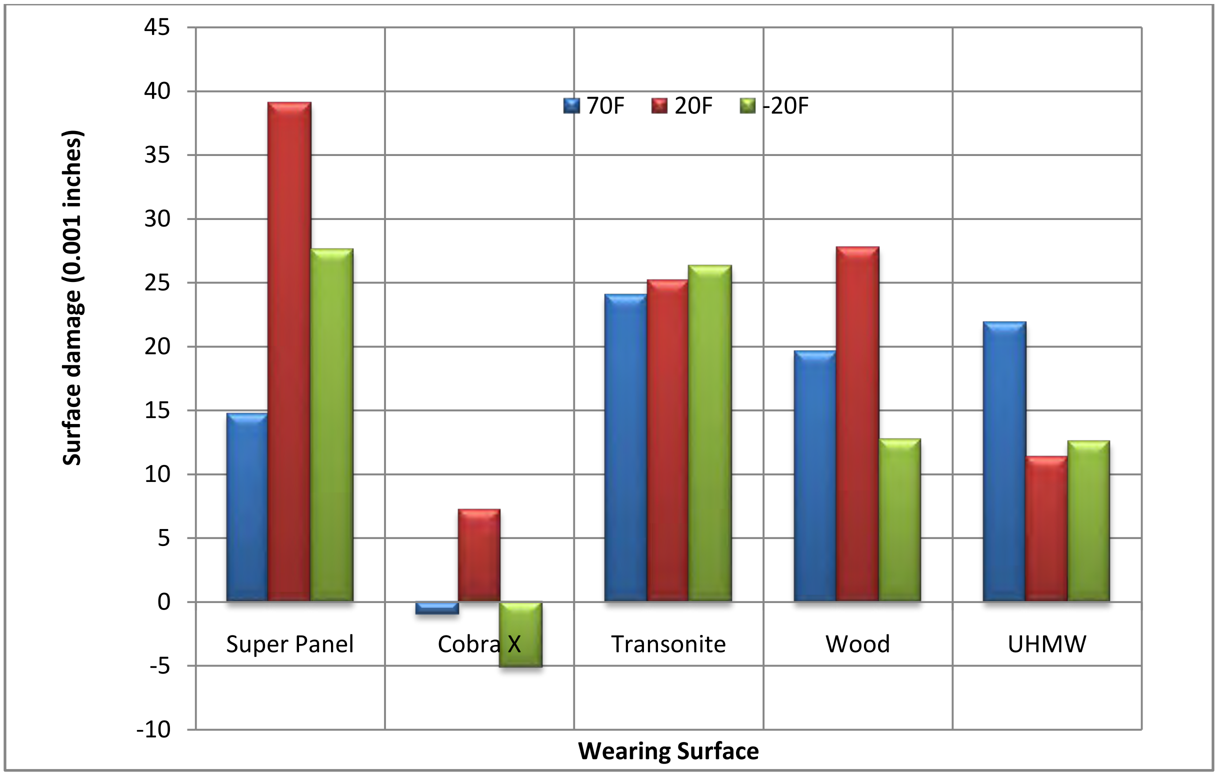

Figure 8.14 Dragging damage after 11 cycles.

Table 8.5 Ranked Wearing Surfaces by Least Dragging Damage (0.001 in.)

Ranking	Surface	Damage
1	Cobra X	-5
2	UHMW	13
3	Wood	13
4	Transonite	26
5	Super Panel	28

Dragging damage to Cobra X resulted in measured negative wear values at 70°F and -20°F. This is likely due to a very small amount of actual wear, combined with errors in measurements of the surface before and after testing. This would indicate that the standard error of measurement methods used is greater than the wear that occurred in testing.

Field Traction Measurements

On June 21, 2007, Zachery Jerla and Wilhelm Muench set up the UAF Findley Irvine Grip Tester equipment and performed preliminary friction tests for the asphalt pavement along Taku Drive. After the equipment was evaluated, Jerla and Muench measured and recorded friction coefficients for the Civil Engineering parking lot, an asphalt surface, at the Duckering Building on the UAF campus. According to UAF, this pavement is older than 10 years. Test results for these asphalt wearing-surface tests are shown in Table 8.6.

Table 8.6 Dynamic Coefficient of Friction

21 Jun 07 Test	Duckering Asphalt Pavement	Average
1:57 PM	0.87	
2:06 PM	0.79	0.84
2:19 PM	0.86	

On June 22, 2007, Jerla and Muench, and Jim Sweeney from AKDOT&PF, traveled to the Yukon River Bridge, where they ran eight series of field traction tests that same day. The tests were taken using a Findlay Irvine Grip Tester, which was pulled behind a vehicle to measure the coefficient of friction. Details of these tests are presented in Appendix E. While at the bridge, Jerla, Muench, and Sweeney also conducted a follow-up inspection. The purpose was to determine how the wearing-surface conditions might have changed in one year. Later in the summer, after the trip, the wearing surface was replaced with a new two-layer temporary timber wearing surface.

The frictional coefficients for four experimental features were measured. Test results for the eight tests are shown in Table 8.7.

Table 8.7 Summary of Average Field Traction Coefficients

Bridge Surfaces	Age (yr)	Test 1 1:24 PM	Test 2 1:35 PM	Test 3 1:39 PM	Test 4 1:47 PM	Test 5 1:54 PM	Test 6 2:00 PM	Test 7 2:07 PM	Test 8 2:13 PM	Avg
Wood	1 to 8	----	----	0.62	0.70	0.73	0.76	0.68	0.72	0.70
Cobra X	15	----	----	0.50	0.64	0.50	0.59	0.51	0.60	0.56
Prodeck 4	2	----	----	0.91	0.91	0.96	0.94	0.94	0.95	0.94
Transonite	2	----	----	0.86	0.92	0.91	0.91	0.89	0.93	0.90

Field dynamic traction coefficients for the four experimental features are presented in Table 8.8.

Table 8.8 Summary of the Range of Field Traction (2007)

	Wood (8 yr)			Cobra X (14 yr)			Prodeck 4 (2 yr)			Transonite (2 yr)		
Test	min	avg	max	min	avg	max	min	avg	max	min	avg	max
1:39 PM	0.2	0.62	0.8	0.5	0.5	0.57	0.59	0.91	1.01	0.78	0.86	0.98
1:47 PM	0.07	0.7	0.9	0.6	0.64	0.7	0.66	0.91	0.99	0.64	0.92	1.01
1:54 PM	0.21	0.73	0.9	0.5	0.5	0.55	0.88	0.96	1.02	0.88	0.91	0.96
2:00 PM	0.09	0.76	0.9	0.6	0.59	0.63	0.8	0.94	1.01	0.7	0.91	1.03
2:07 PM	0.22	0.68	0.8	0.5	0.51	0.56	0.86	0.94	0.99	0.77	0.89	1.02
2:13 PM	0.35	0.72	0.9	0.6	0.6	0.63	0.82	0.95	1.03	0.82	0.93	1.01
Extremes	0.07		0.9	0.5		0.63	0.59		1.01	0.64		1.03

In addition to average values, mean, most often, and values for 80% of the data above and values for 80% of the data below are shown in Table 8.9.

Table 8.9 Traction Coefficients for Wearing Surfaces on Yukon River Bridge, 2007

Run		Avg Speed (mph)	Traction Coefficients				
			80% Above	Average	Most Often	Mean	80% Below
Test 1	1:24 PM	8	0.59	0.69	0.76	0.73	0.79
Test 2	1:35 PM	14	0.59	0.71	0.77	0.77	0.83
Test 3	1:39 PM	9	0.59	0.69	0.77	0.73	0.79
Test 4	1:47 PM	10	0.62	0.71	0.79	0.77	0.81
Test 5	1:54 PM	9	0.59	0.72	0.79	0.75	0.81
Test 6	2:00 PM	8	0.6	0.72	0.8	0.77	0.8
Test 7	2:07 PM	7	0.59	0.7	0.75	0.76	0.81
Test 8	2:13 PM	9	0.59	0.7	0.78	0.76	0.81
Range for tests:			0.59				0.83
Wearing surfaces are wood plus 4 experimental features							

REFERENCES

AASHTO-LRFD Bridge Design Specifications, Second Edition (1998). American Association of State Highway and Transportation Officials, Washington, D.C.

ASTM (2006). ―Standard Test Method of Flatwise Compressive Properties of Sandwich Cores," (C 365/C 365M-05). West Conshohocken, PA: ASTM International.

Creative Pultrusions, Inc. (2002). ―SuperPlank™ Decking Products," Internet Resource: http://www.creativepultrusions.com/

Euclid Chemical Company (2007). ―FLEXOLITH," Internet Resource: http://www.tamms.com/

Huang, Y.H. (2004). ―Design Factors," *Pavement Analysis and Design*, Second Edition. Upper Saddle River, NJ: Pearson Prentice Hall, pp. 26–29.

Hulsey, J.L., Yang, L., Curtis, K., and Raad, L. (1995). ―Yukon River Bridge Deck Strains and Surfacing Alternatives," Final Report No. INE/TRC/RP-94.10, Alaska Department of Transportation & Public Facilities, Institute of Northern Engineering, University of Alaska Fairbanks, September.

Hulsey, J.L., Yang, L., and Raad, L. (1999). ―Wearing Surfaces for Orthotropic Steel Bridge Decks," Transportation Research Record, Paper 991049, National Research Council.

Hulsey, J.L., Raad, L., and Conner, B. (2002). ―Deck Wearing Surfaces for the Yukon River Bridge," ASCE Proceedings, 11th International Conference on Cold Region Engineering, Anchorage, Alaska, May 20–22.

Jerla, Z.C.D. (2008). ―Structural Durability of Wearing Surfaces for the Yukon River Bridge," Master of Science in Civil & Environmental Engineering, University of Alaska Fairbanks, May 2008.

Johnson, P.R., and McFadden, T.T. (1979). ―Ice Forces on the Yukon River Bridge – 1978 Breakup," Federal Highway Administration, Research & Development, Report No. FHWA-RD-79-82, pp. 13–25.

Kalný, O., and Peterman, R.J. (2005). ―Performance Investigation of a Fiber Reinforced Composite Honeycomb Deck for Bridge Applications," Kansas Department of Transportation, Report No. FHWA-KS-04-1.

Martin Marietta Composites (2008). ―Structural Composite Panel," Internet Resource: http://www.martinmarietta.com/

Matoba, K. (2001). ―Surfaces Hold Up Well Under Heavy Traffic," *Railway and Track Structures*, Vol. 97, No. 6, pp. 23–32.

PCA, 1984. “Thickness Design for Concrete Highway and Street Pavements,” *Engineering Bulletin* No. EB 109.01P, Portland Cement Association, Skokie, IL, 46 pp.

Peratrovich & Nottingham, Inc. (1981). “Yukon River Bridge Use Risk Analysis Criteria Development,” State of Alaska, Department of Transportation and Public Facilities Division of Planning and Programming.

Persichetti, B. (2005). “Lake-Effect: A Bridge in the Snow Belt Gets a New Anti-Icing System,” *Roads & Bridges*, Vol. 43, No. 10, pp. 36–40.

Persichetti, B. (2007). “Accident Reduction Plus Bridge Preservation,” *Bridges*, Vol. 101, No. 6, pp. 16–18.

Prachasaree, W., GangaRao, H.V.S., Laosiriphong, K., Shekar, V., and Whitlock, J. (2007). “Theoretical and Experimental Analysis of FRP Bridge Deck Under Cold Temperatures,” *International Journal of Materials and Product Technology (IJMPT)*, Vol. 28, No.1/2, pp. 103–121.

Ultra Poly, Inc. (2002). “UHMW Physical Properties,” Internet Resource: http://www.ultrapoly.com/

Wanek, M. (2004). “Grade Crossings: From Concrete and Wood to Rubber, Steel and Composite, Manufacturers Continue to Look at New Material,” *Railway and Track Structures*, Vol. 100, No. 6.

Wanek, M. (2005). “Grade Crossings Keep Evolving,” *Railway and Track Structures*, Vol. 101, No. 6, pp. 21–27.

Wolchuk, R. (1997). “Steel Plate Deck Bridges and Steel Box Girder Bridges Section 19,” *Structural Engineering Handbook*, Fourth Edition. Gaylord/Gaylord/Stallmeyer, McGraw-Hill Publishing Co., pp. 17–19.

Wolchuk, R. (2001). “Criteria for Surfacing Selection on Steel Orthotropic Decks,” *Transportation Research Board*, 2001 Annual Meeting, January.

APPENDIX A
STRUCTURAL INTEGRITY: BRIDGE-DECK TEST PANELS

The test panels described herein are Part 1 of this study. The motivation of this research was to investigate potential replacement panels for the bridge deck on the Yukon River Bridge. We tested four panels under different environmental conditions and load cases, and compared results. We designed and constructed a versatile loading frame, and developed a testing procedure as part of this research. These work items were needed to evaluate panel structural properties.

In this section of the report, we provide the design and construction of the loading frame used for the evaluation of the experimental Yukon River Bridge deck panels, along with a detailed description of each panel. We explore the advantages and disadvantages of each panel as well as the geometric and pre-evaluation structural properties. Additionally, we present the composition of the experimental panels, testing objectives, and procedures.

Load Frame

We tested four experimental panels and a control panel representing the temporary timber bridge deck. The test panels were roughly 4 ft square and 5 in. thick. The load frame was designed to accommodate both large panels and smaller specimens cut from larger panels. We tested the smaller specimens to determine unknown structural properties.

We chose a double-acting linear actuator from M-Mac Actuators, Inc. as a load ram for applying either a push- or pull-type load. The actuator has a thrust capability of pushing 40,000 lb or pulling 25,000 lb. The frame was designed for test loads up to 50,000 lb. We chose steel W-shapes as main loading carrying members. We constructed a built-up steel channel section as a mount for the actuator and a load spanner. Threaded rods of 1½ in. in diameter were used as tension members and were chosen so the vertical location of the actuator could be varied. The largest allowable clear span between supports (angle to angle) was 41 in. square, and the smallest adjustable length between supports was 8 in. Figure A.1 shows our loading frame with the actuator mounted in the built-up channel section and the W-shapes set at the default 41 in. clear span.

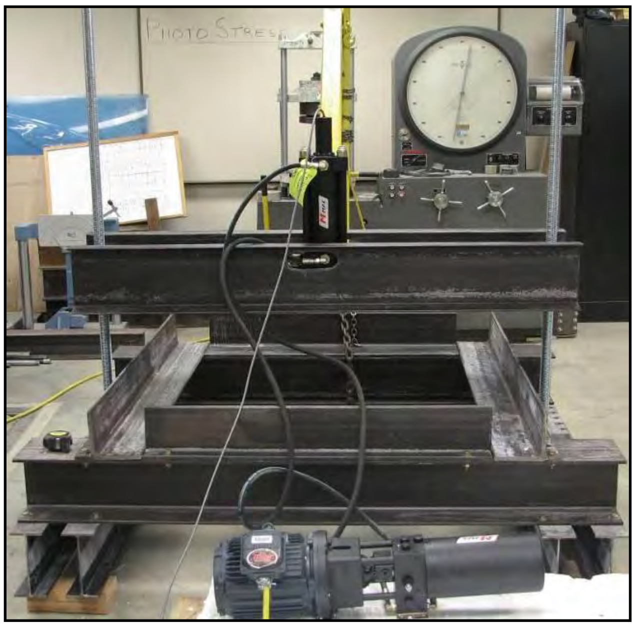

Figure A.1 Structural testing loading frame.

Once the frame was constructed, steel members of the frame could be unbolted and removed so that the large 4-ft-square panels could be easily loaded and unloaded from the frame. Figure A.2 demonstrates how a panel would be slid into place and centered below the actuator for testing through the removal of a steel angle section. Once testing was concluded we unbolted and removed the angle, and slid the panel free from the frame. The next panel was then placed in the frame.

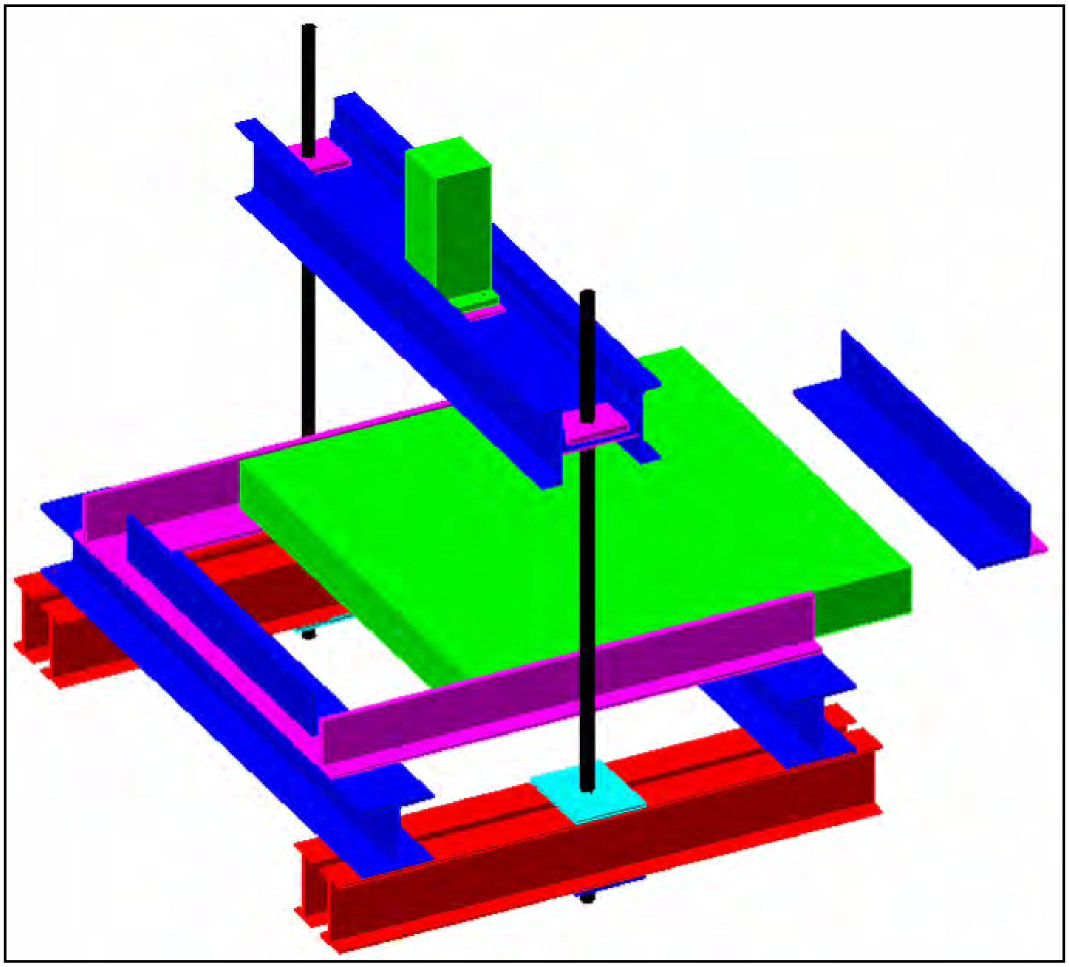

Figure A.2 AutoCAD drawing of loading frame.

Dual Tire Loading Foot Assembly

We used an HS20-44 loading as the basis for testing each panel. One axle was assumed to weigh 32,000 lb, distributing 16,000 lb to each set of dual tires on the axle with tire pressure approximating 110 psi.

Laboratory loads were applied through the footprint shown in Figure A.3. The footprint was obtained from measurements and comparisons of various dual truck tires that travel across the Yukon River Bridge. The load-foot assembly was designed and manufactured by Jerla (2008) in accordance with published standards (PCA, 1984; Huang, 2004).

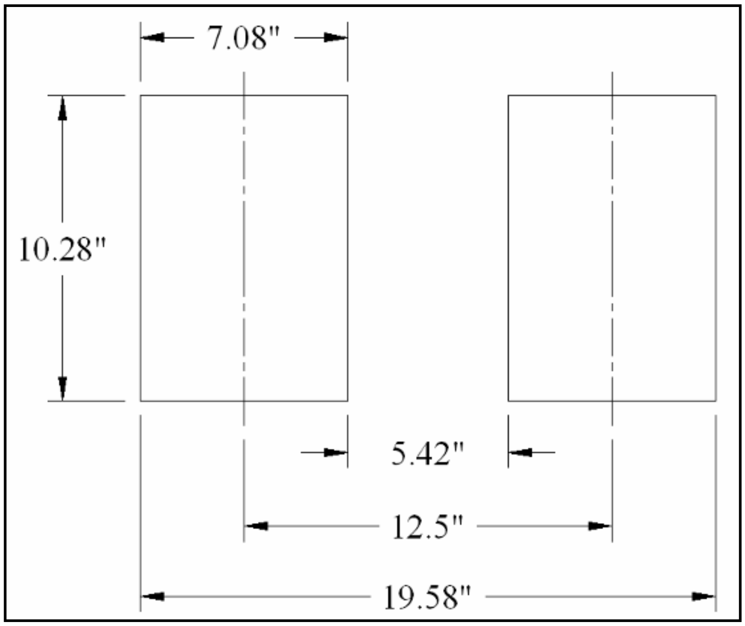

Figure A.3 Dimensions of loading foot.

Figure A.4 shows the completed assembly of the loading foot. We welded four ball joints to steel loading plates. The load cell mount on top of the loading foot was tapped to accommodate three different size load cells. The size was dependent on which test was being executed. Rubber pads for the two steel plates are not shown in this Figure.

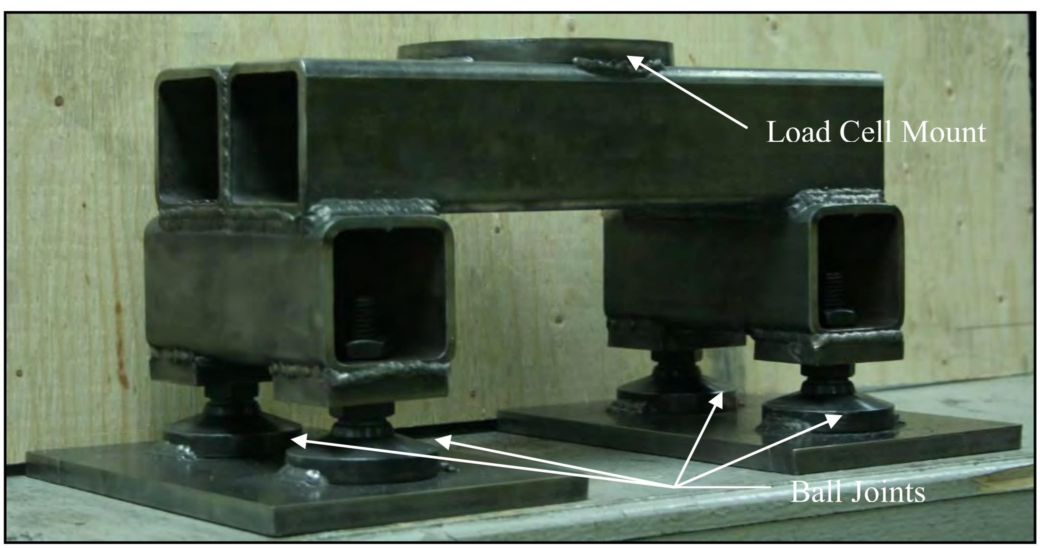

Figure A.4 Loading foot.

Figure A.5 shows the loading foot complete with the loading train that we used for a 16,000 lb static test that simulated duals from a truck. Higher capacity load cells (25,000 lb and 50,000 lb) were used to verify factory calibration data and to confirm that the load being applied was accurate. The load cell with the least amount of electronic noise was used for data analysis.

Figure A.5 Completed loading foot with load train.

Experimental Panels

We tested four experimental bridge-deck panels in the laboratory and compared them with laboratory test results for a control panel that represents the temporary bridge deck on the Yukon River Bridge. The geometry, structural properties, and unique characteristics of each panel are presented herein.

Timber on Timber Panel

The timber on timber panel is the control panel, and it represents the temporary wearing surface on the Yukon River Bridge. The timber/timber panel was constructed from supplemental lumber available from the 2006 Yukon River Bridge decking contract. The lumber specifications were:

- 2½ in. × 12 in. × 16 ft
- number 2 or better Douglas Fir, rough sawn
- surfaced on one side with two edges and rough sawn on one side for the traction surface
- moisture content of 23%–28%

Five 16 ft running planks were provided by AKDOT&PF at no cost for this research. Upon delivery, this lumber (which had been stored outdoors) had a significant amount of moisture. After delivery, it was kept at room temperature for a week. It was then cut and bolted to form the test panel. At test time, these planks had undergone significant shrinkage, and their weight had decreased, resulting in a test panel weight of 218 lb. Initially, top and bottom layers were bolted to be flush. After 30 days, a 1⁄8 in. space between planks developed to ¼ in. The moisture content of this timber/timber panel was 11%. Figures A.6 and A.7 illustrate the top and bottom surface of this timber/timber panel.

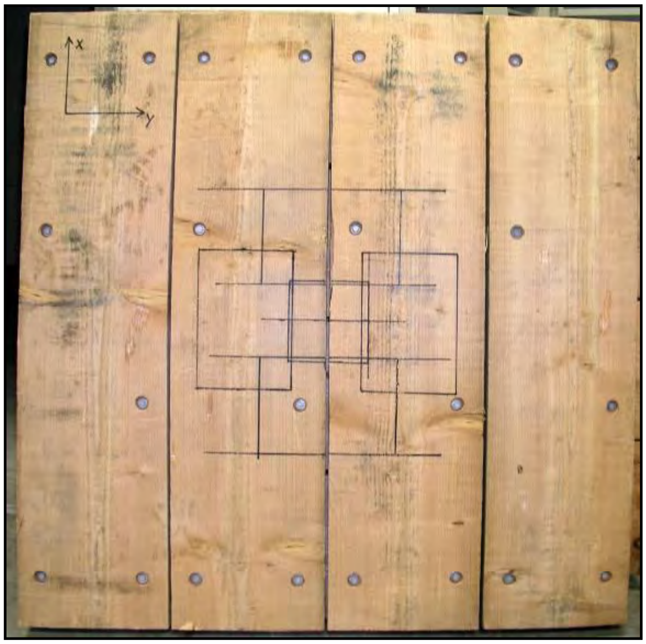

Figure A.6 Timber/timber panel top view.

Figure A.7 Timber/timber panel side view.

Two layers of timbers were attached with ¼ in. diameter by 3 ¾ in. galvanized lag bolts, recessed ¾ in. from the top of the plank. The bolting pattern for the timber/timber panel is shown in Figure A.8. The bolting pattern on the existing bridge deck is shown in Figure A.9. The bolting pattern for this test panel is not the same as that used for the temporary wearing surface; however, the difference is considered insignificant.

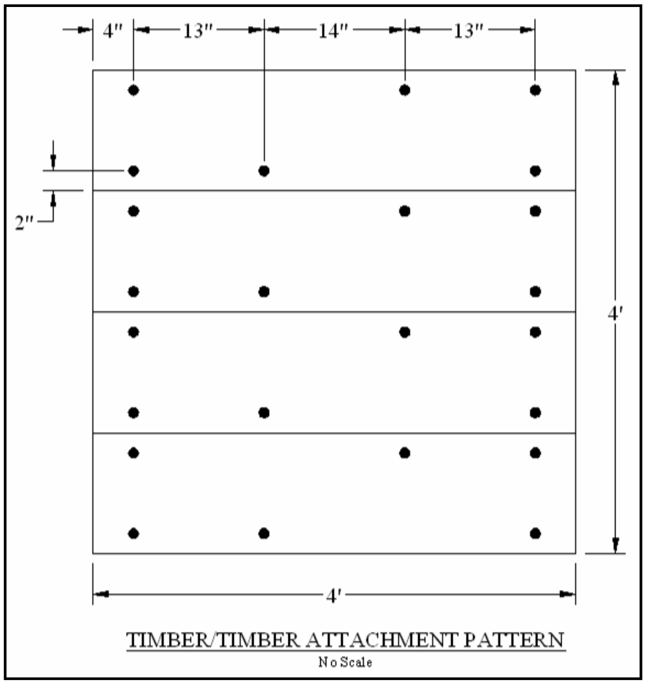

Figure A.8 Timber/timber bolting pattern.

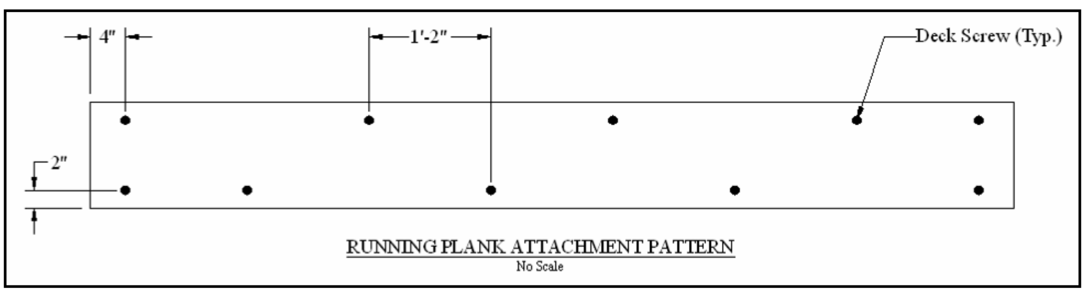

Figure A.9 Existing bridge-deck bolt pattern.

Transonite Panel

A Transonite panel measuring 51 in. by 51 in. by 5-7/8 in. and weighing slightly less than 300 lb was donated by Martin Marietta Composites for experimental testing in this research. This Transonite panel was made up of a two-part composite system. A skid-resistant polymer concrete using a low-modulus epoxy binder—FLEXOLITH—was installed on the panel by Tamms Industries, Inc. This company is now the Euclid Chemical Company (Euclid, 2007). Each Transonite layer was comprised of two sheets of fiber-reinforced polymer laminates, created using a pultrusion process. The laminates formed a top and bottom skin with a foam core in-between, all held together with 3-D fiber insertions. These fiber insertions provided reinforcement strength and durability to the Transonite panel and gave the panel a unique structure. The pultrusion process can result in varying density of the 3-D insertions between panel designs. The panel used in this research had a 3-D insertion density of 8 fibers per square inch in the upper course and 4 fibers per square inch in the lower course. Figure A.10 displays a cross section of the Transonite panel; this figure illustrates section details and corresponding dimensions. Figures A.11 and A.12 show the top and bottom view of the Transonite panel.

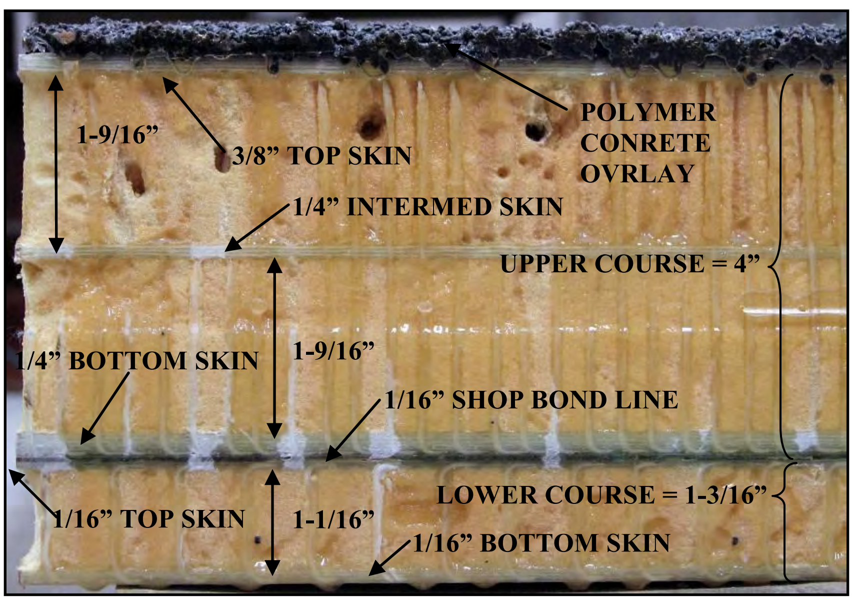

Figure A.10 Transonite cross section.

Figure A.11 Top view of Transonite panel.

Figure A.12 Bottom view of Transonite panel.

Structural properties for this donated Transonite panel were not supplied ,and Transonite properties reported in the literature give a wide range. Table A.1 shows the published values for Transonite for various thicknesses, core types, and fiber-insertion density.

Table A.1 Transonite Structural Properties (Martin Marietta Composites, 2008)

	Tensile Performance Range (Skins) ASTM D3039	Shear Performance Range (Sandwich) ASTM 273	Compressive Performance Range ASTM C365
Thickness range tested	0.15 to 0.30 in.	1.5 to 4.0 in.	1.5 to 4.0 in.
Modulus	2.0 to 3.5 Msi	1,500 to 15,500 psi	60,000 to 160,000 psi
Strength	25 to 60 ksi	Not Available	400 to 1,470 psi

Super Panel

Inspired by an inadequate flooring system in oil well drill housings on the Alaska North Slope, Creative Pultrusions, Inc. developed a fiber-reinforced panel to support and protect workers from deteriorating soils around the massive oil drills. In coordination with Compositech, a Fairbanks-based general contractor/vendor, Creative Pultrusions, Inc., developed a pultruded flooring panel known as the Super Panel.

The Super Panel was donated to UAF by Compositech for this research. Unlike the other four experimental panels, the Super Panel was designed to be a floor panel, not a bridge panel. However, the hollow-core geometry of the Super Panel is similar to that of the Bedford product, a product that was used for bridge panels as an experimental feature on the Yukon River Bridge.

A Super Panel is created through pultrusion. For this particular application, the Super Panel was pultruded into long, narrow sections that incorporated a male joint on one end and a female joint on the other. A high-quality epoxy was applied to the joints, and the panels were fastened together to develop a structurally sound flooring system. The panels shown in

Figure A.13 were being prepared at Compositech for assembly and shipment to the Alaska North Slope.

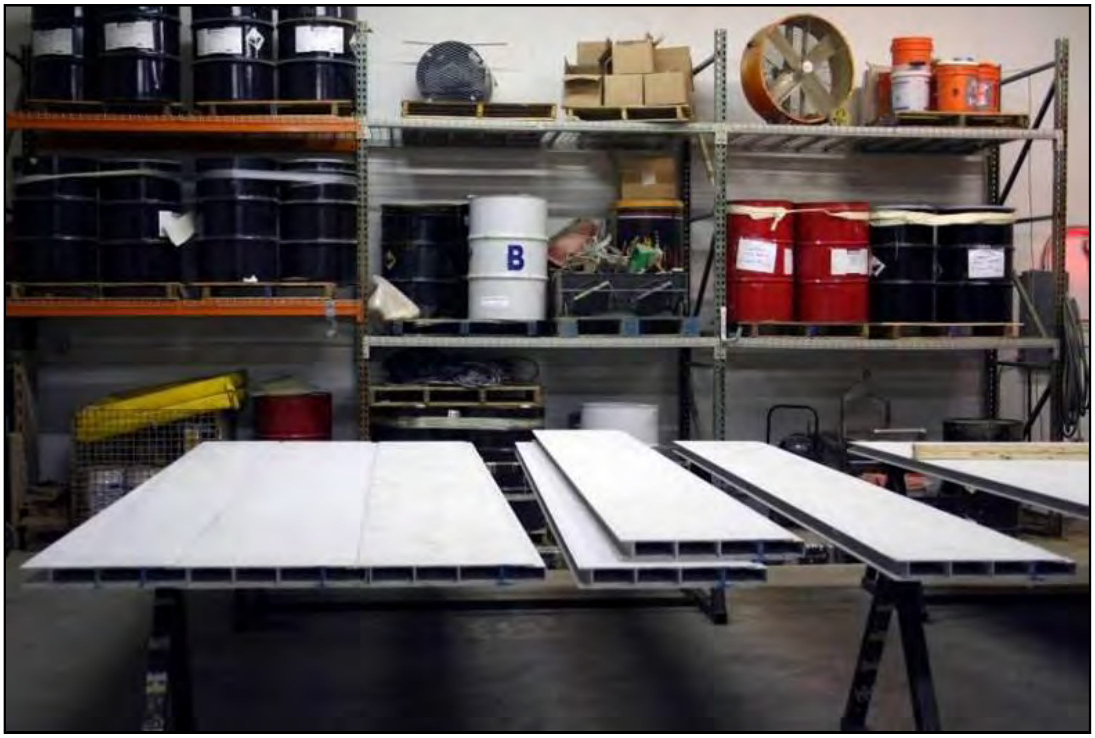

Figure A.13 Super panel assembly at Compositech.

The panel used for structural testing was 48 in. by 20½ in. with a nominal thickness of 2½ in. A Fairbanks aggregate combined with methyl methacrylate was applied to the surface of the panel to form a skid-resistant overlay. Figure A.14 shows the experimental Super Panel prior to testing. Figure A.15 provides a cross-sectional view of the Super Panel and the corresponding dimensions. Structural properties published by Compositech are presented in Table A.2.

Figure A.14 Super Panel.

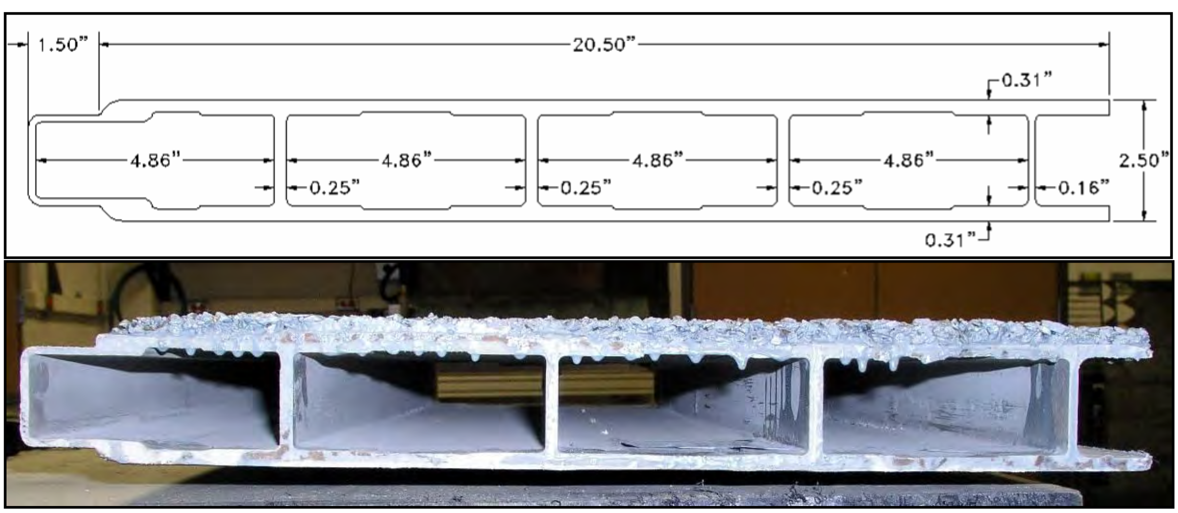

Figure A.15 Super Panel cross section.

Table A.2 Super Panel Published Structural Properties (Creative Pultrusions, Inc., 2002).

Item	Name	Value	Units
1. Mechanical Properties			
Modulus of Elasticity	E	3,500	ksi
Shear Modulus	G	500	ksi
Weight	ρ	6.83	psf
2. Ultimate Strengths for a Simply Supported Section with a Uniform Load			
In-Plane Shear Strength		7,000	psi
Flexural Strength		33,000	psi
Local Buckling Strength		26,213	psi
3. Sectional Properties			
Area of web	Aw	2.77	sq in
Moment of Inertia, major axis	Ix	15.4	$in.^4$
Section Modulus, major axis	Sx	12.33	$in.^3$

Timber on Solid UHMW

Ultra-high molecular weight (UHMW) polyethylene is a polymer with high abrasion resistance and high impact strength. It was chosen as an applicable bridge-deck panel because UHMW polyethylene is similar to Cobra X, an experimental feature that was installed on the bridge in 1992. The Cobra X panel was made of high-density polyethylene and was placed on the Yukon River Bridge as a possible bridge-deck alternative to timber. Except for minor deterioration of the imbedded traction surface, the panel performance was impressive. AKDOT&PF doubted the possibility of creating a bridge deck out of UHMW polyethylene because it was evident from the Cobra X panel that a reliable surface could not be imbedded in plastic and withstand destructive forces experienced by the bridge. Therefore, it was determined that additional research was needed to investigate possible tractable surfaces that could be integrated with UHMW polyethylene.

A proposal was made to AKDOT&PF to use a two-part system that could be altered in the future. The two-part system would consist of a 2½-in.-thick layer of solid UHMW polyethylene on which 2½ in. by 12 in. timber running planks could be fastened. As timber running planks start to fail, they could be replaced, and eventually the deck could be replaced entirely by a composite bridge deck that provided the desired thirty-year design life.

A 48-in.-square by 2½-in.-thick panel was donated by Ultra Poly with the cooperation of Compositech (a local contractor). Four 2½ in. by 12 in. timber running planks were fastened to the panel using the same bolting pattern as the timber on timber panel in Figure A.16. Initially as part of this research, the planks were fastened to the UHMW polyethylene using ¼ in. diameter by 3¾ in. galvanized lag bolts. However, this diameter was not sufficient, as once the lag had developed enough length in the UHMW polyethylene, the plastic would melt and grab the lag causing the bolt head to shear. After several attempts to fasten the timber with ¼ in. lags the size was increased to 5/16 in. lag bolts.

Figure A.16 Timber on timber panel.

Figure A.17 shows timber running planks fastened to 2½ in. of solid UHMW polyethylene to create an experimental bridge-deck panel 48 in. square and 5 in. thick. The solid UHMW polyethylene panel weighed 195 lb, and with the timber running planks attached, weighed 304 lb.

Figure A.17 Timber on solid UHMW panel.

Table A.3 is a summary of structural and physical properties that were found on Ultra Poly's website.

Table A.3 UHMW Polyethylene Structural Properties (Ultra Poly, Inc., 2002)

Item	Name	Value	Units
1. Mechanical Properties			
Flexural Modulus of Elasticity	E	120,000	psi
Weight	Y	58.058	pcf
2. Ultimate Strengths			
Tensile breaking strength		6,000	psi
Elongation at Break		400	%

Timber on M-Shaped UHMW

In the case of timber on M-shaped UHMW, timber is applied to a UHMW section corrugated bottom, giving the same depth but less weight; this was called the M-shaped UHMW panel. We postulated that an M-shaped panel would decrease the cost and weight of the possible bridge-deck alternative and increase constructability of the deck. The 48-in.-square panel weighed 146 lb, compared with the solid panel that weighed 195 lb. Figure A.18 shows the dimensions of the M-shaped panel molded at the Ultra Poly factory.

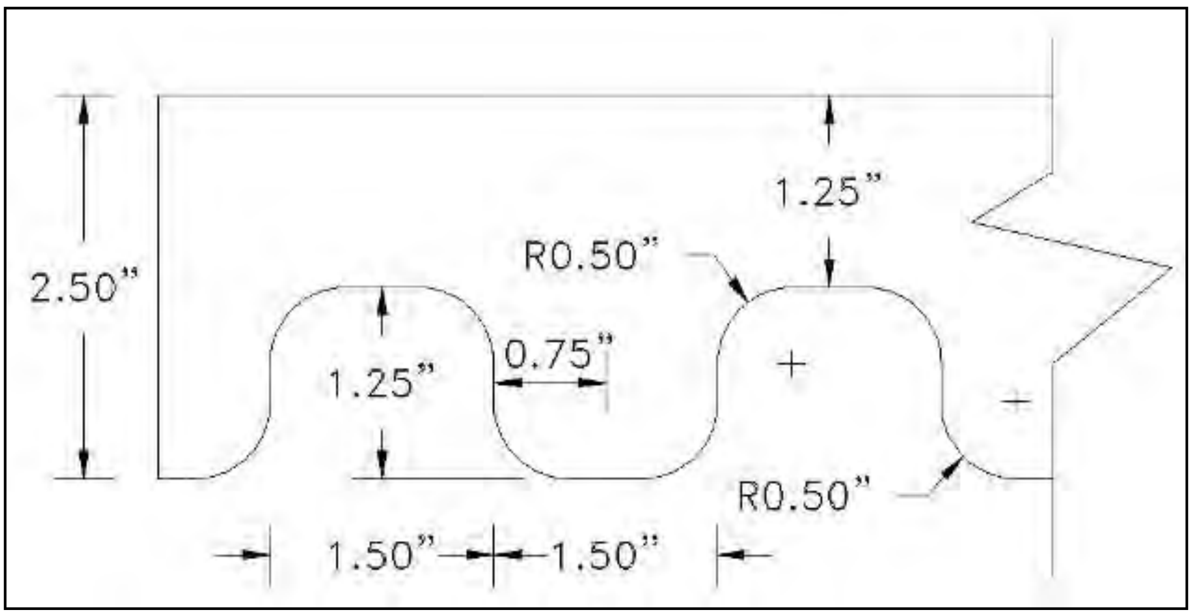

Figure A.18 M-shaped dimensional section.

The ridges molded in the panel run the full length of the panel and the four 2½ in. by 12 in. timber running planks were fastened perpendicular to the ridges. Figure A.19 shows a cross section of the molded M-shaped panel.

Figure A.19 Timber on M-shaped UHMW cross section.

Running planks were fastened to the panel using 5/16 in. diameter by 3¾ in. galvanized lag bolts. The running planks were fastened perpendicular to the ridges because, if the panel were placed on the steel orthotropic deck of the Yukon River Bridge, the ridges would need to be placed perpendicular to the deck. If ridges were placed parallel to the orthotropic deck, the ridges could form stress risers to the steel deck. Figure A.20 and A.21 show the top and bottom views of panel used for experimental testing.

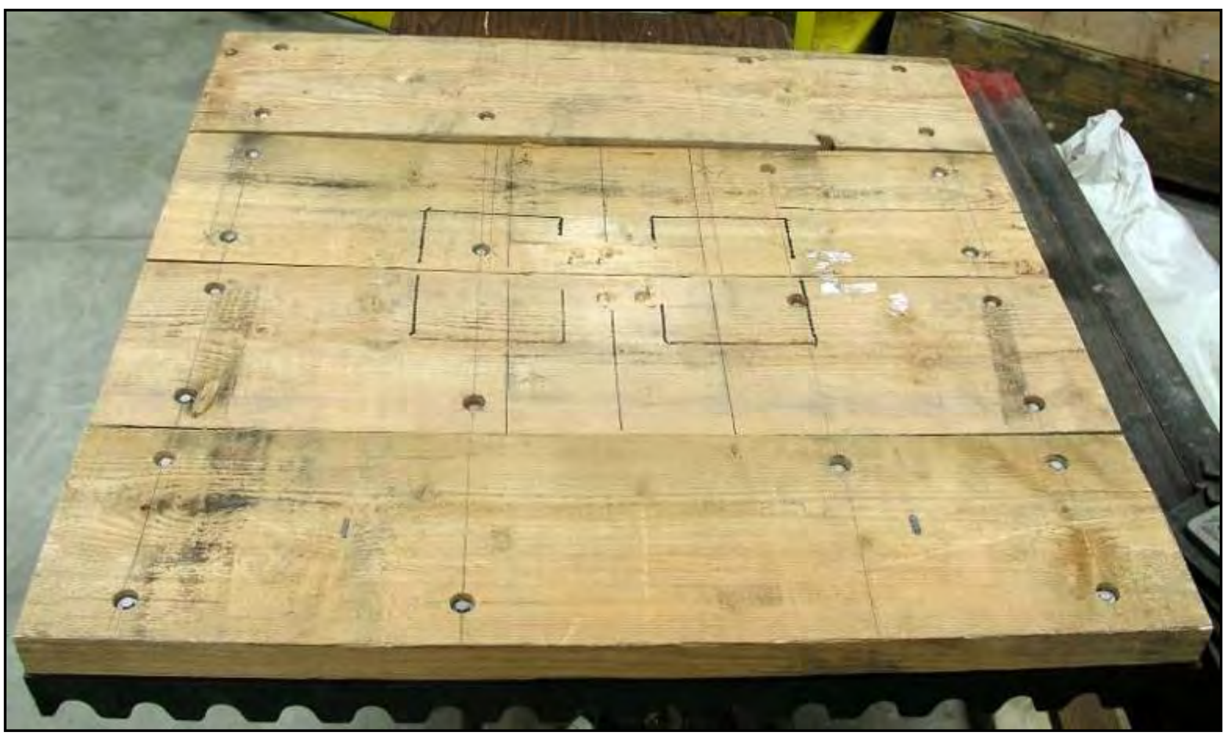

Figure A.20 Timber on M-shaped UHMW panel top view.

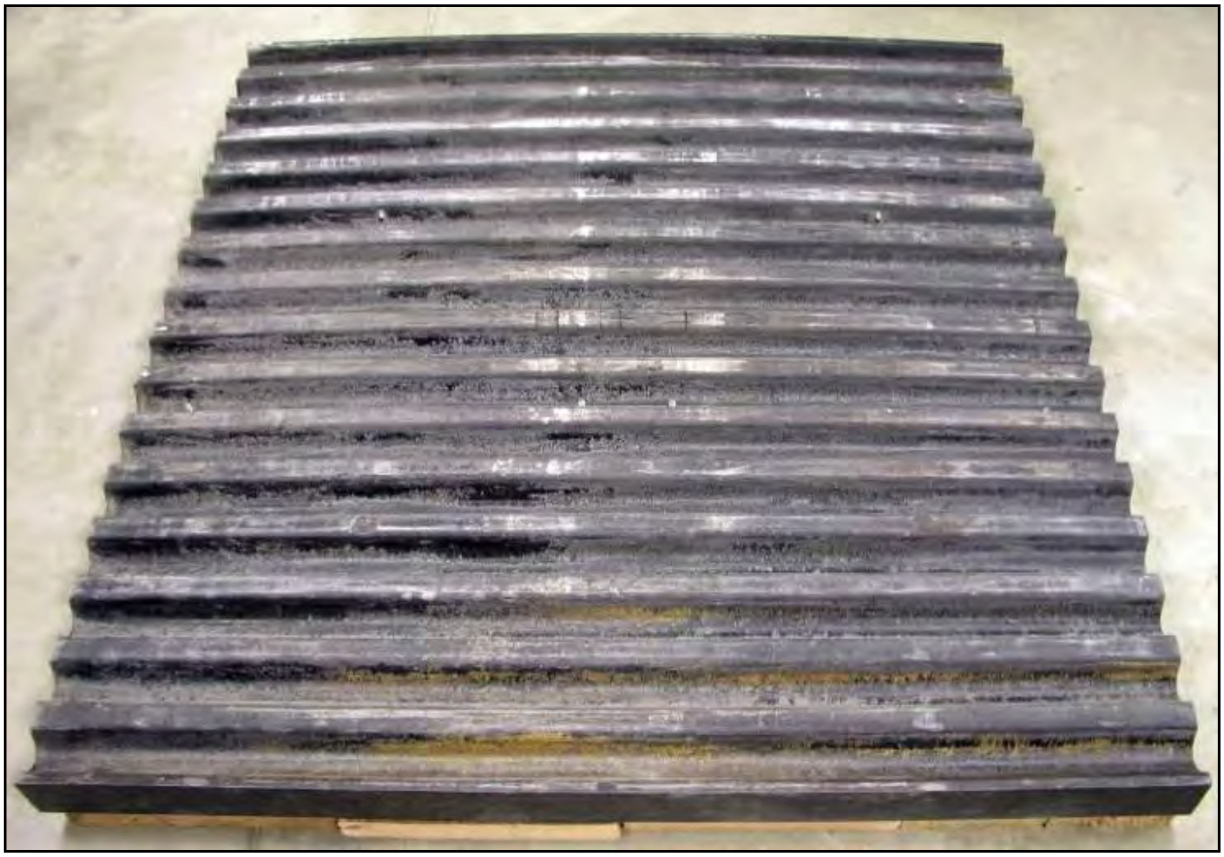

Figure A.21 Timber on M-shaped UHMW panel bottom view.

Experimental Panel Summary

In total, five panels were used for experimental evaluation. The panels were evaluated as potential bridge-deck systems. Evaluating the panels as a system was important for the timber on solid UHMW and timber on M-shaped UHMW panels. Individual parts of these panels were not tested as full-sized panels; they were always tested and evaluated together. Evaluating timber and UHMW polyethylene together made it possible to compare bridge-deck panels as systems, not as individual materials. Table A.4 is a summary of the panels that were tested.

Table A.4 Experimental Panel Summary

Experimental Panel Name	Manufacture	Length (in.)	Width (in.)	Thickness (in.)	Weight (lb/ft^2)	Structural Components
Transonite Panel	Martin Marietta Composites	51.00	51.00	5.88	15.8	FRP, 3-D Fiber Insertions, Foam Core
Super Panel	Creative Pultrusions Inc.	48.00	20.50	2.50	9.4	FRP
Timber/Timber Panel	UAF	48.00	48.00	5.00	13.6	Douglas Fir
Timber on Solid UHMW	Ultra Poly	48.00	48.00	5.00	19.0	Douglas Fir, UHMW Polyethylene
Timber on M-shaped UHMW	Ultra Poly	48.00	48.00	5.00	16.0	Douglas Fir, UHMW Polyethylene

APPENDIX B
WEARING-SURFACE INSPECTION (2006)

General Information

On June 13, 2006, Zachery Jerla and Wilhelm Muench (UAF graduate students) and personnel from AKDOT&PF Research, Bridge Design, and Maintenance inspected the Yukon River Bridge deck wearing surfaces.

While at the bridge, issues with each wearing surface that concern AKDOT&PF bridge design, maintenance, and research were discussed. This trip was taken before conducting any laboratory tests. A year later, after the testing was completed (June 22, 2007), Jerla and Muench returned to the bridge site to measure traction for the bridge-deck wearing surfaces and conduct a follow-up inspection for each surface.

Background

The Yukon River Bridge is a 2295-ft-long six-span orthotropic steel deck. The orthotropic steel deck is supported by two box girders that span between 310 ft and 420 ft between piers. Transverse beams spaced at 15 ft on center support the orthotropic steel deck. This two-lane bridge is on a 6% downgrade from south to north (see Figure B.1). It carries two-way vehicle traffic, heavy truckloads, and the Trans-Alaska pipeline. It was opened to traffic in 1976 with a two-layer temporary timber deck wearing surface.

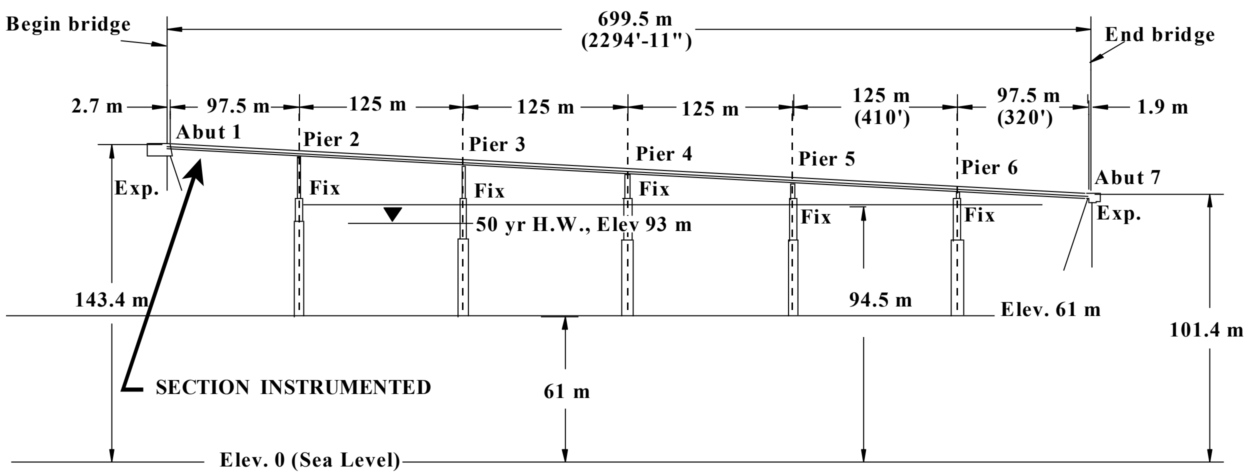

Figure B.1 Elevation view of the Yukon River Bridge.

Since 1976, the cost of timber has been on the rise, and the quality of timber has been on the decline. The timber deck wearing surface has been replaced four times in 33 years. In an attempt to find a better solution, AKDOT&PF funded UAF to evaluate the level of in-service strain in the orthotropic steel deck (Hulsey et al., 1995). In 1992, Cobra X was installed as an experimental feature. Since 1992, three additional experimental wearing surfaces have been installed. Table B.1 summarizes the performance of these wearing surfaces. AKDOT&PF has been seeking a wearing surface that provides better traction, more durability, and longer life at less cost.

Table B.1 Wearing Surfaces for the Yukon River Bridge

Wearing Surface	Installed	Replaced	Life	Performance
Temporary 2-layer timber (5 in. thick):				Short life and expensive
	1976	1981	5	
	1981	1992	11	
	1992	1999	7	
	1999	2007	8	
Experimental features:				
a) Cobra X over timber	1992	2007	15	Good to very good, but expensive
b) Concrete-filled grid	1999	2007	8	As the concrete wears down, the metal grid will be above and could result in a traction problem
c) Bedford Plastics: Prodeck 4	2005	2007	2	Failed
d) Martin Marietta, Inc.: Transonite	2005	2007	2	Poor to medium; first year there was damage to the surface grit at some locations; installation problems; water damage to underside of panel

In 2006, most of the wear surface was a two-layered wood system. This temporary wood deck wearing surface has several issues. The undesirable characteristics include short life, low traction, and increased cost; and with each replacement, the quality of replacement materials is lower. In an effort to find an improved wearing surface, AKDOT&PF provided for test panels to be installed as an experimental feature in the past several construction deck-replacement contracts. Test panels included polyurethane (Cobra X), concrete in a steel grid, and two types of fiberglass composites with supplier-attached wear surfaces (Transonite and Prodeck). Cobra X was installed in 1992, the concrete with steel grid was installed in 1999, and the Transonite and Prodeck were installed in 2005 (see Table B.1). All wearing-surface systems were installed and later visually inspected for wear, loss of traction, and degradation. None of the experimental featured test panels was instrumentated.

Inspection Team

On June 13, 2006, a group of AKDOT&PF and UAF designers and researchers inspected the wear surface of the bridge. The group included Clint Adler, Jake Allen, George Imbsen, Jeff Currey, and Joe Kemp from AKDOT&PF. The research team from UAF included graduate students Wilhelm Muench and Zack Jerla. The AKDOT&PF Maintenance and Operations crew, headed by Earl Ratliff, was replacing boards in the wear deck when the team arrived. The temperature was about 60°F and a rain shower occurred around noon.

Wood

At the time of inspection, wood covered most of the bridge deck. It is a two-layer system. The first layer is 3 in. rough-cut creosote boards, laid transverse to the direction of travel. The boards are held in place by studs at the edge of the deck and near the centerline of the bridge. Above this is a wear surface that consists of 2 in. rough-cut, untreated running planks laid parallel to the direction of travel. This running surface was completely replaced in 1999, and as part of maintenance, some planks are replaced periodically. The running planks are attached to the lower wood deck with ¼ in. lag bolts countersunk into the surface. There are two rows of bolts that are spaced about 2 in. apart in a staggered pattern. Many of the lag bolts showed signs of being pulled out, and some of the running planks showed evidence of warping. Prior to the June trip, AKDOT&PF Maintenance had added more lag bolts to the existing planks and replaced badly damaged planks. Many older planks showed signs of damage due to tire chains, and knots had appeared above the surface where decay (rot) was prevalent. Figure B.2 shows running planks with impressions left by tire chains. In some areas, the wood held up well; in other areas, it was in poor shape.

Figure B.2 Surface wear damage caused by tire chains.

Most of the timber wearing surface damage appeared to be from rot (decay) and splitting. For example, many of the wood surfaces were soft and decayed (see Figure B.3).

Figure B.3 Decay in the top of the wearing surface.

It appeared that these planks had deteriorated from rot, and the rotted material had been abraded and removed by traffic.

While decay seemed to be a problem, a treated test plank was installed in 1991 as a running board, and this plank did not show any significant improvement in wear resistance. Perhaps this is due to a difference in the type of wood used or increased wear due to the presence of incisions from pressure treating. These planks were replaced with the rest of the running surface in 1999 and, therefore, were not inspected during this trip.

A lack of traction for the wood plank driving surface on this bridge appears problematic. For example, during the inspection, a 10-yard dump truck towing an equipment trailer loaded with a small bulldozer was driving south over the bridge (uphill) and was stopped by a flagger. In an attempt to start moving, one set of duals spun on the running planks. The driver had to engage the rear axle because, on this type of truck, front wheels engage without the rears. Evidence of this problem is shown in Figure B.4, where rubber track marks were left on the running planks. It had rained several hours earlier, prior to the truck stopping, but the surface had since dried. This illustrates that the wood driving surfaces on this bridge have very little traction even when dry.

Figure B.4 Rubber tire marks caused by loss of traction.

Many of the most damaged planks were replaced prior to our field inspection and were not available for evaluation. Figure B.5 shows a typical repair. Except near the ends, the planks were satisfactory. At the bridge ends, boards were typically damaged, but the cause is unknown.

Figure B.5 Wood wearing surface: A typical replacement by Maintenance.

Our inspection initiated the following questions and observations:

1. Do some new planks have irregularities that may lead to premature failure? (Conditions to watch for include pockets of rot, irregular grain, loose knots, and internal splitting.)
2. Some of the planks may experience unusual in-service damage from snow removal equipment or other heavy equipment.

3. It would be informative to know how quickly damage spreads across several boards. It would be helpful to document where damage first begins, and how it spreads. Is it possible to limit the damage to one plank if it is inspected and replaced sooner?
4. Will damage continue to spread in partially damaged planks? Will a proactive approach to running-plank replacement lead to a longer time period between complete replacements?

Although our questions are beyond the intent of this inspection report, further study of these issues by AKDOT&PF may extend the life of the bridge deck wearing surface and reduce costs to Maintenance and Operations, as this and many other bridges in the state use wood wearing surfaces.

Cobra X

This is a polyurethane product that was designed for use at railroad crossings. In 1992, an experimental test section of this product was placed on the Yukon River Bridge for observation as an alternative wearing surface. It was not inspected during this trip, but according to Maintenance, it has performed well. When wet, it is supposedly very slick. The company that manufactured this product is no longer in business, so it is not an option for use on the Yukon River Bridge.

Concrete in Steel Grid

A test section of concrete in a steel grid was installed in July 1999. While it continues to serve as a wear surface, it shows signs of impending failure. The concrete above the top of the grid is starting to separate from the grid, and only concrete blocks are left within the grids (see Figure B.6).

Figure B.6 Concrete-filled steel grid wearing surface (7 years old).

Because of concrete loss over time, it is likely that in the distant future only the steel grid will be left. Once there is only a steel grid, the expected traction will be very low or similar to a slick surface typical of metal grid decking. The concrete wearing surface at the in-place experimental test panels were slightly higher than the surrounding wood deck. Figure B.6 shows that the most damaged area is at the end of the test section. The direction of traffic in this figure is from left to right. This suggests that the majority of damage may be due to snow-removal equipment blades scraping the higher surface. We believe this could be eliminated if the surface of this test section and surface of the wood were at the same elevation. Not all damage was at the ends. There were some areas with concrete missing near the center of the test panels, and much of the concrete surface showed signs of cracking along lines of the steel grid below (see Figure B.7).

Figure B.7 Another concrete-filled steel grid wearing-surface test section.

Generally, the concrete-filled steel grid test panels performed well. They offer better traction than other choices and appear to be durable, but they have a life expectancy of only seven years (see Figure B.8). Wear marks shown in Figure B.8 are likely caused by tire chains, studs, and snow removal equipment.

Figure B.8 Concrete-filled metal grid: Possible chain damage (age is 7 years).

Though there is surface damage to the concrete-filled steel grid, the damage did not seem to reduce the effectiveness of the wearing surface or its ability to absorb further wear. Except for weight, it appears from our visual field inspection that concrete is a viable wearing surface. A weight restriction of 30 psf means that a normal-weight concrete alternative must be no thicker than 2½ in. (about 145 pcf).

Transonite

In August 2005, several test panels of Transonite, a proprietary fiberglass composite manufactured by Martin Marietta, were placed on the bridge. Two panels were installed as a wearing surface between the bridge rails. The joint between the panels was between traffic lanes or the bridge centerline.

Three sets of test panels were placed in the direction of travel, creating a six-panel test section. These panels were bolted to the steel deck with steel studs field-welded to the deck.

Each panel was a three-part system: a top layer, inner layer, and bottom layer. The top layer consisted of a wear surface bonded to the panel. This wear surface was about 3/8 in. thick and appeared to be an epoxy concrete with an aggregate broadcast. The inner layer consisted of a 4 in. thick Transonite panel. Transonite panels are made of foam sandwiched between fiberglass panels, with pillars of fiberglass connecting the panels through the foam. The bottom layer was bonded to the inner layer. This bonded bottom layer was a 1-3/16-in.-thick Transonite panel. The bottom layer did not exist over the bolt splice plates in the steel deck. In this area, a neoprene strip was located over the bolt heads, and a plate of sheet metal was bonded to the panel. Figure B.9 shows a panel in place on the deck. This figure shows both the layered system and the neoprene strip. The panel assembly was bolted to the steel deck with studs.

Figure B.9 Fastening details between deck and the Transonite.

The wear surface showed signs of damage. Marks formed by tire chains and grader teeth were clearly visible. Since the surface is only 3/8 in. thick, even a small amount of wear damage is a concern. One of the panels appeared to have a thinner surface than the others had; and in many places, the fiberglass was damaged and the wear surface was gone (see Figure B.10). This figure illustrates that the surface wore more along the edges.

Figure B.10 Early delamination of the Transonite wearing surface (1 year old).

The remaining panels with the 3/8 in. thick wearing surface appeared to have less wear damage, but early stages of cracking and delamination were still evident. The performance of these one-year-old test panels was poor in comparison with the other experimental features that have been tested on this bridge deck. Cracks in a spider pattern exist around many of the attachment holes (see Figure B.11). The length of these cracks appears to be growing.

Specifically, cracks appear to be noticeably wider at the hole. This may mean that water is getting into the cracks and forcing them open. If this is the cause, early delamination of the surface and damage to the panel is likely.

Figure B.11 Cracks around attachment hole: Transonite wearing surface.

Figure B.12 shows a panel with a sharp delaminated edge. This sharpness suggests that the damage is from a break or breaks—not from wear. At this same location, there is a crack that exists across both panels. This crack appeared to follow the edge of the bolt splice plate that is fastened to the steel deck and the edge of the 1-3/16 in. Transonite layer (this a probable change in support stiffness).

Figure B.12 Possible delamination caused by a bolt in the splice plate.

Edge caps were attached to the exposed ends of the panels, presumably to keep water from entering the foam. The caps were held in place using aluminum pop rivets; if another attachment was used, it is not visible. Several of the pop rivets were missing heads (see

Figure B.13). If rivets are the only form of attachment, this is a problem, as the other rivets will also likely fail.

Figure B.13 Transonite edge strip with missing pop rivets.

The underside of the Transonite was investigated with the assistance of an AKDOT&PF operator and a boom truck. The panel underside revealed additional problems. For example,

Figure B.14 shows that the seal between the panel bottom and the end caps failed, which allows water to enter the panel freely.

Figure B.14 Leaky seal under the Transonite panel.

At the notch over the bolt plate in the steel deck, we noted damage, again in the seals around the panel. The exposed foam shown in Figure B.15 was apparently painted with a rubberized sealer; however, the sealer cracked and the foam behind it was damp and very soft, and the pillars of fiberglass were broken at either the top or the bottom. This problem extended back into the panel for 1 in. to 3 in. The sealer (green) did not stop water and dirt from entering the panel (see Figure B.15). Besides problems already stated, the bottom of the fiberglass panel was separated from the foam.

Figure B.15 Cracked sealer and foam on the Transonite panel.

The dirt and wet foam was easily removed with our fingers. Once the dirt and foam was removed, we found that many of the pillars within the foam were broken; they also were easily removed without tools. Figure B.16 shows a hole in the foam that is about 1½ in. deep.

Figure B.16 Damaged fiberglass pillars and foam in the Transonite panel.

All first-row pillars and many second-row pillars along the cut edge of the panel were broken. This may have been caused by water entering the foam followed by freezing and forcing the panel apart, and may cause the panel to degrade over time as more water enters the foam. No sealer was found around the attachment holes. Fastening studs welded to the steel deck penetrate the first layer of Transonite and are sleeved with FRP inserts. This penetration was not bonded or sealed.

Martin Marietta shop drawings for these test panels show a typical section for an attachment hole (see Figure B.17).

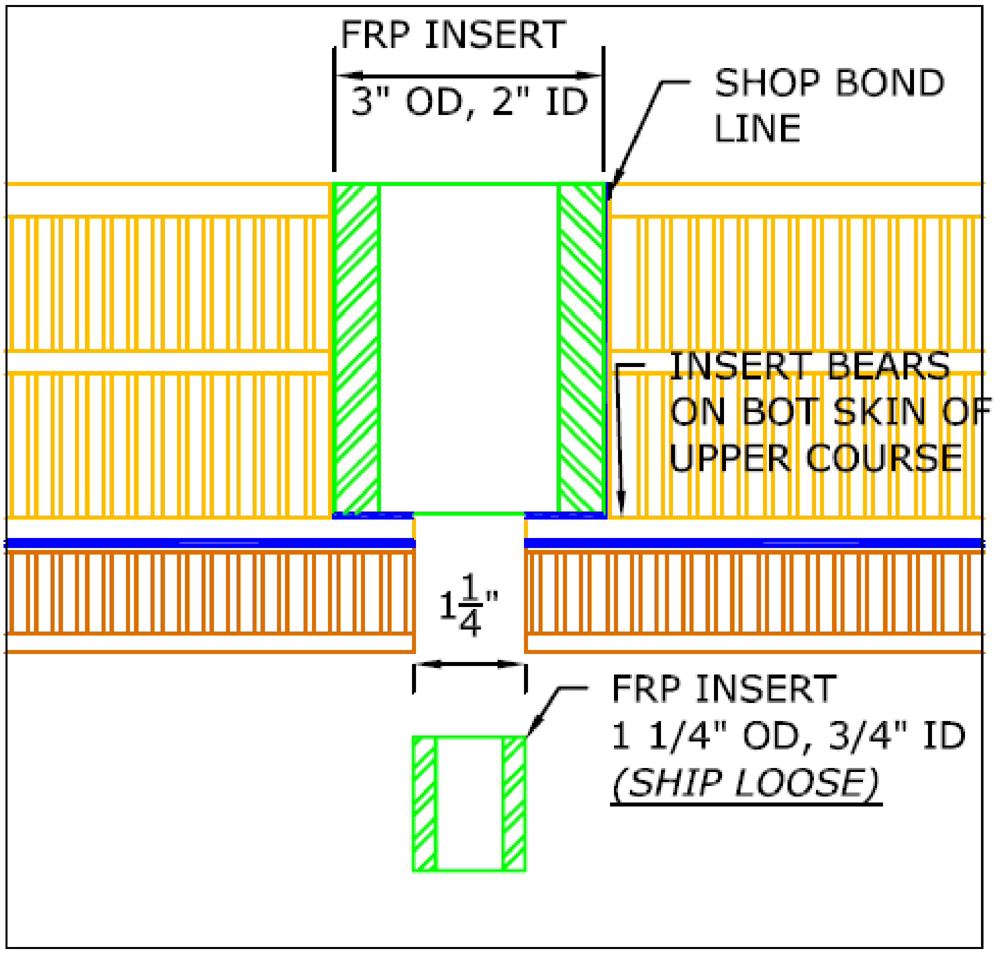

Figure B.17 Insert detail: Martin Marietta shop drawing.

In this case, sealant was to be placed over the top of the nut. The idea was to prevent water from entering from the top. In many cases, however, the sealant had collapsed into the hole, allowing water to enter. Further, no sealer was placed around the insert, and this allowed water to enter the foam. Figure B.18 shows one of these holes from the bottom side of the panel; the FRP insert is removed in this picture. Foam inside the hole was wet, degraded, and soft. The foam in another hole nearby was dry and showed no sign of foam damage. Based on these observations, the foam will likely suffer from freeze damage.

Figure B.18 Hole for the insert: looking from the bottom.

Panels appeared to be sliding on the steel deck. The bolts in the splice plate had worn shiny spots on the metal above them (see Figure B.19). This does not appear to be causing damage to the bolts or the panel, where the metal protects the fiberglass.

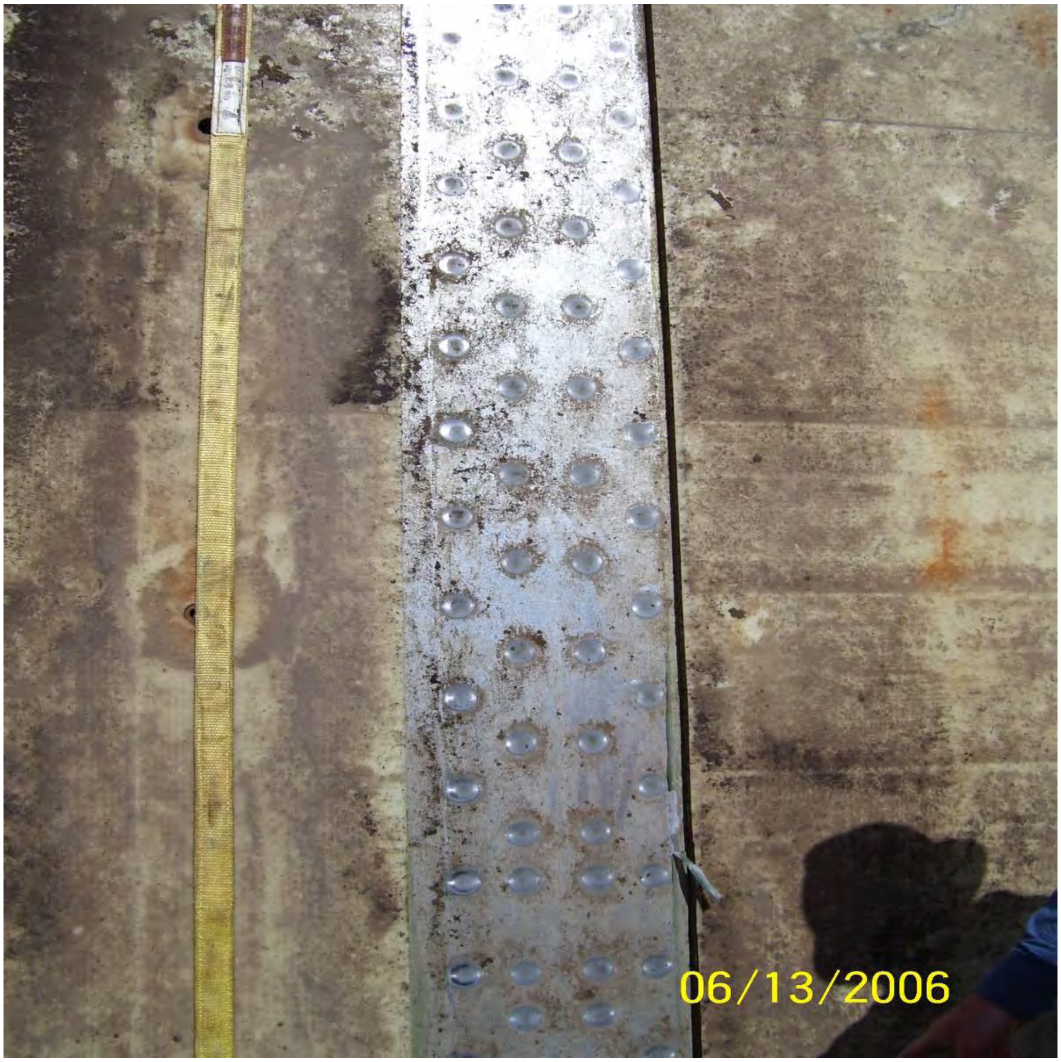

Figure B.19 Bolted splice plate supporting deck panels

Unless the panel fiberglass is protected, relative movement between the panel and the deck may be problematic. Panel under-surfaces are susceptible to damage, so the old timber surface was removed before the panels were placed. Studs used to hold the timber down were cut off and ground to be flush with the deck surface. Two studs appeared to have been left higher than the others, and they punctured the lower surface of the Transonite (see Figure 20).

Figure B.20 Punctured bottom surface of the Transonite test panel.

Panel damage existed at those studs that extended above the surface by as much as 1/16 in. to 1/8 in. above the surface of the deck. Prior to inspection, water had entered the panel at these punctures and discolored fiberglass around the hole. This was verified by turning the panel on its side and observing water running out of the holes.

If Transonite is used, we recommend a smooth support surface to avoid punctures. Workers must take care with their tools to prevent damage to this fragile panel. For the most part, the steel deck looked to be in good condition. Except where the studs were ground off, the anticorrosion coating held up well. There were instances where rust was found around some studs (see Figure B.21). Areas around some studs were rusted; other areas were not. Figure B.21 shows a rusted stud (one of the worst). A better long-term treatment is needed around these studs.

Figure B.21 Deck rust at a welded stud; loss of anticorrosion coating.

Prodeck 4

In July 2005, several test panels of Prodeck 4, a proprietary fiberglass composite manufactured by Bedford Reinforced Plastics, were placed on the bridge. Two panels were used to cover the width of the bridge with a joint at centerline. Three sets of panels were placed along the direction of travel, creating a six-panel test section.

The test panels were bolted to the steel deck using weld on studs. The panels are a two-part system. The top layer (wear surface) was bonded to the panel. This wear surface was about ¾ in. thick and appeared to be an epoxy concrete. The second layer was a 4 in. thick FRP Prodeck panel. Prodeck panels have fiberglass at the top and fiberglass at the bottom, with webs of fiberglass connecting the top to the bottom. These panels are a composite that is much like a hollow-core concrete slab with rectangular voids. Voids were at both ends, open and orientated perpendicular to the bridge, allowing the panel to drain.

The Prodeck panels were not lifted to inspect below. However, according to shop drawings, Prodeck panels were placed on 1½ in. FRP spacers to provide clearance over the bolts and splice plates in the steel deck. The panels were attached to the steel deck using studs that fit through holes in the spacers at the bottom sheet of the panel. The studs were accessed through holes in the upper layer of the panel. Sealant was placed around the holes, but collapsed and allowed water to enter. Unlike Transonite, water was not trapped in the foam (see Figure B.22). The wear surface showed signs of damage, but was generally in good condition. Though marks from tire chains and graders were present, most of the marks were only surface scratches and did not extend into the wear surface. Figure B.22 shows a mark left by a grader (top to bottom).

Figure B.22 Grader scratch to the wearing surface on the Prodeck test panel.

The left-to-right marks are part of the original wearing surface. The surface is about ¾ in. thick, so some wear is allowable before failure. Cracks appeared near corners of several of these test panels. Cracks appeared to initiate in the fiberglass and not in the wear surface (see Figure B.23).

Figure B.23 Prodeck 4 test panel: Cracks propagated from the fiberglass.

A crack was found to run along one of the webs in the FRP panel below the wear surface. There was a crack in the FRP web at the edge of the panel. It would appear that the crack is the result of bending in the panel. The failure of the panel may be due to the unevenness of the steel deck. When installed, all of the panels on the northbound lane were higher than the surrounding surface at their southwest corners. Heavy trucks deflect the panels downward, but the panels return when load is removed.

Figure B.24 provides a closer view of the panel failure and similar to that seen in Figure B.23. The end web was detached from the top, and the end cap had debonded from the main panel. This was the only place where debonding was observed. However, the failure at the top of the end web was common, and in some cases, a similar fracture could be seen at the bottom.

Figure B.24 Prodeck 4 test panel: Cracked fiberglass end.

At time of inspection, the panels did not sit flat on the steel deck. While no panels were lifted on this date, the following information was obtained from Bedford Reinforced Plastics, Inc. shop drawings and pictures of the installation.

The panels were supported on five FRP spacers that are parallel to traffic. The spacers have holes that are placed over studs welded to the deck. Figure B.24, provided by AKDOT&PF, shows the steel deck with spacers in place and ready for the panels to be placed. These narrow strips transmit the traffic line loads, which cause high states of stress. Orthotropic steel decks like the one used on the Yukon River Bridge are sensitive to fatigue and have been shown to have problems with cracking. Subsequently, spacers should be positioned so that the load is applied to the ribs below the deck plate. This would minimize future problems.

Installation reports for these test panels were provided by AKDOT&PF. These reports are identified by ―Yukon River Bridge Rehabilitation Test Panel Installation (Surface Deck) DP-065-2(13)/60431." Drawings were provided by the supplier. It was not possible to determine from the installation pictures and from these reports if the spacers were located over the ribs. No matter what spacing is used for the FRP spacers, inspections should be conducted to check for damage to the steel deck (see Figure B.25).

Figure B.25 Installation of Prodeck 4 on the Yukon River Bridge (after AKDOT&PF).

APPENDIX C
HISTORY OF WEARING SURFACES FOR THE YUKON RIVER BRIDGE

A steep grade, severe climate, and use by heavy trucks requiring tire chains to gain traction on slick timber running planks have been a wearing-surface challenge for the Yukon River Bridge. Timber quality is on the decline, as timber replacement costs are on the incline. The condition of the timber wearing surface in 2007, prior to replacement, is shown in Figure C.1. Intermediate sections of the deck were replaced in the summer of 2006. The age of the failed timbers in the photograph are estimated to be only a few years.

Figure C.1 Timber wearing surface, months before it was replaced.

Cobra X

In 1992, AKDOT&PF took the initiative and installed an experimental wearing surface on the Yukon River Bridge. A 55-ft-long by 30-ft-wide test section of 2½-in.-deep lightweight Cobra X high-density polyethylene (HDPE) grade-crossing module was placed over a lower course of 2½-in.-thick timbers. Cobra X, created by Railroad Friction Products, was used extensively in railroad crossings throughout Alaska. The skid surface for the Cobra X module used as a bridge-deck panel was improved by the addition of quartz particles embedded in an epoxy coating. This product is not available, as the company is no longer in business.

A 1996 bridge inspection concluded that the Cobra X panels had performed successfully throughout the period of the study. The skid surface showed minimal wear, and it was recommended that annual inspections be continued until it was possible to estimate the service life of the wearing surface. It was stated in the 1996 bridge inspection report that the Cobra X test panels were in place for 15 years and were performing comparatively well in comparison with the timber running planks that had only been on the bridge for 5 years. The lag screw method for attaching the panel to the underlying timber running planks had been an area of failure. The photograph shown in Figure C.2 shows the failure of a number of panels. The test section was replaced in the summer of 2007 with two new layers of timber running planks.

Figure C.2 Cobra X crossing module; summer of 2007.

Concrete-Filled Steel Grate

In summer 1999, two 18-in.-wide concrete-filled steel grate wearing surfaces were installed as a second experimental feature on the Yukon River Bridge. Documentation from a 2003 evaluation of the concrete tests reported that a considerable amount of degradation was observed and the material was not enduring well. The concrete had begun to show surface-tension cracks, this was due to the weakness in tension and the stiff behavior of the concrete. In the summer of 2007, the concrete-filled steel grates were removed, and no future consideration was given to that experimental feature.

FRP Panels (Bedford Reinforced Plastics, Inc.)

The realization that a new wearing surface for the Yukon River Bridge would have to be an engineered product specifically designed for the unique characteristics of the bridge led AKDOT&PF to explore modern composite materials. In the spring of 2005, a ―Letter of Interest” was sent to prospective suppliers expressing an interest in using a synthetic material as a replacement for the timber deck surface on the Yukon River Bridge. Suppliers were asked to provide materials for a 25-ft minimum length, full-width test section. A bulleted list of ―suggested deck wearing-surface requirement and properties” was drafted to aid suppliers in their design, The bulleted list is shown in Appendix D.

Two FRP composite bridge-deck manufacturing companies were selected for the installment of two experimental bridge-deck sections. Bedford Reinforced Plastics, Inc. installed six panels measuring15 ft by 8 ft to create a 24-ft-long test section spanning both sides of the bridge centerline. The product they proposed for a replacement bridge deck was a 4-in.-deep Prodeck 4 hollow-box core FRP composite bridge deck with a ¾ in. polymer concrete overlay as the traction surface. Panels were orientated so that the hollow-box core ran transverse to traffic. Panels were placed on 1½ in. FRP composite spacers; this provided clearance over splice plates on the steel deck. Each panel was set into place over ten Nelson studs, ⅝ in. in diameter, welded to the steel deck, and secured with a nut and washer.

A year after installment (2006), the FRP composite bridge deck showed signs of fatigue; yet traction of the polymer concrete surface was reliable and little wear was seen. A close inspection revealed web-flange intersections and concrete surfaces with signs of high tensile strains. Figure C.3 (summer 2006) shows a traction surface, cracked polymer concrete, and fracture of the web-flange intersection.

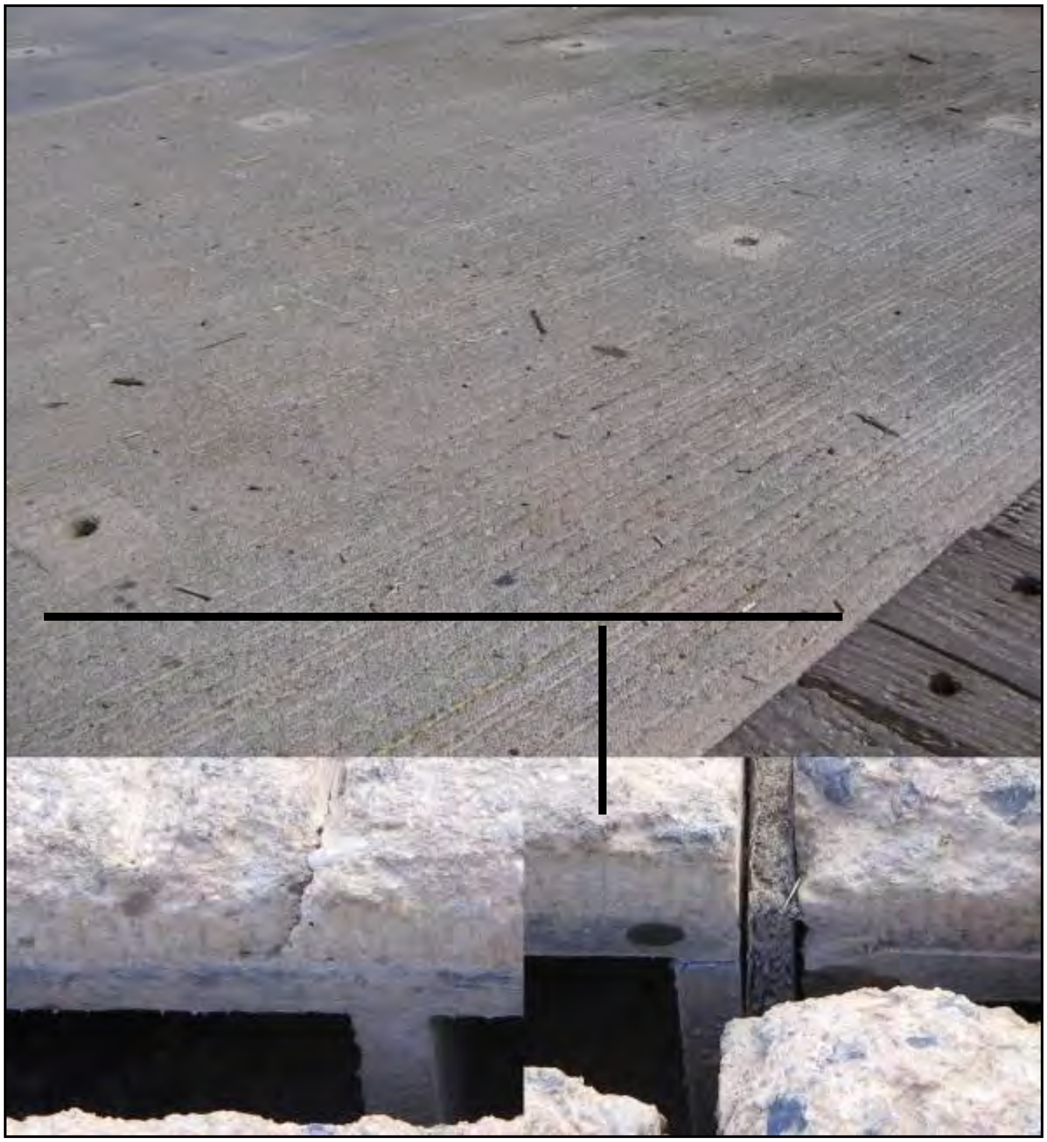

Figure C.3 Bedford Reinforced Plastics, Inc. Prodeck 4 panel.

It was believed that the Bedford Prodeck 4 panel was too stiff to be used on the Yukon River Bridge. The steel orthotropic deck is a flexible system. Subjecting a contrasting stiff system to the flexibility in the deck may cause tension failure in the surface. Cracking of the polymer concrete traction surface and fracture of the web-flange intersection were valid as evidence that this wearing-surface system was too stiff. The Bedford Prodeck 4 panel is not recommended as an alternative wearing surface for the Yukon River Bridge. The photograph in Figure C.4, taken during summer 2007, shows that the polymer concrete overlay was beginning to delaminate from the FRP.

Figure C.4 Prodeck 4, surface delaminating.

Prior to this research contract, Prodeck 4, provided by Bedford Reinforced Plastics, Inc., was withdrawn from the market, and it was not available for laboratory testing and future analysis.

FRP Panels (Transonite by Martin Marietta Composites)

The second FRP composite bridge deck installed in the summer of 2005 was distributed by Martin Marietta Composites. Martin Marietta supplied a FRP composite bridge deck known as the Transonite panel. The Transonite panel was made up of a two-course composite system with a skid-resistant polymer concrete overlay. Similar to the installation of the Prodeck 4 bridge deck, the Transonite was installed as six separate panels. Each panel had the dimensions of 15 ft by 8½ ft. The Transonite panel encompassed an area of 25½ ft by 30 ft on the Yukon River Bridge. Nine ⅝-in.-diameter Nelson studs secured the panel to the steel orthotropic deck, and a 12½-in.-wide by ⅞-in.-deep channel was cut from the panel to span the splice plates. During a bridge inspection trip in the summer of 2006, one of the six panels installed was lifted so that the bottom of the panel and the steel orthotropic deck could be examined. Figure C.5 provides a photograph of the bottom of one of six panels installed on the Yukon River Bridge.

Figure C.5 Transonite panel, bottom side inspection.

The lower FRP sheet of the Transonite panel had been penetrated by Nelson studs that were intended to be grinded down flush with the steel deck prior to installation of the panel. Water had infiltrated into the foam core through these penetrations and around the holes manufactured to allow the panel to be fastened to the deck. The presence of water seemed to be deteriorating the foam, but the neighboring FRP sheet remained intact. The 3-D fiber insertions that were exposed due to the cut in the bottom of the panel to allow for the splice plates were seen to be failing along the edge. It was believed that the failure of the 3-D fiber insertions was caused by shear failure or possible crushing, but the failure did not appear to affect the integrity of the system. The structural durability of the panel appeared to be sufficient despite the fatigued appearance of the bottom of the panel. The traction surface of the Transonite panel showed signs of wear as a 3 in. section of the polymer concrete overlay had been chipped away. Figure C.6 shows the wear in the traction coating of the Transonite panel.

During a return inspection of the Yukon River Bridge in the summer of 2007, the traction surface of the Transonite panel showed very little signs of additional wear from the previous year. It was believed that the chip section in the polymer concrete would progress and cause a greater loss of area, but this was not seen. Figure B.6 provides a photograph of the same chipped area seen in Figure B.7, but one year later.

The Transonite panel was a more flexible system than the Bedford Prodeck 4 panel. Added flexibility of the system allowed the panel to conform to movement of the steel orthotropic deck, thus limiting high levels of strain in the traction surface. However, panel deterioration after two years of installation on the bridge was cause for concern, and it is not recommended as an alternate wearing surface for this structure.

Figure C.6 Transonite panel, 2006 (1 year old).

Figure C.7 Transonite panel, 2007 (2 years old).

APPENDIX D
SUGGESTED DECK WEARING-SURFACE REQUIREMENTS AND PROPERTIES

Design criteria attached to the ―Request for Letters of Interest” drafted by AKDOT&PF:

Suggested Deck Wearing-Surface Requirements and Properties
Yukon River, BN 271

- Allowable deck surface weight:
    - 30 pounds per square foot.
- Viscosity:
    - Bridge is on a 6% grade. It must be possible to place viscous material on a 6% grade.
- Coefficient of linear expansion:
    - Provide slip plane between materials with incompatible coefficients
    - For composite materials, ensure compatible coefficients.
    - Provide sufficient expansion joints for 2295-foot-long bridge.
- Ability to inspect underlying orthotropic-steel deck:
    - Removable wearing surface.
    - Accessible anchorage system.
- Friction coefficient:
    - Establish minimum requirement.
    - Ability to reestablish the wearing surface friction coefficient.
- Flexural, tensile, and compressive strength:
    - Identify acceptable values.

    - For composite materials, ensure compatible strengths. Example: If a flexible material is overlaid with a material having low flexural strength, then cracks and/or debonding may occur.
- Minimum required thickness:
    - Wearing surface must cover splice bolts extending 1.22 inches (1/2 inch plate + 35/64 inch bolt head +0.177 inch washer) above steel deck surface. Suggest field verifying bolt height.
- Wearing surface anchorage:
    - Existing anchorage consists of 5/8-inch-diameter threaded studs (approximately 3¼ inch long) welded to the orthotropic-steel deck 6 inches from deck sides and 12 inches from deck centerline (4 total) at 11½ inch spacing.
    - Additional welded anchors require Bridge Section approval.
- Design temperature range:
    - Approximately –60°F to +100°F (research verify range).
- Installation weather requirements:
    - Minimum required wearing-surface installation and re-texturing temperature is 50°F.
    - Humidity/precipitation limits.
    - (Suggest discussing with Bridge Maintenance Crew for confirmation)
- Material handling and safety requirements:
    - Identify appropriate material handling and safety requirements.
- Environmental considerations:
    - Volatile organic compounds (VOC) limits may apply to some products.

    - Other environmental considerations.

- Other properties:
    - Freeze-thaw durability.
        - Low permeability.
        - Resistance to salts and petroleum products.
        - Toughness (non-polymer materials)
        - Polymer glass transition temperature (brittleness/toughness).

Other items:

- If polymer materials are used, then additional material properties may be important. Refer to AASHTO-AGC-ARTBA Joint Committee, Task Force 34 Report, “Guide Specifications for Polymer Concrete Deck Overlays,” October 1995.
- Through a research project in the early 1990, the Missouri Department of Transportation identified an appropriate polymer overlay for an orthotropic-steel deck bridge.
  They also routinely place an epoxy polymer concrete overlay on concrete bridge decks.
  Refer Missouri 2004 Standard Specifications Sections 623 and 1039.
- Require consultant to develop material and construction specifications for our review.

APPENDIX E
FIELD TEST RESULTS

Yukon River Bridge Traction Tests

On June 22, 2007, we measured the coefficients of friction for the wood deck and four experimental features. The friction coefficients were measured for wood, Cobra X, Transonite (a Martin Marietta product), and Prodeck 4 (a Bedford Plastics product). It was the purpose of these tests to provide a comparison between the laboratory tests and the conditions in the field.

Except for Cobra X (14 years old when it was removed from the bridge) and a sample of asphalt pavement (14 years old) the materials tested in the laboratory were at the beginning of their life. The materials tested in the field were at the end of their life. The wood deck was between 1 and 8 years old, Cobra X was 15 years old, Transonite was 2 years old, and the Prodeck 4 was 2 years old. During the summer of 2007, the wearing surface was completely replaced with a two-layer timber deck wearing surface.

The test results are provided herein for review and consideration. They are listed in Figures E.1 to E.8. The coefficients were within 0.59 to 0.83 for 80% of the data being either below or above these values. The tests were conducted by first driving upgrade from north to south. The researchers turned around and drove downgrade, taking data. This was repeated four times for a total of eight tests. Locations of the experimental features were recorded, and the friction data for these sites were recorded for Tests 3 to 8.

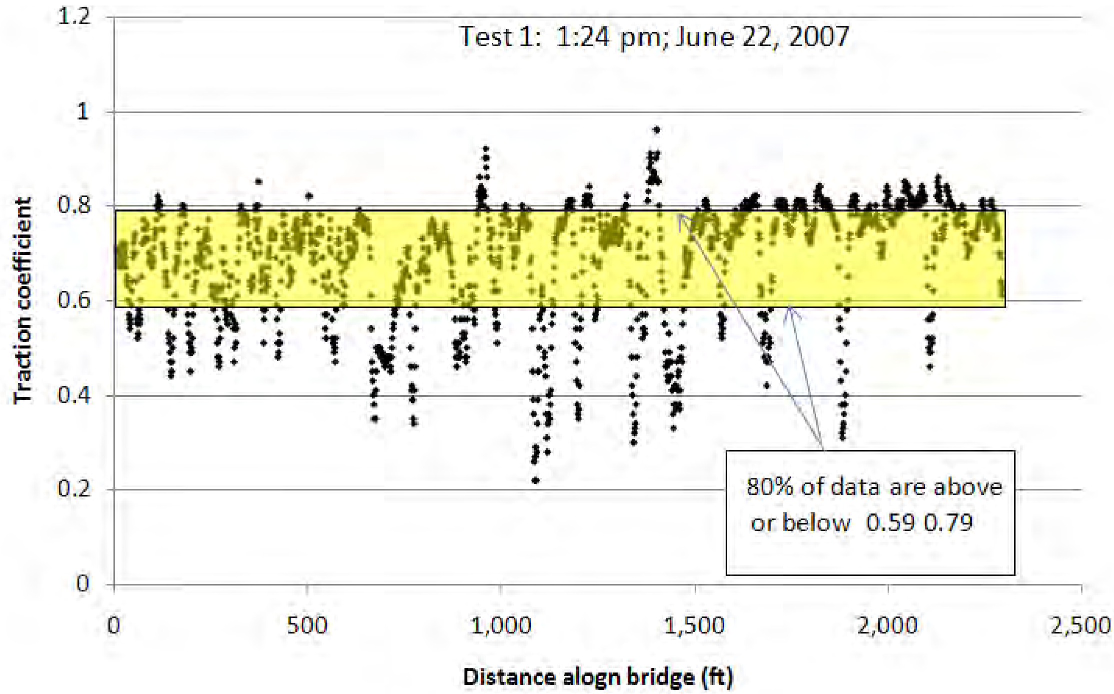

Figure E.1 Traction data for the Yukon River Bridge.

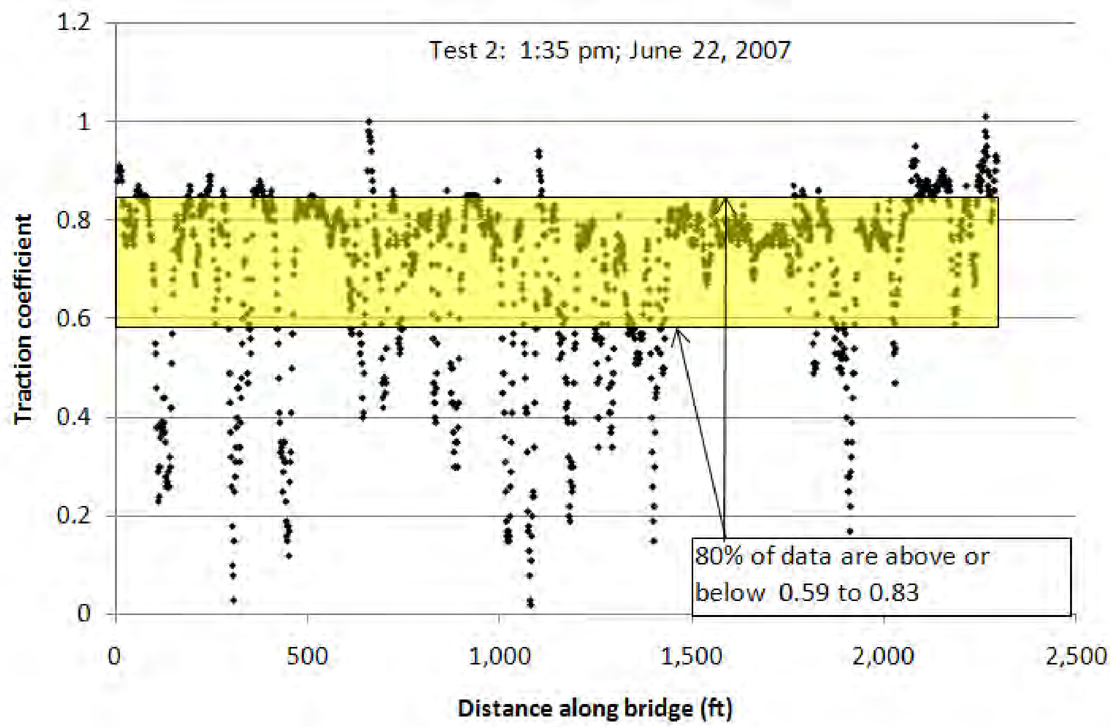

Figure E.2 Traction data for the Yukon River Bridge.

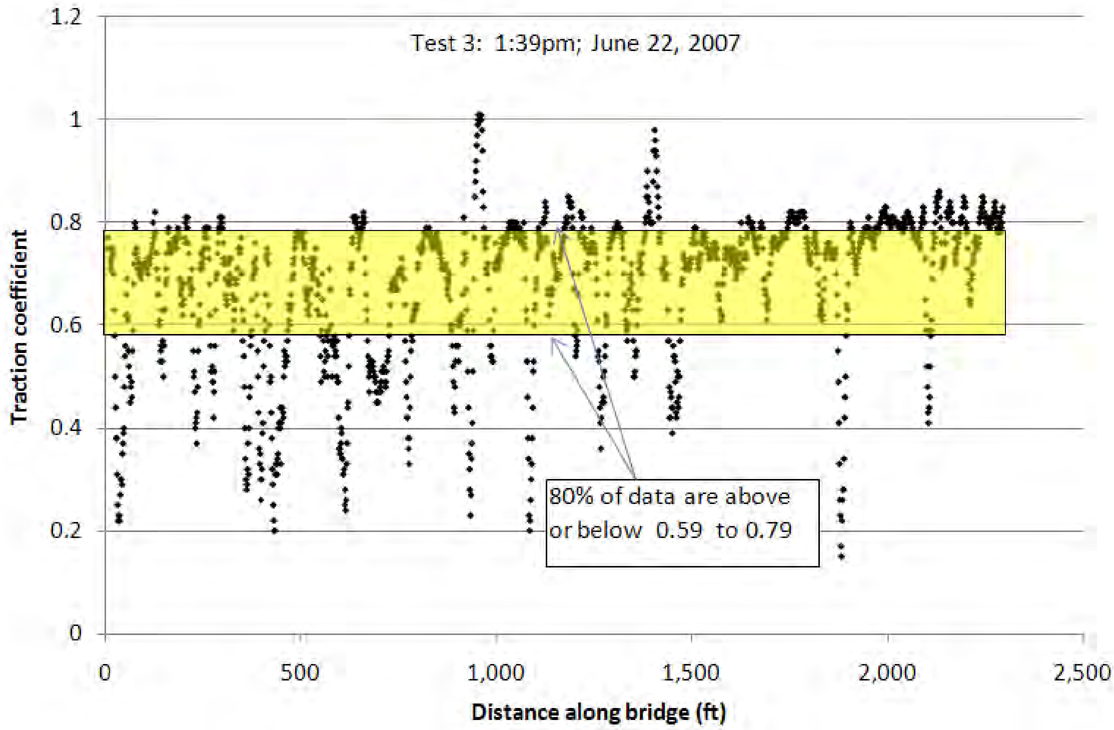

Figure E.3 Traction data for the Yukon River Bridge.

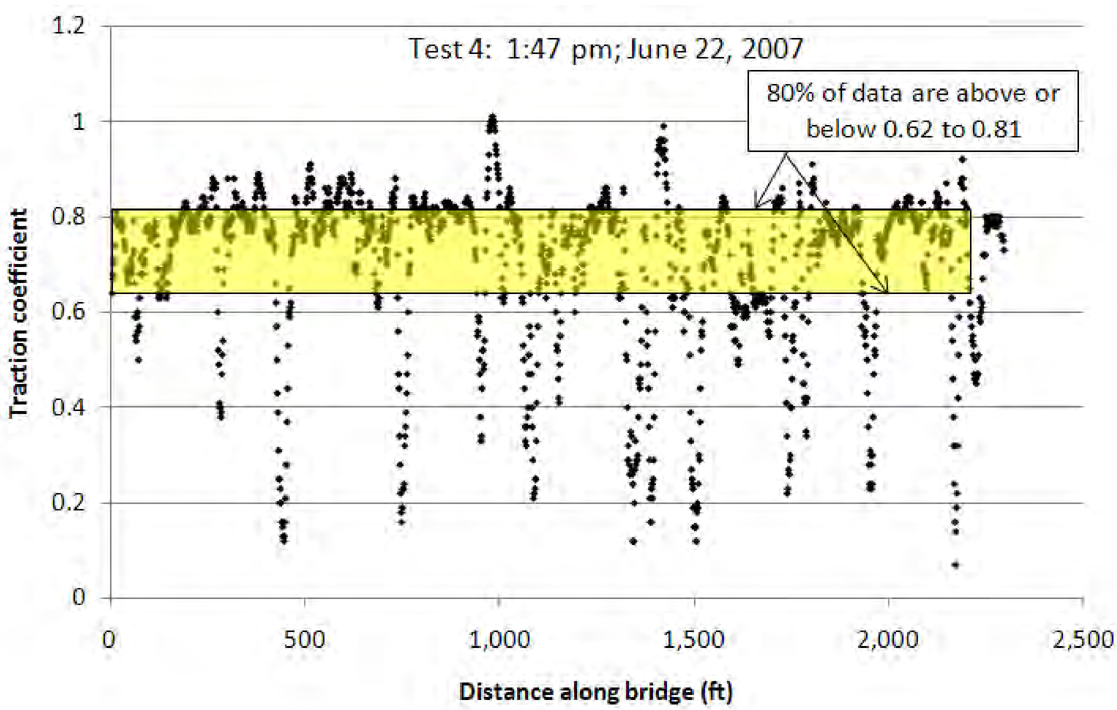

Figure E.4 Traction data for the Yukon River Bridge.

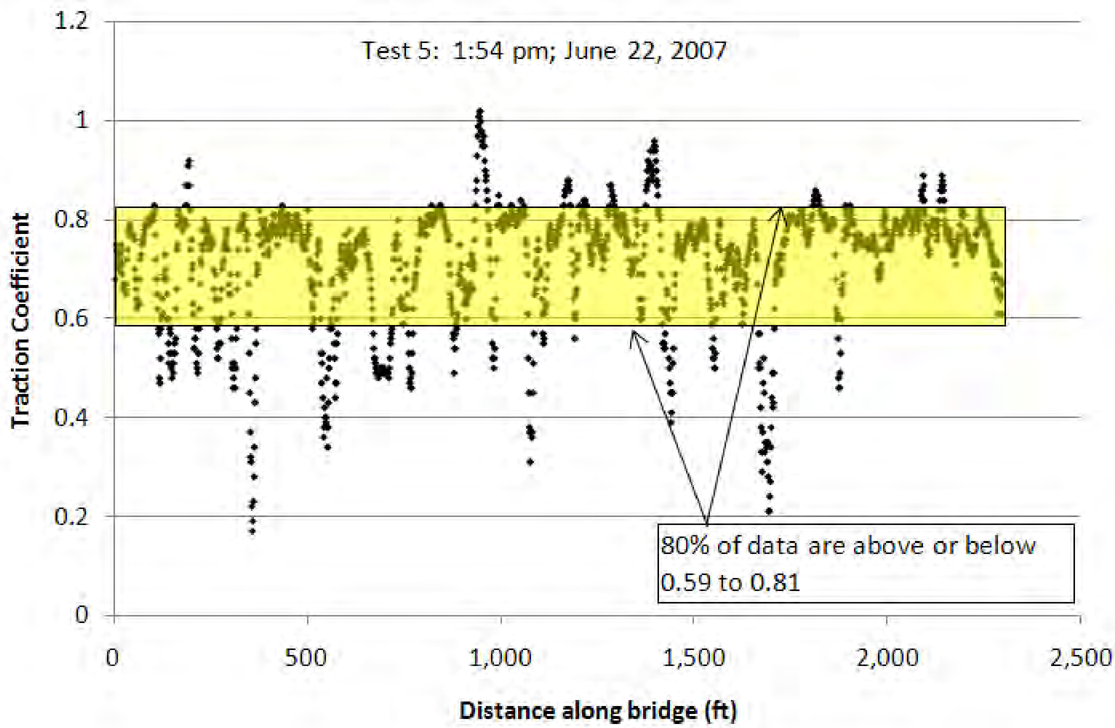

Figure E.5 Traction data for the Yukon River Bridge.

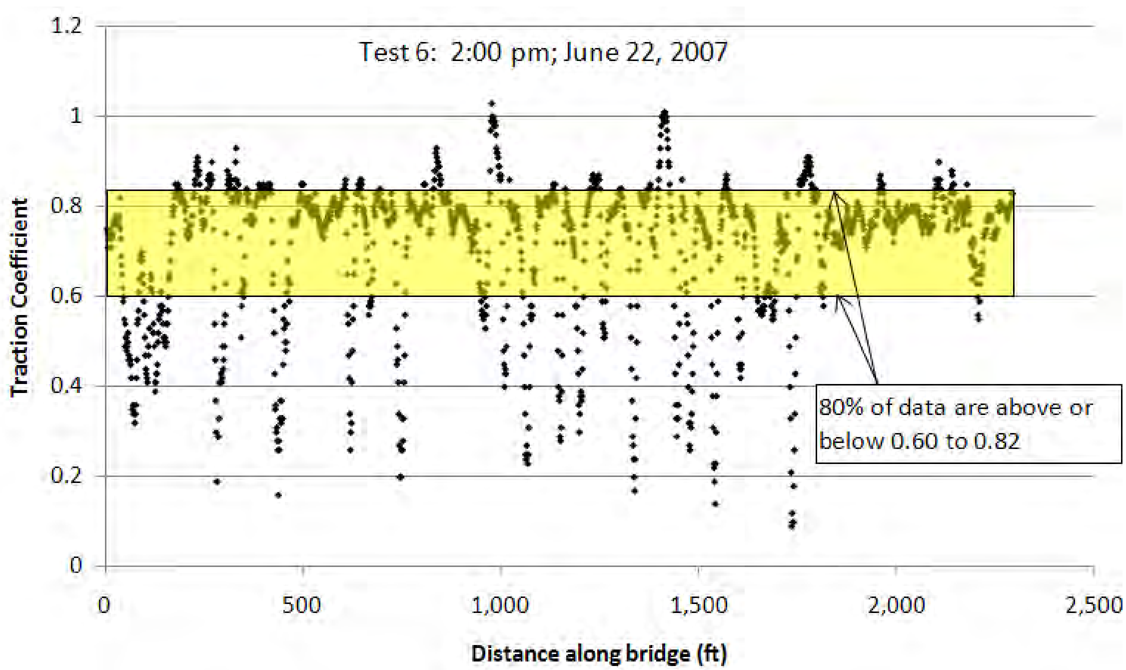

Figure E.6 Traction data for the Yukon River Bridge.

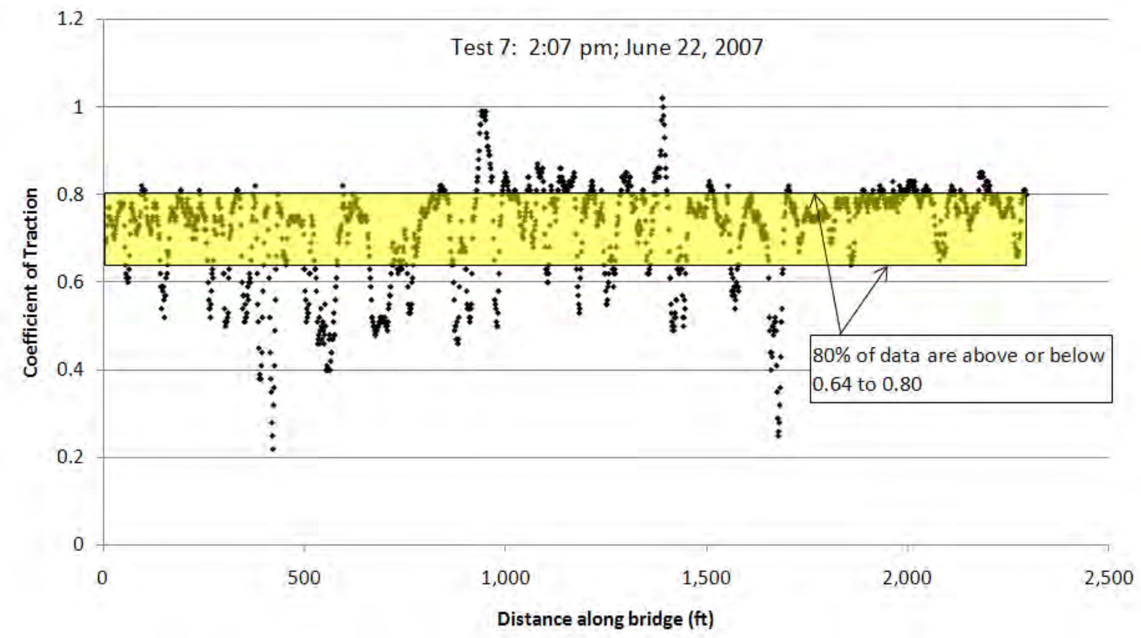

Figure E.7 Traction data for the Yukon River Bridge.

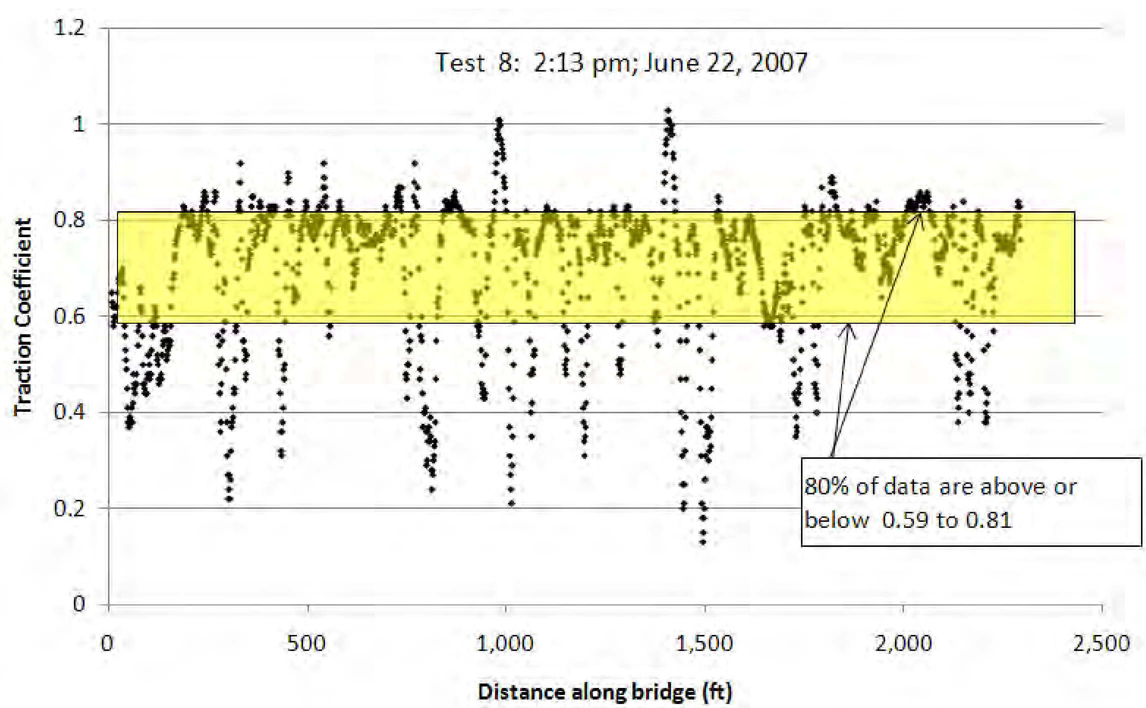

Figure E.8 Traction data for the Yukon River Bridge.